November 2015

Photochemical Tools for Fluorescent Labeling of Endogenous Proteins

Stephen T. McCarron
University of Massachusetts Amherst

PHOTOCHEMICAL TOOLS FOR FLUORESCENT LABELING OF ENDOGENOUS PROTEINS

A Dissertation Presented

by

STEPHEN T. MCCARRON

Submitted to the Graduate School of the
University of Massachusetts Amherst in partial fulfillment
of the requirements for the degree of

DOCTOR OF PHILOSOPHY

September 2015

Department of Chemistry

PHOTOCHEMICAL TOOLS FOR FLUORESCENT LABELING OF ENDOGENOUS PROTEINS

A Dissertation Presented

by

STEPHEN T. MCCARRON

Approved as to style and content by:

_____
James J. Chambers, Chair

_____
Vincent Rotello, Member

_____
Nathan Schnarr, Member

_____
Alejandro Heuck, Member

_____
Craig T. Martin, Department Head
Department of Chemistry

DEDICATION

To my family, friends, and mentors. Thank you for providing me with so much love, support, and inspiration. To my grandpa, one of the greatest men I will ever know.

ACKNOWLEDGMENTS

First and foremost, I would like to thank my advisor, Professor James Chambers for his patience, guidance, and contributions to my research over the past six years.

Thank you to my committee members, Professors Vince Rotello, Nate Schnarr, and Alejandro Heuck for their insight and guidance.

I would also like to thank my collaborators: Dr. Amy Hauck Newman and Dr. Ulrik Gether for providing ligands for the dopamine and serotonin nanoprobes as well as conducting the imaging experiments. Dr. Doug Johnson and Dr. Joshua Judkins at Pfizer for your excellent work on the ketamine probe.

Thank you to Dr. Peter Samal and Dr. Chris McDaniel for your mentorship during my TA assignments. Thank you to the Chambers group for all your insights during group meeting.

Finally, thank you to all my friends and family for making the last six years so enjoyable.

ABSTRACT

PHOTOCHEMICAL TOOLS FOR FLUORESCENT LABELING OF ENDOGENOUS PROTEINS

SEPTEMBER 2015

STEPHEN T. MCCARRON

B.S., SIENA COLLEGE

Ph.D., UNIVERSITY OF MASSACHUSETTS AMHERST

Directed by: Assistant Professor James J. Chambers

The study of the dynamic movements of membrane bound proteins is typically achieved through an exogenously applied fluorescent tag or genetic modification of a receptor of interest to spatiotemporally monitor protein location. Techniques often used for labeling proteins include overexpression of a fluorescent protein such as GFP fused to a target protein or the application of antibodies. These methods benefit from superb specificity towards a receptor of interest, but may impose unforeseen consequences when studying natural protein movements. Thus, it is advantageous to development small, modular probes that would allow for visualization of endogenous membrane bound receptors in a minimally perturbed state.

Several strategies employing photochemical small molecules were pursued to label important neuronal receptor targets on live cells. One method, photoaffinity labeling, requires a highly specific ligand outfitted with a UV photoreactive group and an orthogonal handle to covalently bind the ligand to the receptor for experimental analysis of the target. Using this technique we synthesized high affinity photoaffinity labels to

study sigma receptors, which are believed to be involved in several neurodegenerative disorders and cancer pathologies.

Another method is fluorescently tethered small molecule ligands that utilize a pharmacophore covalently bound to a fluorophore for specificity and subsequent visualization of a receptor of interest. We have designed small, minimally-perturbing modular probes that enable labeling and subcellular visualization of endogenous receptors on live cells. This technology allows for silent labeling of a receptor of interest, which allows for the receptor to be tagged with a fluorescent moiety in a non-ligated and thus active state. Using these probes we labeled the presynaptic dopamine and serotonin transporters and NMDA receptors on live cells.

Finally, we have developed a method for facile alkylation of biological substrates utilizing a small, photoactivatable, electrophilc moiety that is compatible with aqueous buffer. We demonstrated that the molecule is reactive only in the presence of UV light, which gives the user temporal control over the alkylation of a nucleophile.

In sum, these small molecule probes will provide chemical biologists novel tools for labeling membrane-bound receptors to visualize their location and trafficking, which will give fundamental insight into their endogenous activity.

TABLE OF CONTENTS

Page

LIST OF TABLES

Table Page

LIST OF FIGURES

Figure Page

LIST OF SCHEMES

Scheme Page

CHAPTER 1

GENERAL LABELING STRATEGIES

1.1 Introduction

The use of fluorescent molecules has revolutionized the way we can observe proteins, receptors, and ion channels in and on cells. These molecules have allowed for the study of several membrane bound proteins that can give insight into not only the structure of the protein, but function as well. Techniques that are widely used to label membrane bound proteins include overexpression of a fluorescent protein fused to a target protein or the application of antibodies[1]. Overexpression of a fluorescent protein generally relies on a gene construct being introduced to a target cell that encodes the gene of interest with the fusion protein. In addition, hybrid chemical/genetic strategies such as the tetracysteine FlAsH/ReAsH or the tetraserine RhoBo systems have also been developed[2,3]. Enzyme catalyzed processes are also utilized for selective chemical modification of expressed proteins, which include the use of Bir[4], Lp1[5], SrtA[6], and phosphopantetheinyl transferases[7]. Although these systems benefit from the superior specificity that is built into the system, overexpression of some fluorescent proteins are known to cause oligomerize under certain conditions[8]. In addition, overexpression of tagged monomeric subunits of heteromultimeric proteins have been shown to bias receptor subtype composition and function, which will make it difficult to study receptors in their natural state[9].

Another widely used method for labeling native receptors is the application of antibodies. This technique utilizes fairly large proteins to label and track the movement of receptors. Much like the case with genetically modified proteins, antibody labeling

provides high specificity for a target of interest due to the evolved nature of their binding. Unfortunately, due to the large size of the antibody coupled with the addition of a fluorescently labeled secondary antibody, this technique may impose unforeseen consequences on the natural movement of a receptor on the surface of a cell. This factor is especially significant when studying neuronal receptors that are moving in and out of a synapse, which is a distance that is not much larger than the antibody-receptor complex[10].

Ideally, a labeling strategy should not only be selective towards the receptor of interest, but also be small to be minimally perturbing to the native system. The strategy should be modular so it can be easily adapted for numerous uses and targets. In addition, if the method is also silent, one would be able to visualize the receptor in a non-ligated and thus non-perturbed state. Towards these ends, new small molecule probes were designed and synthesized for visualization of various neuronal receptors on live cells. They were derived from carefully chosen high affinity ligands from the literature to ensure selective labeling of the receptors of interest.

As general background for this work, two methods of small molecule labeling will be discussed as alternatives to genetic modification or antibody labeling approaches. First, there will be a brief description of design strategies for photoaffinity labeling, which utilizes a ligand outfitted with a photoreactive group and orthogonal handle. Next, the three key features for fluorescently tethered ligands will be discussed: pharmacophore, linker, and fluorescent reporter. Finally, the development of multifunctional probes will be introduced, focusing on a method for silently labeling endogenous proteins on live cells.

1.2 Small Molecule Labeling

Fluorescently labeled small molecule ligands have become powerful tools that can be utilized to study proteins on living cells. These probes generally consist of a high affinity ligand covalently modified in some fashion to a fluorescent reporter for binding and visualization of a receptor of interest, respectively[11,12]. There are two key advantages that are provided by the utilization of small molecules for imaging neuronal targets. First one must consider the minute size of a typical organic dye in comparison to the previously mentioned genetic and antibody techniques. Organic fluorophores generally consist of multiple conjugated and/or aromatic ring structures that are much smaller than proteins or quantum dots. Fluorescent proteins are generally in the range of 30 kDa and 4 nm on their longest axis whereas quantum dots can be in the 15-50 nm diameter range[8]. In these cases, the fluorescent label could be similar in size to the receptors of interest, thereby increasing the likelihood of disruption to normal trafficking. Second, small molecule probes can be applied to native systems that have not been genetically altered. As stated earlier, genetic modification with a fluorescent protein can lead to receptor subtype biasing as well as oligomerization, which can lead to unforeseen changes in receptor trafficking. By applying small molecule probes to native receptors it increases the likelihood of viewing natural movement of the protein. The combination of the diminutive size of organic fluorophores coupled with recent advances in imaging techniques makes for an unprecedented confluence that allows us to study neuronal receptor dynamics in detail that was not possible just a few years ago[13]. Two small molecule techniques that will be discussed in the following chapters to label neuronal receptors are photoaffinity labeling and fluorescently tethered ligands.

1.2.1 Photoaffinity Labeling

Photoaffinity labeling (PAL), a technique that was developed more than five decades ago[14], is a valuable small molecule tool that can be used to study the interactions of ligands with their target proteins. PAL utilizes a ligand possessing a UV-photoreactive group that can be incubated with a receptor of interest to form a noncovalently bound ligand-receptor complex. Following binding, UV irradiation triggers the photoreactive group to produce a highly reactive intermediate that will form a covalent link between the ligand and the receptor at the binding site (Figure 1.1). In addition, photoaffinity labels typically contain orthogonal groups to facilitate the detection and identification of the photolabeled biomolecules. When designing photoaffinity ligands, it is important to establish that the incorporated photoreactive group does not significantly alter the binding affinity of the ligand towards the receptor when compared with the parent compound. The formation of a covalent ligand-receptor complex aids the study of the receptor because it allows for the use of more rigorous and harsher analysis tools such as SDS-PAGE, HPLC, and mass spectrometry, which would normally lead to the dissociation of the ligand-receptor complex[15].

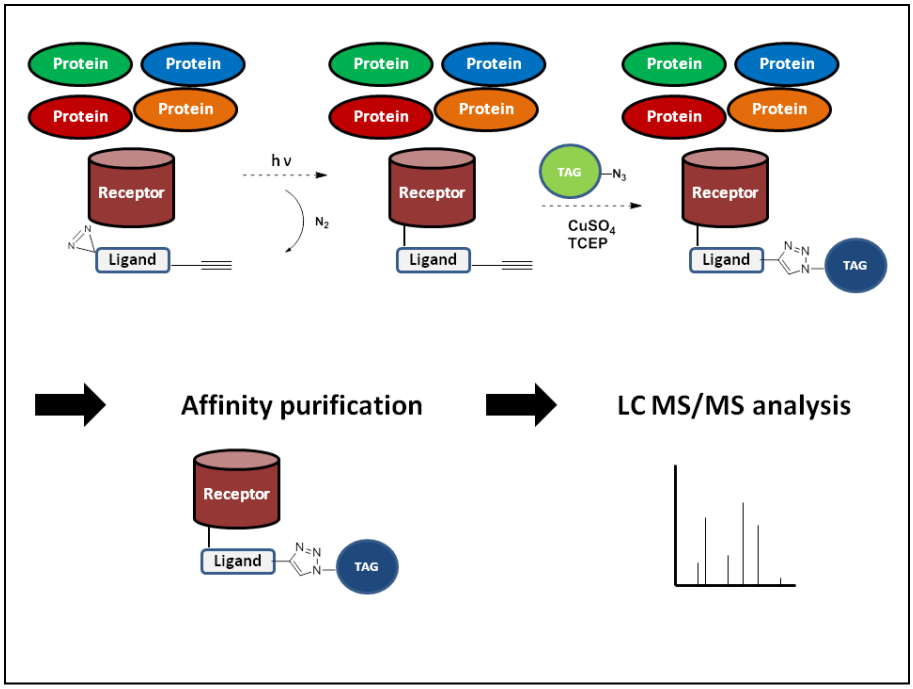

Figure 1.1. Cartoon depiction of PAL. The ligand will give specificity towards the receptor of interest, which will put the photoreactive group in close proximity to the receptor. Following irradiation with UV light the photoreactive group will create a covalent bond with the receptor that can then be tagged utilizing the alkyne handle. The tag can facilitate visualization of the receptor or affinity purification that will allow for subsequent mass spectroscopy studies.

The choice of photoreactive group used to covalently link the ligand and receptor is of critical design importance for labeling experiments. In most cases, the photolabeling compound is a derivatized receptor agonist or antagonist. The photoreactive group is usually synthetically inserted into the ligand of interest, however, some ligands may contain moieties that are capable of intrinsic photoactivation such as sulfides, enones, dienones, and halogenated compounds[16]. The photoreactive group should demonstrate several of the following characteristics in order to successful label a receptor of interest. First, the molecule chosen should be as small as possible to minimize any steric interactions that would impact ligand-receptor binding affinity. Ideally, once a probe is chosen, control experiments should be performed to ensure that the binding affinity of the derivatized ligand for the receptor being studied is not significantly altered from the

parent compound[15]. Second, the half life of the photoactivated species should be short enough to encourage covalent linkage between the photoaffinity ligand and receptor before disassociation can occur. At the same time, the excited state of the molecule should last long enough for the photoreactive group to remain in close contact with the binding site so that the labeling efficiency is high. Lastly, the photoreactive group should be capable of attacking both C-H and nucleophilic X-H bonds at an activation wavelength that would not damage proteins[15].

The most commonly used photoreactive groups for PAL studies are aryl azides, diazirines, and benzophenone based compounds (Figure 1.2)[17,18]. The aryl azide and diazirines moieties are precursors of nitrene and carbene groups, while benzophenone based probes rely on the reactivity of aryl ketones[19]. Nitrene and carbene intermediates are capable of rapidly reacting with double bonds or heteroatoms in addition to chemically 'inert' aliphatic C-H bonds[20]. Benzophenones generate reactive triplet carbonyl states upon irradiation with 350 nm light. They are generally more stable to solvent than other photoreactive groups, however, they require long irradiation periods that bears a risk for non-specific labeling[21]. The broad reactivity of these photoreactive moieties allow for almost all functional groups found in biomolecules to be available for forming covalent bonds.

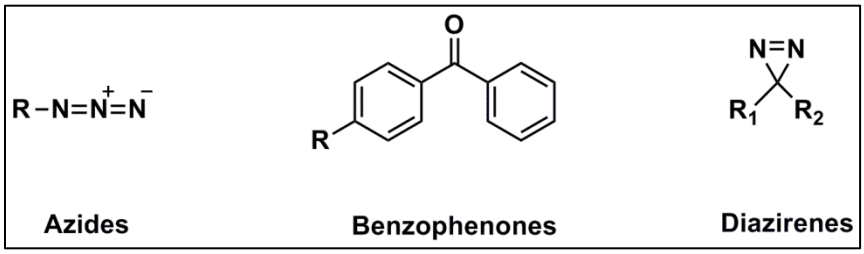

Figure 1.2. General photoreactive groups utilized for PAL.

As mentioned previously, photoaffinity labels often contain an orthogonal handle in addition to the photoreactive group to facilitate further study of the ligand-receptor complex. Most often these groups are biotin, radioactive isotopes, fluorescent groups, and alkyne moieties, which all help with the detection of a receptor in a complex matrix such as cell lystate[15]. For example, after cross-linking a photoaffinity label to a receptor of interest, an alkyne handle can be reacted with biotin-azide in a highly specific 1,3-dipolar cycloaddition reaction. The biotin will allow for affinity purification of the labeled receptor, which can be followed by trypsin digest and analysis by mass spectroscopy. The coupling of receptor labeling with mass spectroscopy allows for information on receptor-ligand interactions to be obtained on several levels. For instance, these techniques can be used to screen for the target of a particular ligand or drug candidate, find information of the binding region through mass spectroscopy based sequencing, or identify specific amino acids involved in interaction with the ligand in the binding pocket[15]. The results obtained at this level will be useful in developing 3D models of the ligand-receptor complex, and therefore become a key component in effective structure based drug design.

1.2.2 Fluorescently tethered ligands

The first fluorescent labeling with a selective small molecule ligand that targeted the β-adrenergic receptors was reported in 1976[22]. In this work, the authors conjugated the antagonist propranolol to a 9-aminoacridine fluorophore, which was then used to label β-receptors in rat cerebellum. Since then, many more have followed, displaying that receptor selective fluorescent ligands are powerful tools for studying receptor physiology or pathophysiology on the cellular or subcellular level[23]. Fluorescent small molecule probes have become increasingly sought after for use in the drug discovery process to

replace radioligands due their expense, health risks, and disposal issues[23]. Fluorescent molecules not only solve many of these drawbacks, but also can provide other advantages. Fluorescent molecules allow for real-time visualization and tracking of the labeled receptor, which can provide information on dynamic changes like agonist-stimulated receptor internalization, endocytosis, and receptor recycling[24].

There are several factors that must be considered when designing small molecule fluorescent ligands (Figure 1.3). The ligand and fluorophore must work together to not only bind to the proper target of interest, but also provide high efficiency fluorescence for visualization of the receptor. The pharmacophore should be potent and selective, as well as allow for chemical functionalization via coupling to a linker and fluorophore. If there are no easily available sites for modification, functionalization can be built into the system by chemical means. In one such instance, Bai et al. described the synthesis of a fluorescent molecule for the study of the cannabinoid receptor, CB2[25]. The pharmacophore chosen, SR144528, didn't easily allow for a fluorophore to be conjugated through a linker. However, the parent compound was modified to contain an alkyl bromide group, which was followed by a substitution reaction with an amine linker for conjugation to a near-infrared dye[25]. Another factor to consider is the location of the fluorophore on the ligand chosen, which may alter affinity towards the receptor of interest. For example, Yates et al. were interested in studying the CB2 receptor by conjugating the fluorescent dye nitrobenzodiazole (NBD) directly to a CB2 agonist. The new fluorescent probe lost extensive binding affinity towards CB2, which was ultimately attributed to the addition of NBD[26].

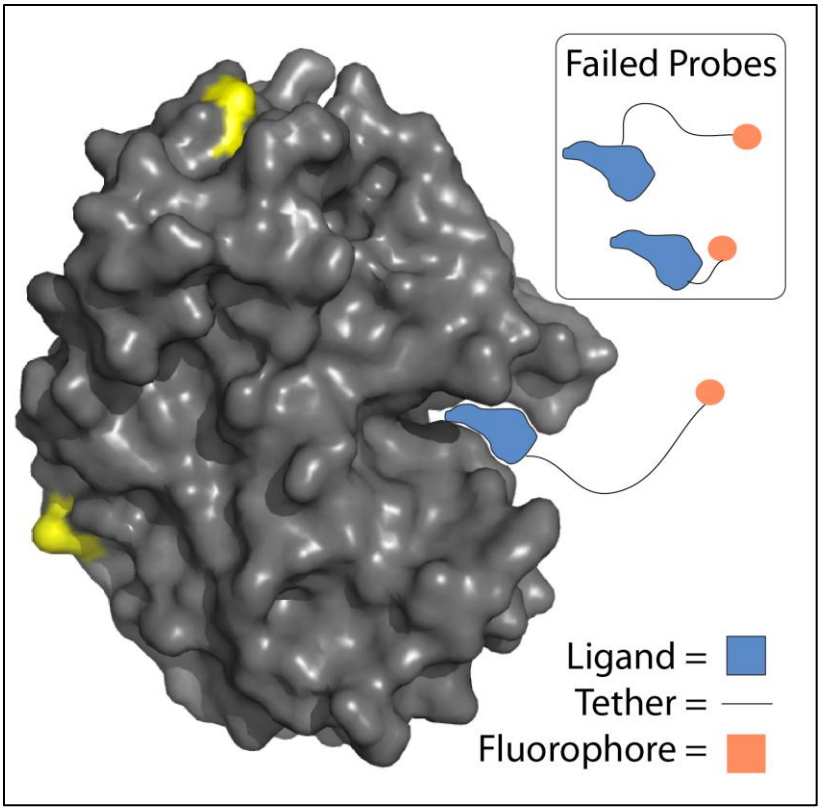

Figure 1.3. Cartoon representation of an ideal ligand/fluorophore pairing. Representation of a ligand that is appropriately decorated with a tethered fluorophore bound to the protein. In this specific case, the ligand is able to bind properly in the binding pocket due to the optimized length of the tether and fluorophore positioning. The upper right box shows two probes that will not work for this protein. One probe is functionalized with the tether in the wrong spot on the pharmacophore that would not allow the pharmacophore to bind properly with the protein. The other has a tether to the fluorophore that is too short, which would put the fluorophore too close to the protein and not allow the pharmacophore to enter the binding pocket.

The choice of the size and composition of the linker between the pharmacophore and fluorescent dye also plays an important role in potency as well as where the fluorophore will be positioned in proximity to the receptor[27]. The ideal spacer length should be derived from an optimization process taking into account the specific pharmacophore, fluorophore, and the environment in which they will be applied. To date, only a few studies have reported systematic evaluation of spacer length for the fluorescent probe being studied[28,29]. In general, longer linkers have been used for bulky fluorophores, such as near-infrared fluorophores, to reduce the likelihood of unfavorable

steric interactions with the target protein[25,30]. Another important consideration is that lipophilicity can play a factor in contributing to non-specific binding of some reported probes[31,29 ,32]. However, this issue can be circumvented through the use of polyethylene glycol linkers[33].

Finally, the chosen fluorophore should have high fluorescence intensity, be photostable, and have the proper excitation and emission profile for system being studied[23]. Fluorophores that are often used for fluorescent imaging include fluorescein, coumarin, dansyl, cyanine, rhodamine derivatives, and NBD as mentioned previously. More recently, there have also been several reported BODIPY based probes as well[23]. Fluorophores with excitation or emission wavelengths in the region of the visible light spectrum where cells exhibit high levels of autofluorescence and light scattering should be avoided to improve signal to noise ratio[34]. Care must also be taken to avoid any other fluorescent markers that are already present in the cells of interest such as a GFP-tagged protein.

Fluorescently tethered ligands can provide a multitude of valuable information about a receptor of interest. Tight binding of these fluorescent small molecules can give information regarding the mechanism of ligand binding, the fate of the receptor after binding events such as internalization, and the structure of the binding pocket[11,35,36]. Small molecule fluorophores have allowed for the development of pharmacological assays on the single cell level through their combination with fluorescent techniques such as fluorescence recovery after photobleaching, fluorescence correlation spectroscopy, and fluorescence resonance energy transfer microscopy[37]. Environment-sensitive fluorophores such as dansyl, 4-aminophthalimide derivatives, and PRODRAN, have been

employed to study the surrounding environments of these receptors. These molecules exhibit low quantum yields in aqueous solution, but become much more fluorescent when bound to a hydrophobic site in proteins or membranes[28,38,39]. Probes that contain red to near infrared emitting fluorophores have potential for use in vivo studies due to their longer excitation wavelengths, which not only allow for deeper penetration in living tissues, but are also less damaging to the cellular environment. In addition, these fluorophores allow for less light scattering compared to dyes with shorter excitation wavelengths, which reduces background noise and improves sensitivity[34].

1.2.3 Multifunctional small molecule probes

As previously discussed, small molecule fluorescent probes are powerful tools that have been used to label and track membrane bound receptors. However, there are some drawbacks to the current technology that limit their use. Due to the reliance on maintained receptor occupancy by these probes during imaging, one would only be able to observe receptors in a ligand bound, and thus perturbed, state. It has been shown that persistence of receptor activation by an agonist can cause conformational changes of several receptor types and also induce clathrin-mediated endocytosis or differential trafficking patterns[40,41,42]. Ideally, a molecular probe should not only be highly specific for a target of interest and contain a high contrast agent easily detected from the background fluorescence, it should also be traceless with regard to the ligand binding site to minimize the difference between the labeled and unlabeled state. Previous work in our lab was toward the development of a small, minimally-perturbing fluorescent probe that enabled labeling and subcellular visualization of endogenous glutamatergic α-amino-3-hydroxy-5-methyl-4-isoxazolepropionic acid (AMPA) receptors on live, wild-type

neurons[43]. Nanoprobe 1 much like the small molecule probes discussed earlier, utilizes a ligand for specificity towards AMPA receptors and a Cy3 dye for visualization (Figure 1.4).

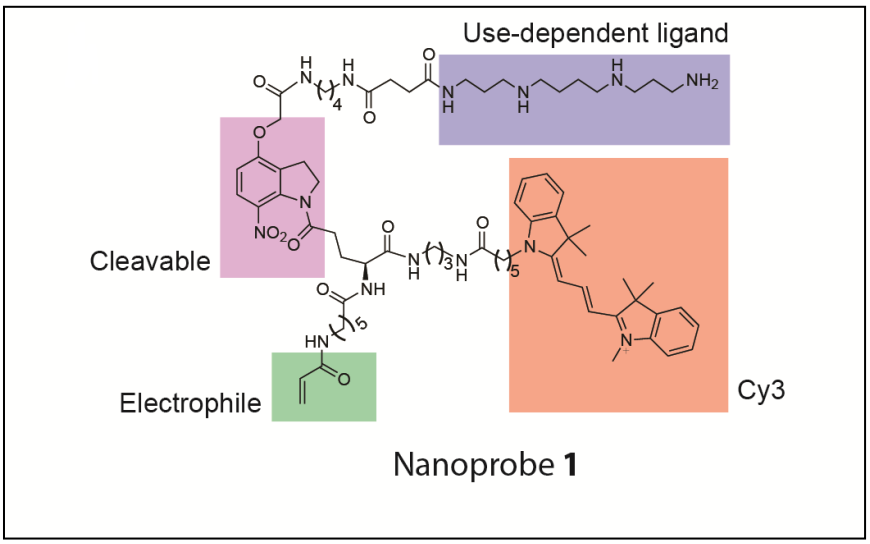

Figure 1.4. Structure of Nanoprobe 1.

This probe exceeds the previous discussed technology because there are two key additions to the molecule that allow for the permanent labeling of the receptor, as well as a method for excising the ligand: a promiscuous acrylamide electrophile for crosslinking to the receptor of interest and a photolabile nitroindoline core that facilitates the removal of the ligand following irradiation with 365 nm light (Figure 1.5)[43]. The combination of these functional groups allow for a receptor to be tagged with a fluorescent moiety in a non-ligated and thus active state. This technology has allowed us to visualize and track the endogenous receptor in live neurons in a time-resolved manner[43,44].

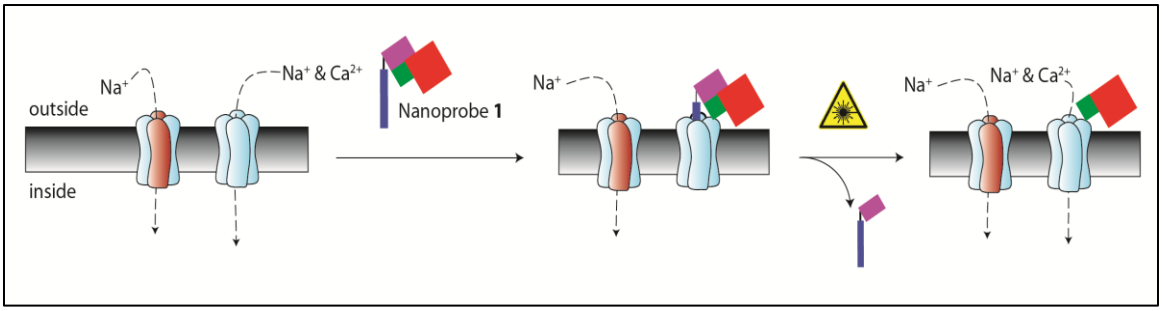

Figure 1.5. Cartoon depiction of nanoprobe labeling. Binding of the ligand (purple rectangle) to the receptor of interest brings the acrylamide electrophile (green square) in close proximity to a nucleophile to covalently bond the probe to the receptor. Following irradiation with UV light to cleave the photolabile core (purple square), the ligand is removed from the binding site to leave behind a fluorophore (red square) covalently bond to the receptor.

The background described above is applied to several of the following chapters, which describes the work done towards designing and synthesizing small molecule fluorescent tools for labeling endogenous proteins. Some of these probes were used to directly to label neuronal receptors on live cells, the results of which are described in each appropriate section.

1.3 References

(1) Giepmans, B. N. G.; Adams, S. R.; Ellisman, M. H.; Tsien, R. Y. *Science* **2006**, *312*, 217.

(2) Griffin, B. Albert, Adams, Stephen R., Tsien, R. Y. *Science (80-.).* **1998**, *281*, 269.

(3) Halo, T. L.; Appelbaum, J.; Hobert, E. M.; Balkin, D. M.; Schepartz, A. *J. Am. Chem. Soc.* **2009**, *131*, 438.

(4) Lin, M. Z.; Wang, L. *Physiology* **2008**, *23*, 131.

(5) Fernandez-Suarez, M.; Baruah, H.; Martinez-Hernandez, L.; Xie, K. T.; Baskin, J. M.; Bertozzi, C. R.; Ting, A. Y. *Nat Biotech* **2007**, *25*, 1483.

(6) Popp, M. W.-L.; Ploegh, H. L. *Angew. Chemie Int. Ed.* **2011**, *50*, 5024.

(7) Vivero-Pol, L.; George, N.; Krumm, H.; Johnsson, K.; Johnsson, N. *J. Am. Chem. Soc.* **2005**, *127*, 12770.

(8) Toseland, C. P. *J. Chem. Biol.* **2013**, *6*, 85.

(9) Lu, W.; Shi, Y.; Jackson, A. C.; Bjorgan, K.; During, M. J.; Sprengel, R.; Seeburg, P. H.; Nicoll, R. A. *Neuron* **2014**, *62*, 254.

(10) Sobolevsky, A. I.; Rosconi, M. P.; Gouaux, E. *Nature* **2009**, *462*, 745.

(11) Eriksen, J.; Rasmussen, S. G. F.; Rasmussen, T. N.; Vaegter, C. B.; Cha, J. H.; Zou, M.-F.; Newman, A. H.; Gether, U. *J. Neurosci.* **2009**, *29*, 6794.

(12) Mizukami, S.; Hori, Y.; Kikuchi, K. *Acc. Chem. Res.* **2014**, *47*, 247.

(13) Joubert, J.; Dyk, S. V; Malan, S. F. *Mini Rev. Med. Chem.* **2013**, *13*, 682.

(14) Singh, A.; Thornton, E. R.; Westheimer, F. H. *J. Biol. Chem.* **1962**, *237* , PC3006.

(15) Robinette, D.; Neamati, N.; Tomer, K. B.; Borchers, C. H. *Expert Rev. Proteomics* **2006**, *3*, 399.

(16) A. Fleming, S. *Tetrahedron* **1995**, *51*, 12479.

(17) Weber, P. J. A.; Beck-Sickinger, A. G. *J. Pept. Res.* **1997**, *49*, 375.

(18) Dormán, G.; Prestwich, G. D. *Trends Biotechnol.* **2000**, *18*, 64.

(19) Dorman, G.; Prestwich, G. D. *Biochemistry* **1994**, *33*, 5661.

(20) Brunner, J. *Annu. Rev. Biochem.* **1993**, *62*, 483.

(21) Vodovozova, E. L. *Biochemistry. Biokhimiia*, 2007, *72*, 1–20.

(22) Melamed, E.; Lahav, M.; Atlas, D. *Experientia* **1976**, *32*, 1387.

(23) Kozma, E.; Suresh Jayasekara, P.; Squarcialupi, L.; Paoletta, S.; Moro, S.; Federico, S.; Spalluto, G.; Jacobson, K. A. *Bioorg. Med. Chem. Lett.* **2013**, *23*, 26.

(24) Gironacci, M. M.; Adamo, H. P.; Corradi, G.; Santos, R. A.; Ortiz, P.; Carretero, O. A. *Hypertens.* **2011**, *58* , 176.

(25) Bai, M.; Sexton, M.; Stella, N.; Bornhop, D. J. *Bioconjug. Chem.* **2008**, *19*, 988.

(26) Yates, A. S.; Doughty, S. W.; Kendall, D. A.; Kellam, B. *Bioorg. Med. Chem. Lett.* **2005**, *15*, 3758.

(27) Baker, J. G.; Middleton, R.; Adams, L.; May, L. T.; Briddon, S. J.; Kellam, B.; Hill, S. J. *Br. J. Pharmacol.* **2010**, *159*, 772.

(28) Berque-Bestel, I.; Soulier, J.-L.; Giner, M.; Rivail, L.; Langlois, M.; Sicsic, S. *J. Med. Chem.* **2003**, *46*, 2606.

(29) Middleton, R. J.; Briddon, S. J.; Cordeaux, Y.; Yates, A. S.; Dale, C. L.; George, M. W.; Baker, J. G.; Hill, S. J.; Kellam, B. *J. Med. Chem.* **2007**, *50*, 782.

(30) Höltke, C.; von Wallbrunn, A.; Kopka, K.; Schober, O.; Heindel, W.; Schäfers, M.; Bremer, C. *Bioconjug. Chem.* **2007**, *18*, 685.

(31) Korlipara, V.; Ells, J.; Wang, J.; Tam, S.; Elde, R.; Portoghese, P. *Eur. J. Med. Chem.* **1997**, *32*, 171.

(32) Middleton, R. J.; Kellam, B. *Curr. Opin. Chem. Biol.* **2005**, *9*, 517.

(33) Tahtaoui, C.; Parrot, I.; Klotz, P.; Guillier, F.; Galzi, J.-L.; Hibert, M.; Ilien, B. *J. Med. Chem.* **2004**, *47*, 4300.

(34) Leopoldo, M.; Lacivita, E.; Berardi, F.; Perrone, R. *Drug Discov. Today* **2009**, *14*, 706.

(35) Madsen, B. W.; Beglan, C. L.; Spivak, C. E. *J. Neurosci. Methods* **2000**, *97*, 123.

(36) Turcatti, G.; Zoffmann, S.; Lowe, J. A.; Drozda, S. E.; Chassaing, G.; Schwartz, T. W.; Chollet, A. *J. Biol. Chem.* **1997**, *272*, 21167.

(37) Michalet, X.; Weiss, S.; Jäger, M. *Chemical Reviews*, 2006, *106*, 1785–1813.

(38) Krieger, F.; Mourot, A.; Araoz, R.; Kotzyba-Hibert, F.; Molgó, J.; Bamberg, E.; Goeldner, M. *ChemBioChem* **2008**, *9*, 1146.

(39) Vázquez, M. E.; Blanco, J. B.; Salvadori, S.; Trapella, C.; Argazzi, R.; Bryant, S. D.; Jinsmaa, Y.; Lazarus, L. H.; Negri, L.; Giannini, E.; Lattanzi, R.; Colucci, M.; Balboni, G. *J. Med. Chem.* **2006**, *49*, 3653.

(40) Carroll, R. C.; Beattie, E. C.; von Zastrow, M.; Malenka, R. C. *Nat Rev Neurosci* **2001**, *2*, 315.

(41) Dhami, G. K.; Ferguson, S. S. G. *Pharmacol. Ther.* **2006**, *111*, 260.

(42) Thiagarajan, T. C.; Lindskog, M.; Tsien, R. W. *Neuron* **2005**, *47*, 725.

(43) Vytla, D.; Combs-Bachmann, R. E.; Hussey, A. M.; Hafez, I.; Chambers, J. J. *Org. Biomol. Chem.* **2011**, *9*, 7151.

(44) Combs-Bachmann, R. E.; Johnson, J. N.; Vytla, D.; Hussey, A. M.; Kilfoil, M. L.; Chambers, J. J. *J. Neurochem.* **2015**, *133*, 320.

CHAPTER 2

PHOTOAFFINITY LIGANDS FOR SIGMA RECEPTORS

2.1 Introduction

Sigma receptors were initially classified as a subclass of opioid receptors proposed by Martin et al[1]. Further studies, however, showed that the sigma binding sites were a distinct class of receptors located in both the central nervous system (CNS) as well as a variety of tissues and organs. These studies demonstrated that there were at least two types of sigma receptors; sigma 1 and sigma 2, which were distinguished based on their affinity towards [^{3}H]-(+)-pentazocine and [^{3}H]-1,3-di(2-toyl)guanidine ([^{3}H]-DTG). Both receptors bind pentazocine whereas only the sigma 2 receptor binds DTG[2].

Sigma 1 receptors reside at the endoplasmic reticulum (ER)–mitochondrion interface called the mitochondrion-associated ER membrane (MAM). At the MAM, the sigma 1 receptor regulates the stability of inositol 1,4,5-trisphosphate receptors, which ensures proper Ca^{2+} signaling between the ER and mitochondrion[3]. These receptors also regulate of the level of reactive oxygen species to control the dendritic spine arborization in neurons. The sigma 1 receptor consists of 223 amino acids and has been cloned from several mammalian species, which has been found to be 90% identical and have 95% similar amino acid sequences across species[3]. Although the sequence of sigma 1 has been characterized, the physiological role it plays remains largely elusive. There is increasing evidence that links the sigma 1 receptor to neuroprotective/neuroregulatory functions as well as to CNS pathologies such as schizophrenia, depression, and Alzheimer's and Parkinson's diseases[4,5,6]. More recently, it has been shown that juvenile amyotrophic

lateral sclerosis (ALS) is caused by a mutation in the gene encoding the sigma 1 receptor[7].

The sigma 2 receptor, unlike sigma 1, has yet to be cloned and its exact distribution is still not clear. Despite this, the sigma 2 receptor has been validated as a biomarker for tumor cell proliferation and as a target for chemotherapy. Sigma 2 receptors are expressed in high density of nearly all human and rodent tumor cell lines[8]. The density of these receptors in proliferating mouse mammary adenocarcinoma cells was found to be about ten-fold higher than that in the corresponding quiescent tumor cells both in vitro and in vivo[9,10]. Therefore, the sigma 2 receptor has become an attractive target for the development of small molecule probes for diagnostic imaging of solid tumors and as a druggable site for cancer treatment[11,12,13].

At the start of our work on this project, it was clear that both sigma receptors were interesting targets due to their involvement in various neurodegenerative diseases and the lack of information concerning the identity of sigma 2. We sought to synthesize small molecule probes that would allow for labeling and subsequent visualization of these receptors in live cells. One method of small molecule labeling is the use of photoaffinity ligands, which was described in chapter 1. Briefly, photoaffinity labeling utilizes a highly specific ligand outfitted with a UV photoreactive group and an orthogonal handle. Following binding to the receptor, UV irradiation produces a reactive intermediate that covalently links the ligand to the receptor. The orthogonal handle can then be utilized for the attachment of a tag that will facilitate the detection or purification of the labeled receptor.

Our first step was to identify various ligands that were potent towards the sigma receptor and were also amendable for modification with a photoreactive group. The main goal of the project was to synthesis photoaffinity ligands that could be used to label sigma 1 receptors on live cells. We chose the sigma 1 receptor because it was a more validated target, which would make it easier to determine that the ligand was reacting with the right receptor. However, because the pharmacology of the sigma receptors tends to overlap in several ways, we anticipated that the probe may also provide information on the identity of sigma 2.

2.1.1 Probe design

One of the first pharmacological models used to understand structural requirements for ligand binding to sigma receptors was developed by Glennon et al[14]. The model, based on analysis of different flexible sigma 1 ligands determined that one basic amine flanked by two hydrophobic regions was necessary for binding (Figure 2.1). The distances between the basic amino group and the primary and secondary hydrophobic regions should be in the range of 6-10 Å and 2.5-3.9 Å, respectively[14]. In addition, the basic amino group could be a secondary or tertiary amine and each hydrophobic region tolerates steric bulk at those positions. More recently, a 3D model developed by Laggner et al confirmed many of the details from the original Glennon model[15].

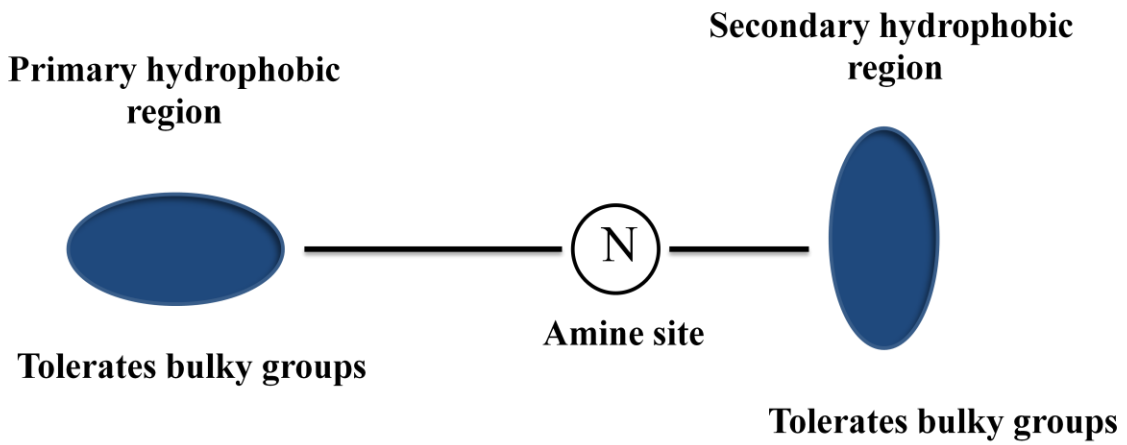

Figure 2.1. Glennon model for ligand binding to sigma receptors

With this model in mind, we searched through several structurally diverse ligands with high affinity towards sigma receptors, which include benzomorphans, arylalkylamines[16,17], spirocyclic compounds[18], steroids[19], and haloperiodol[20]. Of these structures, we were most interested in the arylalkylamines and haloperiodol because we could easily modify the phenyl rings of these compounds with a photoreactive group. Synthetic arylalkylamine compounds that are targeted to the sigma receptors often utilize a piperazine ring as the basic amine moiety in the compound. The addition of a cyclohexyl ring to the piperazine moiety also appears to increase the binding affinity of these compounds[21]. This information along with the structure of haloperiodol led us to the design of two new possible photoaffinity ligands for sigma receptors (Figure 2.2). In our proposed structures, we have utilized a piperazine ring as outlined from the previous examples. Both ligands make use of an aryl azide photoreactive group due to its small size and facile synthesis from an aniline precursor. We also chose to vary the position of the alkyne handle on either structure to allow for the cyclohexyl moiety to be placed on probe 2, which might produce a compound with higher binding affinity for the sigma

receptors. Upon completion of the synthesis of both these compounds, we have attempted to label the sigma 1 receptor in live cells.

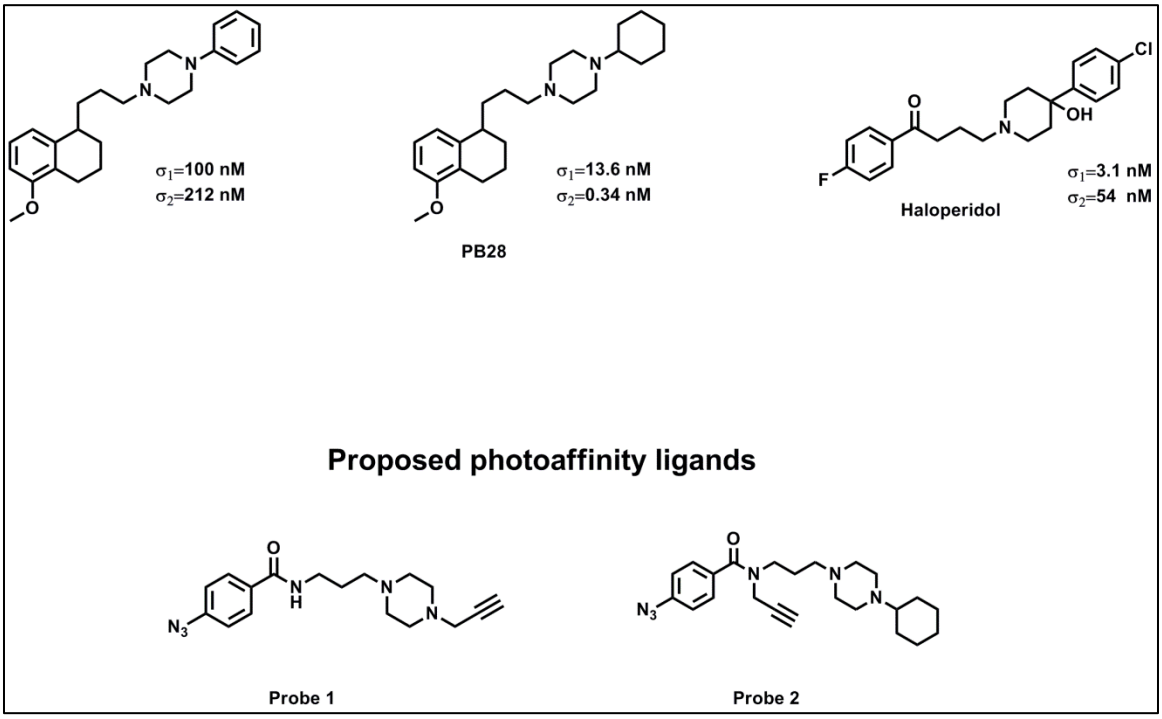

Figure 2.2. Proposed structures of photoaffinity labels for sigma receptors compared to examples of arylalkylamines and haloperiodol.

2.2 Experimental methods

2.2.1 Probe 1 synthesis

Starting with *p*-nitrobenzoic acid, intermediate **1** was synthesized under standard peptide coupling conditions with EDC and HOBt. Alkylation of **1** with Boc-piperazine to form **2** was followed by acid deprotection to yield piperazine **3**. The alkyne handle was affixed to the scaffold by reacting piperazine **3** with propargyl amine under peptide coupling conditions to form alkyne **4**. Reduction of the nitro group in alkyne **4** with tin (II) chloride ($SnCl_2$) produced aniline **5**, which was then converted to the aryl azide under Sandmeyer conditions to complete the synthesis of probe 1 (Scheme 2.1).

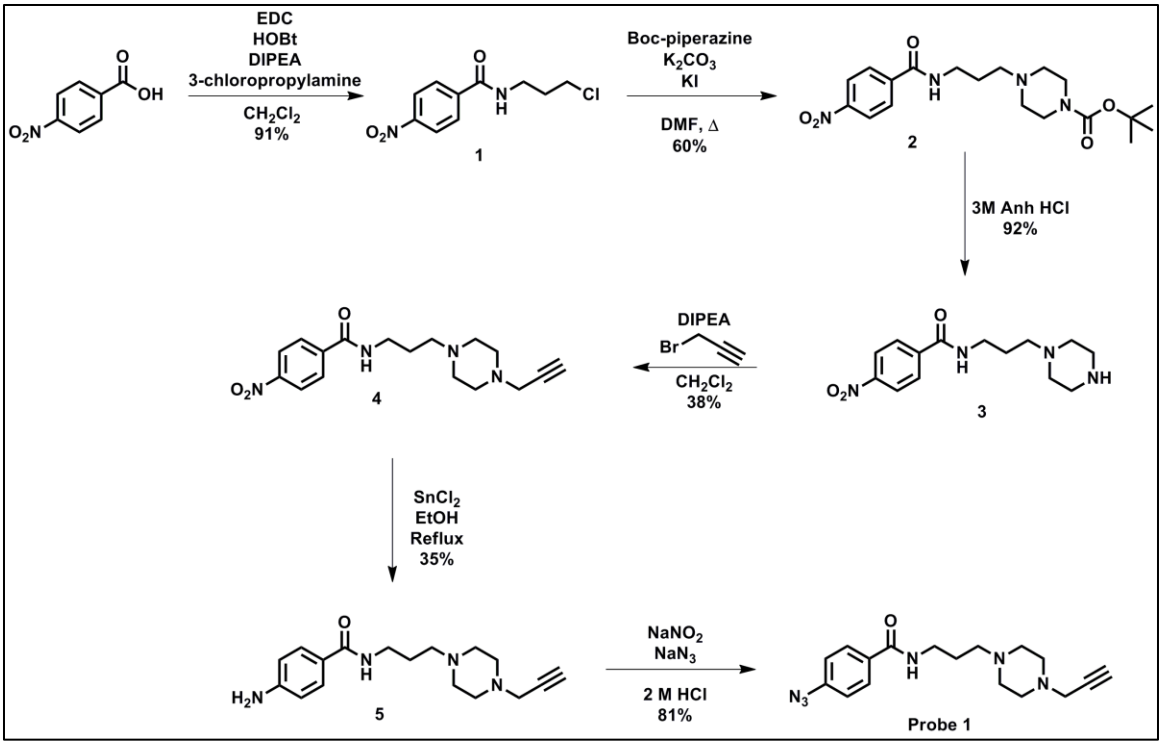

Scheme 2.1. Synthesis of photoaffinity ligand probe 1.

2.2.2 Probe 2 synthesis

Similar to the strategy used previously, probe **2** was synthesized through the peptide coupled intermediate **1** from *p*-nitrobenzoic acid. Alkylation of compound **1** with cyclohexylpiperazine led to intermediate **6**, which underwent $SnCl_2$ reduction to yield aniline **7**. Aryl azide **8** was synthesized as previously described utilizing Sandmeyer conditions from aniline **7**. The amide of intermediate **8** was then alkylated under basic conditions to complete the synthesis of probe 2 (Scheme 2.2).

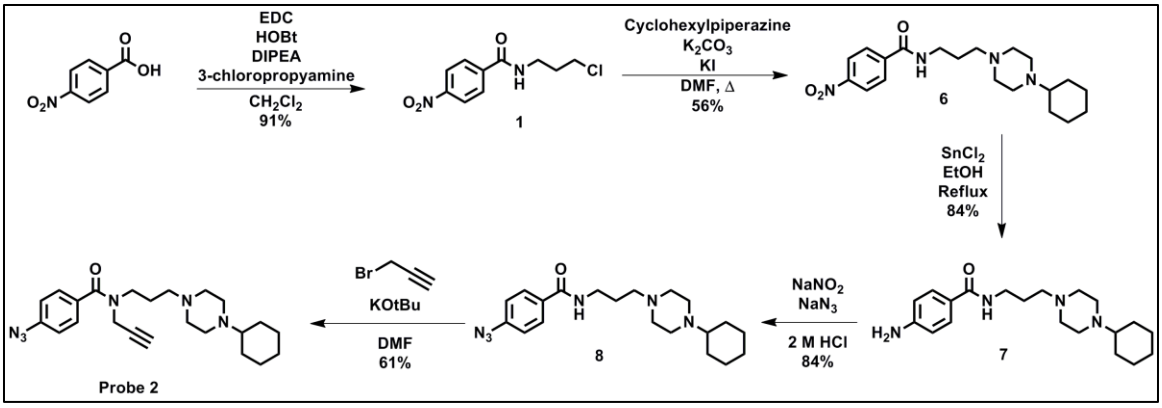

Scheme 2.2. Synthesis of photoaffinity ligand probe 2.

2.3 Results and Discussion

The original strategy for the synthesis of probe 1 and probe 2 was to utilize *p*-azidobenzoic acid as the starting point for both probes. This would incorporate the photoreactive group immediately in the synthesis and facilitate the completion of these probes in 3-4 steps. However, following the successful peptide coupling with 3-chloropropyl amine, it was found that the aryl azide moiety was not stable enough to survive the reflux conditions needed for the subsequent alkylation with Boc-piperazine or cyclohexylpiperzine. Therefore, the azido starting material was replaced with p-nitrobenzoic acid, which would be more stable under reflux conditions and can later be converted to an aryl azide following reduction with $SnCl_2$.

The alkylation of the amide bond in compound **8** to yield photoaffinity ligand probe 2 was also a reaction of particular interest. The first attempts to complete the synthesis under mild basic conditions with potassium carbonate (K_2CO_3) or N,N-diisopropylethylamine (Hunig's base) were unsuccessful despite evidence in the literature for this transformation[22,23]. However, following the addition of the stronger base potassium tert-butoxide, alkylation of the amide bond was successful in 61% yield.

Probe 1 and probe 2 were sent to the Psychoactive Drug Screen Program at the University of North Carolina to evaluate their binding affinity towards the sigma receptors. Probe 1 was found to be slightly more selective towards the sigma 2 receptor over sigma 1, with binding affinities of 230 nM and 821 nM, respectively (Figure 2.3). Similarly, probe 2 was more selective for sigma 2 than sigma 1, but was found to have a much higher binding affinity towards both receptors (1.9 nM, 29 nM, respectively) (Figure 2.4). This increase in binding affinity was likely due to the addition of the cyclohexyl group found in compound probe 2, which agrees with literature precedent. Probe 2 was chosen as the lead compound for receptor labeling studies due to its high potency towards both sigma receptors.

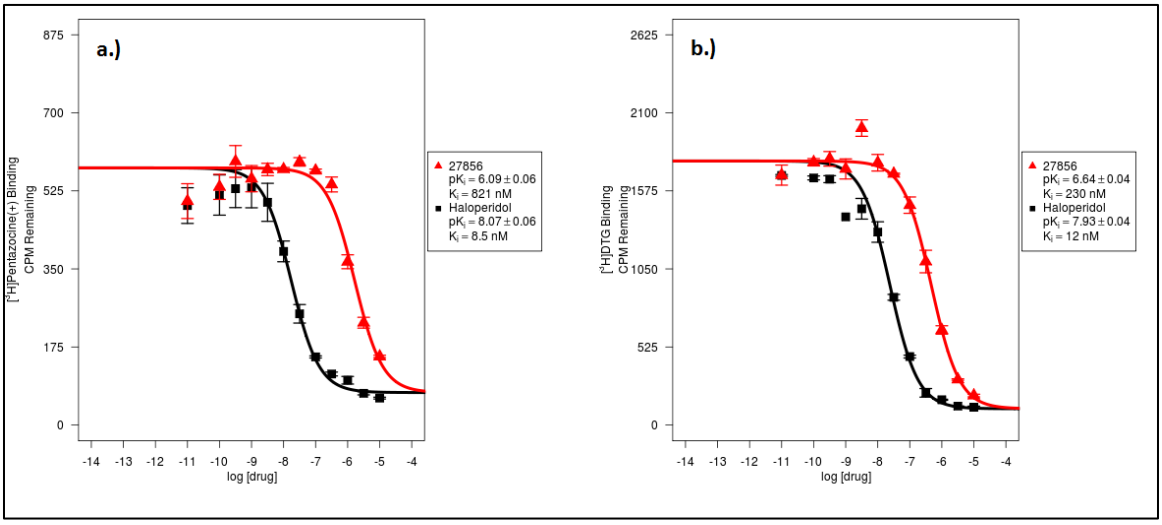

Figure 2.3. Binding curves for photoaffinity ligand probe 1. a.) Sigma 1 binding. b.) Sigma 2 binding

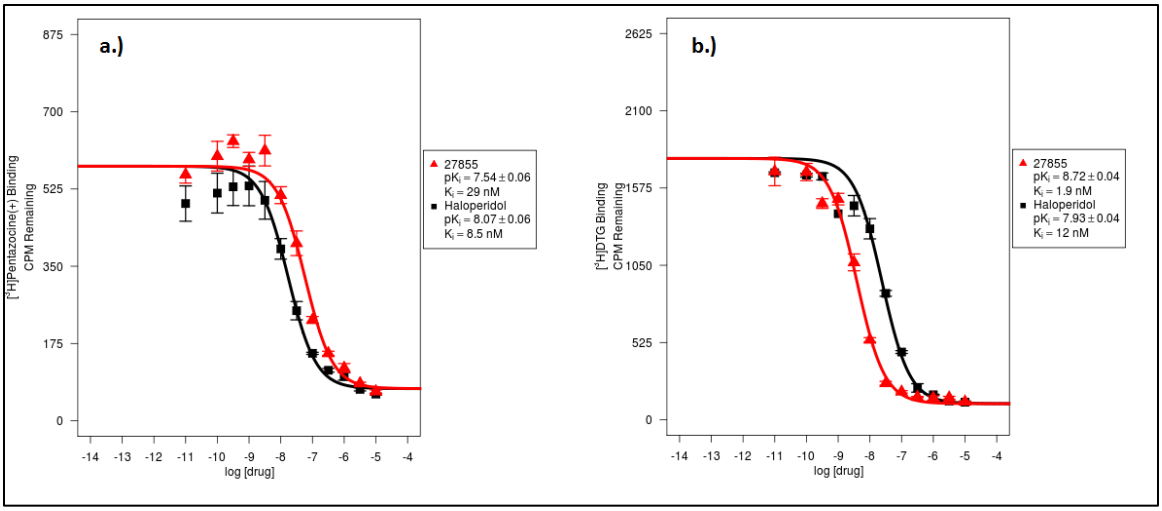

Figure 2.4. Binding curves for photoaffinity ligand probe 2. a.) Sigma 1 binding. b.) Sigma 2 binding

To demonstrate specific labeling of the sigma receptors with probe 2, several different cell lines and the lysates from these cell lines were incubated with concentrations of probe varying from 0.1 nM up to 100 μM. These cell lines included HEK, sigma 1-transfected HEK, HeLa, sigma 1-transfected HeLa, MCF7, and primary rat cerebellar neurons, all of which have a high level of sigma 1 and sigma 2 receptor expression. Rat organs including the liver, brain, spine, and kidney were also incubated with probe to visualize these receptors in whole tissues. During the course of the experiment, some samples were irradiated with 365 nm light to crosslink the ligand its binding partner, while others were kept in the dark. Despite the potency of probe 2 for both sigma receptors, no significant labeling in any of these experiments was observed. In most cases there was no difference between the irradiated and non-irradiated samples. This could possibly be due to the aryl azide moiety not being in close enough proximity to the receptor to form a stable covalent bond. If the aryl azide moiety is in a large hydrophobic pocket that tolerates steric bulk, as depicted in the Glennon model, then the

azide moiety could be facing into the pocket and react with solvent rather than the receptor.

2.4 Conclusion

Probe 2 is a potent compound for the sigma receptors. Despite its affinity, the probe does not provide an effective method for labeling these receptors on live cells. Further iterations of the probe could utilize a longer linker between the piperazine moiety and the aryl azide, which might allow for labeling of the receptor by placing the aryl azide in closer proximity to a potential nucleophile.

2.5 Materials and Methods

2.5.1 General information

All reagents, biological and chemical, were purchased through Fisher Scientific (Fair Lawn, NJ, USA). All reactions involving air- and moisture-sensitive reagents were performed under an argon atmosphere using syringe-septum cap techniques. DMF and CH_2Cl_2 were dried by storing over molecular sieves (4Å). Analytical thin-layer chromatography (TLC) was carried out using Merck Silica gel 60 F254 aluminum sheets. Compounds were detected as single spots on TLC plates and visualized using UV light (254 or 366 nm) and ninhydrin. Merck silica gel (35–70 mesh) was used for flash chromatography. ^{1}H NMR spectra were recorded on a 400 MHz Bruker NMR spectrometer using the residual proton resonance of the solvent as the standard. Chemical shifts are reported in parts per million (ppm). When peak multiplicities are given, the following abbreviations are used: s, singlet; bs, broad singlet; d, doublet; t,

triplet; q, quartet; m, multiplet. Mass spectra were measured on a Waters ZQ device for LRMS.

2.5.2 Synthesis of PAL for sigma receptors

Synthesis of N-(3-chloropropyl)-4-nitrobenzamide (1)

P-nitrobenzoic acid (2.0 g, 12 mmol), EDC (2.3 g, 12 mmol), and HOBt (1.8 g, 12 mmol) were dissolved in dry CH_2Cl_2 (15 mL) under argon and stirred for 10 minutes. 3-chloropropyl amine HCl (1.2 g, 9.2 mmol) and DIPEA (2.4 mL, 14 mmol) were dissolved in dry CH_2Cl_2 (5 mL) and added dropwise to the reaction mixture. After stirring the reaction overnight the solvent was removed and the residue was dissolved in EtOAc (50 mL). The organic layer was washed with 0.5 HCl (50 mL), saturated aq. $NaHCO_3$ (2x25 mL), brine (25 mL), and dried with $MgSO_4$. The organic layer was removed by rotary evaporation and column chromatography was performed with 2:1 EtOAc:Hexanes as the mobile phase to yield 1.96 grams (90% yield) of an off white solid.

^{1}H NMR (400 MHz, $CDCl_3$) δ ppm 8.32 (d, *J* = 9.09 Hz, 2 H) 7.96 (d, *J* = 8.84 Hz, 2 H) 6.51 (br s, 6 H) 3.69 (dt, *J* = 6.06, 3.03 Hz, 4 H) 2.13 - 2.22 (m, 2 H) 2.06 (s, 1 H)

Synthesis of tert-butyl 4-(3-(4-nitrobenzamido)propyl)piperazine-1-carboxylate (2)

To a stirring solution of **1** dissolved in DMF (10 mL) was added K_2CO_3 (0.870 g, 6.27 mmol), KI (0.170 g, 1.05 mmol), and Boc-piperazine (0.580 g, 3.14 mmol). The reaction mixture was heated to 80˚C and stirred under argon for 18 hours. After cooling to room temperature the mixture was poured into H_2O (20 mL) and was extracted with EtOAc (3 x 25 mL). The combined organic layers were washed with brine (25 mL) and dried with $MgSO_4$. The organic layer was removed using rotary evaporation and column

chromatography was performed using 4:1 CH_2Cl_2:MeOH as the mobile phase to obtain 0.492 grams (60% yield) of a white solid.

^{1}H NMR (400 MHz, $CDCl_3$) δ ppm 8.30 - 8.33 (m, 2 H) 7.99 (d, *J* = 8.34 Hz, 2 H) 3.63 (q, *J* = 5.81 Hz, 2 H) 3.47 (br s, 4 H) 2.43 - 2.72 (m, 5 H) 1.89 (br. s., 2 H) 1.48 (s, 9 H)

Synthesis of 4-nitro-N-(3-(piperazin-1-yl)propyl)benzamide (3)

Boc-Piperzine **2** (0.170 g, 0.433 mmol) was dissolved in 3 M anhydrous HCl (2 mL) and stirred for 1.5 hours at room temperature. The solvent was removed via rotary evaporation to yield 0.131 grams (92% yield) of a white solid. The compound was used without further purification.

^{1}H NMR (400 MHz, CD_3OD) δ ppm 8.29 - 8.37 (m, 2 H) 8.02 - 8.10 (m, 2 H) 3.47 - 3.70 (m, 10 H) 2.06 - 2.18 (m, 2 H) 1.53 - 1.61 (m, 2 H)

Synthesis of 4-nitro-N-(3-(4-(prop-2-yn-1-yl)piperazin-1-yl)propyl)benzamide (4)

Piperazine **3** (0.500 g, 1.52 mmol) and DIPEA (784 μL, 4.56 mmol) was dissolved in dry CH_2Cl_2 (4 mL) under argon at 0˚C. Propargyl bromide (143 μL, 1.52 mmol) dissolved in CH_2Cl_2 (1 mL) was then added dropwise. The solution was allowed to warm to room temperature and stir for 16 hours. The solvent was removed in vacuo and the residue was dissolved in EtOAc (40 mL). The organic layer was washed with $NaHCO_3$ (2 x 20 mL), brine (20 mL), and dried with $MgSO_4$. The solvent was removed via rotary evaporation to and column chromatography was performed using 4:1 CH_2Cl_2:MeOH as the mobile phase to give 0.188 grams (38%) of a yellow oil.

^{1}H NMR (400 MHz, CD_3OD) δ ppm 8.30 - 8.38 (m, 2 H) 8.00 - 8.07 (m, 2 H) 3.47 (t, *J* = 6.95 Hz, 2 H) 2.60 - 2.72 (m, 3 H) 2.46 - 2.57 (m, 2 H) 1.79 - 1.90 (m, 2 H)

Synthesis of 4-amino-N-(3-(4-(prop-2-yn-1-yl)piperazin-1-yl)propyl)benzamide (5)

Alkyne **4** (0.230 g, 0.670 mmol) dissolved in EtOH (5 mL) was treated with $SnCl_2$ (0.470 g, 2.10 mmol) and heated to reflux for 16 hours. The mixture was allowed to cool to room temperature, poured onto ice, and was made basic with the addition of 1 N $NaHCO_3$. The solution was carefully filtered through celite and the filter cake was washed several times with CH_2Cl_2. The layers were separated and the aqueous layer was extracted with CH_2Cl_2 (3x15 mL). The organic layers were combined, washed with brine (25 mL), dried with $MgSO_4$, and the solvent was removed via rotary evaporation to yield 73 mg (35%) of a yellow oil. The product was used without further purification.

^{1}H NMR (400 MHz, CD_3OD) δ ppm 7.60 (d, *J* = 8.59 Hz, 2 H) 6.68 (d, *J* = 8.59 Hz, 2 H) 3.40 (t, *J* = 6.82 Hz, 14 H) 2.61 - 2.76 (m, 4 H) 2.46 - 2.54 (m, 2 H) 1.77 - 1.86 (m, 2 H)

Synthesis of Probe 1

To a 0˚C solution of **5** (69 mg, 0.23 mmol) dissolved in 2 N HCl (5 mL) was added slowly a solution of $NaNO_2$ (16 mg, 0.24 mmol) in water (300 μL). After stirring for 15 minutes, the reaction vessel was covered with aluminum foil and a solution of NaN_3 (15 mg, 0.24 mmol) in water (600 μL) was added dropwise and the reaction was allowed to warm to room temperature and stirred for 4 hours. The mixture was poured slowly into H_2O (10 mL), basified with 1 N NaOH, and extracted with EtOAc (3x20 mL). The combined organic layers were washed with brine, dried with $MgSO_4$, and the solvent was removed via rotary evaporation. Column chromatography was performed using 4:1 CH_2Cl_2: MeOH as the mobile phase to obtain 60 mg (81% yield) of a yellow product.

^{1}H NMR (400 MHz, CD_3OD) δ ppm 7.87 (d, *J* = 8.84 Hz, 2 H) 7.17 (d, *J* = 8.84 Hz, 2 H) 3.43 (t, *J* = 6.95 Hz, 2 H) 2.60 - 2.74 (m, 4 H) 2.46 - 2.53 (m, 2 H) 1.79 - 1.88 (m, 2 H)

LCMS (ESI-TOF) Calc for $C_{17}H_{22}N_6O$ [M+1]; 327.40, Found: 327.41

Synthesis of N-(3-(4-cyclohexylpiperazin-1-yl)propyl)-4-nitrobenzamide (6)

To a stirring solution of **1** (0.710 g, 2.97 mmol) dissolved in dry CH_3CN (20 mL) was added K_2CO_3 (0.820 g, 5.94 mmol), KI (50.0 mg, 0.297 mmol), and cyclohexylpiperzine (1.00 g, 5.94 mmol). The reaction mixture was heated to reflux and stirred under argon for 18 hours. After cooling to room temperature the mixture was evaporated to dryness and water (20 mL) was added to the residue. The aqueous phase was extracted with EtoAc (3 x 25 mL) and the combined organic layers were washed with brine (25 mL) and dried with $MgSO_4$. The organic layer was removed using rotary evaporation and. column chromatography was performed using 4:1 CH_2Cl_2:MeOH as the mobile phase to yield 0.616 grams (56% yield) of a white solid.

^{1}H NMR (400 MHz, $CDCl_3$) δ ppm 8.27 - 8.32 (m, 2 H) 8.02 (d, *J* = 8.59 Hz, 2 H) 3.62 (d, *J* = 5.31 Hz, 2 H) 3.51 (s, 1 H) 2.47 - 2.69 (m, 7 H) 2.22 - 2.33 (m, 1 H) 1.77 - 1.89 (m, 6 H) 1.67 (d, *J* = 12.63 Hz, 1 H) 1.06 - 1.34 (m, 6 H)

Synthesis of 4-amino-N-(3-(4-cyclohexylpiperazin-1-yl)propyl)benzamide (7)

Nitro compound **6** (0.470 g, 1.26 mmol) dissolved in EtOH (15 mL) was treated with $SnCl_2$ (0.833 g, 3.69 mmol) and stirred at reflux for 16 hours. The mixture was allowed to cool to room temperature, poured onto ice, and was made basic with the addition of 1 N $NaHCO_3$. The solution was carefully filtered through celite and the filter cake was washed several times with CH_2Cl_2. The layers were separated and the aqueous layer was extracted with CH_2Cl_2 (3x15 mL). The organic layers were combined, washed with brine (25 mL), dried with $MgSO_4$, and the solvent was removed via rotary

evaporation to obtain 0.367 grams (84% yield) of product. The product was used in the next step without further purification.

^{1}H NMR (400 MHz, CD_3OD) δ ppm 7.60 (d, *J* = 8.59 Hz, 2 H) 6.64 - 6.71 (d, 2 H) 5.51 (s, 1 H) 3.40 (s, 2 H) 2.45 - 2.82 (m, 8 H) 2.33 (d, *J* = 3.03 Hz, 1 H) 1.96 (d, *J* = 10.61 Hz, 2 H) 1.77 - 1.89 (m, 4 H) 1.67 (d, *J* = 12.63 Hz, 1 H) 1.09 - 1.37 (m, 6 H)

Synthesis of 4-azido-N-(3-(4-cyclohexylpiperazin-1-yl)propyl)benzamide (8)

To a 0˚C solution of aniline **7** (0.290 g, 0.842 mmol) dissolved in 2 N HCl (5 mL) was added slowly a solution of $NaNO_2$ (60.0 mg, 0.859 mmol) in water (300 μL). After stirring for 15 minutes, the reaction vessel was covered with aluminum foil and a solution of NaN_3 (56.0 mg, 0.859 mmol) in water (600 μL) was added dropwise and the reaction was allowed to warm to room temperature and stirred for 2 hours. The mixture was poured slowly into water (10 mL), basified with 1 N NaOH, and extracted with EtOAc (3x20 mL). The combined organic layers were washed with brine, dried with $MgSO_4$, and the solvent was removed via rotary evaporation to obtain 0.357 grams (84% yield) of a off white solid. The product was used without further purification.

^{1}H NMR (400 MHz, CD_3OD) δ ppm 7.86 (d, *J* = 8.59 Hz, 2 H) 7.16 (d, *J* = 8.59 Hz, 2 H) 3.44 (t, *J* = 6.82 Hz, 2 H) 2.43 - 2.75 (m, 8 H) 2.28 (d, *J* = 3.28 Hz, 1 H) 1.94 (d, *J* = 11.12 Hz, 2 H) 1.79 - 1.88 (m, 4 H) 1.67 (d, *J* = 12.63 Hz, 1 H) 1.05 - 1.37 (m, 6 H)

Synthesis of probe 2

Azido compound **8** (0.130 g, 0.350 mmol) and potassium tert-butoxide (60.0 mg, 0.525 mmol) was dissolved in dry DMF (3 mL) under argon at 0˚C. Propargyl bromide (32.0 μL, 0.420 mmol) dissolved in DMF (0.5 mL) was then added dropwise and the solution was allowed to warm to room temperature and stir overnight. The mixture was

poured into water (30 mL) and extracted with EtOAc (3x25 mL). The combined organic fractions were washed with brine (25 mL), dried with $MgSO_4$, and the solvent was removed via rotary evaporation. Column chromatography was performed using 4:1 CH_2Cl_2:MeOH as the mobile phase to yield 86 mg (61% yield) of a yellow oil.

^{1}H NMR (400 MHz, $CDCl_3$) δ ppm 7.52 (br s, 2 H) 7.05 - 7.12 (m, 2 H) 5.32 (s, 1 H) 1.83 (br s, 4 H) 1.08 - 1.33 (m, 6 H)

LCMS (ESI-TOF) Calc for $C_{23}H_{32}N_6O$ [M+1]; 409.54, Found: 409.55

2.6 References

(1) Martin, W. R.; Eades, C. G.; Thompson, J. A.; Huppler, R. E.; Gilbert, P. E. *J. Pharmacol. Exp. Ther.* **1976**, *197* , 517.

(2) Walker, J. M.; Bowen, W. D.; Walker, F. O.; Matsumoto, R. R.; De Costa, B.; Rice, K. C. *Pharmacol. Rev.* **1990**, *42* , 355.

(3) Su, T.-P.; Hayashi, T.; Maurice, T.; Buch, S.; Ruoho, A. E. *Trends in pharmacological sciences*, 2010, *31*, 557–566.

(4) Jansen, K. L. R.; Faull, R. L. M.; Storey, P.; Leslie, R. A. *Brain Res.* **1993**, *623*, 299.

(5) Mishina, M.; Ishiwata, K.; Ishii, K.; Kitamura, S.; Kimura, Y.; Kawamura, K.; Oda, K.; Sasaki, T.; Sakayori, O.; Hamamoto, M.; Kobayashi, S.; Katayama, Y. *Acta Neurol. Scand.* **2005**, *112*, 103.

(6) Mishina, M.; Ohyama, M.; Ishii, K.; Kitamura, S.; Kimura, Y.; Oda, K.; Kawamura, K.; Sasaki, T.; Kobayashi, S.; Katayama, Y.; Ishiwata, K. *Ann. Nucl. Med.* **2008**, *22*, 151.

(7) Al-Saif, A.; Al-Mohanna, F.; Bohlega, S. *Ann. Neurol.* **2011**, *70*, 913.

(8) Vilner, B. J.; John, C. S.; Bowen, W. D. *Cancer Res.* **1995**, *55* , 408.

(9) Mach, R. H.; Smith, C. R.; Al-Nabulsi, I.; Whirrett, B. R.; Childers, S. R.; Wheeler, K. T. *Cancer Res.* **1997**, *57* , 156.

(10) Wheeler, K. T.; Wang, L.-M.; Wallen, C. A.; Childers, S. R.; Cline, J. M.; Keng, P. C.; Mach, R. H. *Br J Cancer* **2000**, *82*, 1223.

(11) John, C. S.; Gulden, M. E.; Li, J.; Bowen, W. D.; McAfee, J. G.; Thakur, M. L. *Nucl. Med. Biol.* **2015**, *25*, 189.

(12) Mach, R. H.; Huang, Y.; Buchheimer, N.; Kuhner, R.; Wu, L.; Morton, T. E.; Wang, L.-M.; Ehrenkaufer, R. L.; Wallen, C. A.; Wheeler, K. T. *Nucl. Med. Biol.* **2015**, *28*, 451.

(13) Kawamura, K.; Elsinga, P. H.; Kobayashi, T.; Ishii, S.; Wang, W.-F.; Matsuno, K.; Vaalburg, W.; Ishiwata, K. *Nucl. Med. Biol.* **2015**, *30*, 273.

(14) Glennon, R. a.; Ablordeppey, S. Y.; Ismaiel, A. M.; El-Ashmawy, M. B.; Fischer, J. B.; Howie, K. B. *J. Med. Chem.* **1994**, *37*, 1214.

(15) Laggner, C.; Schieferer, C.; Fiechtner, B.; Poles, G.; Hoffmann, R. D.; Glossmann, H.; Langer, T.; Moebius, F. F. *J. Med. Chem.* **2005**, *48*, 4754.

(16) Glennon, R. A. *Mini Reviews in Medicinal Chemistry*, 2005, *5*, 927–940.

(17) Ablordeppey, S. Y.; Fischer, J. B.; Law, H.; Glennon, R. A. *Bioorg. Med. Chem.* **2002**, *10*, 2759.

(18) Jasper, A.; Schepmann, D.; Lehmkuhl, K.; Vela, J. M.; Buschmann, H.; Holenz, J.; Wünsch, B. *Eur. J. Med. Chem.* **2009**, *44*, 4306.

(19) Maurice, T.; Urani, A.; Phan, V.-L.; Romieu, P. *Brain Res. Rev.* **2001**, *37*, 116.

(20) Monnet, F. P.; Debonnel, G.; de Montigny, C. *J. Pharmacol. Exp. Ther.* **1992**, *261* , 123.

(21) Berardi, F.; Abate, C.; Ferorelli, S.; Colabufo, N. A.; Perrone, R. *Central nervous system agents in medicinal chemistry*, 2009, *9*, 205–219.

(22) Jones, T. R.; Smithers, M. J.; Betteridge, R. F.; Taylor, M. A.; Jackman, A. L.; Calvert, A. H.; Davies, L. C.; Harrap, K. R. *J. Med. Chem.* **1986**, *29*, 1114.

(23) Katoono, R.; Kawai, H.; Fujiwara, K.; Suzuki, T. *Tetrahedron Lett.* **2004**, *45*, 8455.

CHAPTER 3

SILENT, FLUORESCENT LABELING OF THE DOPAMINE AND SEROTOIN TRANSPORTERS WITH MULTIFUNCTIONAL PROBES

3.1 Introduction

As discussed previously in chapter 1, our lab has developed a small, minimally perturbing and multifunctional probe that has allowed us to label endogenous neuronal receptors. Nanoprobe 1, bearing a use dependant spermine ligand, was specifically design to label and track calcium permeable AMPA receptors. To expand the use of our nanoprobe technology, we can exploit the modular design of the probe to substitute portions of the probe to allow it to function differently. In this work, we were particularly interested in replacing the spermine ligand for other pharmacophores to target other receptors of interest. Two important molecular targets that can be studied using this method are the presynaptic dopamine and serotonin transporters.

The dopamine transporter (DAT) regulates levels of dopamine at the synapse and is a target for widely abused psychostimulants such as cocaine and amphetamines. DAT belongs to the SLC6 Na^+/Cl^- dependent transporter family, which includes the serotonin transporter (SERT) and norepinephrine transporter[1]. Dopamine is an important neurotransmitter that modulates several processes including attention, arousal, cognition, reward, and motor activity[2]. However, disruption of normal dopamine signaling has been related to several neurodegenerative diseases including Parkinson's disease[3], schizophrenia[4], bipolar disorder[5], and attention deficit hyperactivity disorder[6]. DAT is particularly challenging to study due to the lack of an efficient antibody[2] and the difficulty to obtain neuronal cultures containing a high amount of dopaminergic neurons[7].

The SERT is an integral membrane protein expressed in neurons of the raphe nuclei in the brain. Similar to the function of the DAT, SERT is responsible for rapid clearance of the neurotransmitter serotonin from the synaptic cleft, thereby terminating the chemical signal transduction in serotonergic neurons[8]. As a result, SERT plays a critical role in centrally mediated functions associated with serotonin such as sleep, mood, and appetite[9]. This transporter is also the primary target for selective serotonin reuptake inhibitors and tricyclic antidepressants, which are prescribed for the treatment of depressive disorders and anxiety[10]. These drugs are designed to bind to the SERT and prevent reuptake of serotonin at the synapse back into the cell. However, despite proven clinical success, the mechanisms underlying why these drugs are effective remains elusive.

Previous work in the Newman lab was toward the development of two fluorescently tethered ligands for the DAT and SERT[11,12,13]. One high affinity fluorescent probe developed by Cha et al (JHC-1-64) utilized a tropane analogue of cocaine to enable visualization of the DAT in live cells (Figure 3.1)[12]. This new probe contained a rhodamine fluorophore that had both higher photostability and quantum yield than previously reported probes[14]. In addition, JHC 1-64 applied to neuronal culture revealed a uniform distribution of the DAT labeling of somas, extensions, and varicosities[11]. The Newman group also designed a fluorescent tool based off the antidepressant drug Citalopram, which can give insight into the mechanisms underlying depression (Figure 3.1)[13]. Fluorescent compound 8 was used to demonstrate the specific labeling of SERT in a HEK293 cell line expressing hSERT with EGFP fused to the N-terminus. This effect was also blocked in the presence of a SERT inhibitor, paroxetine[13].

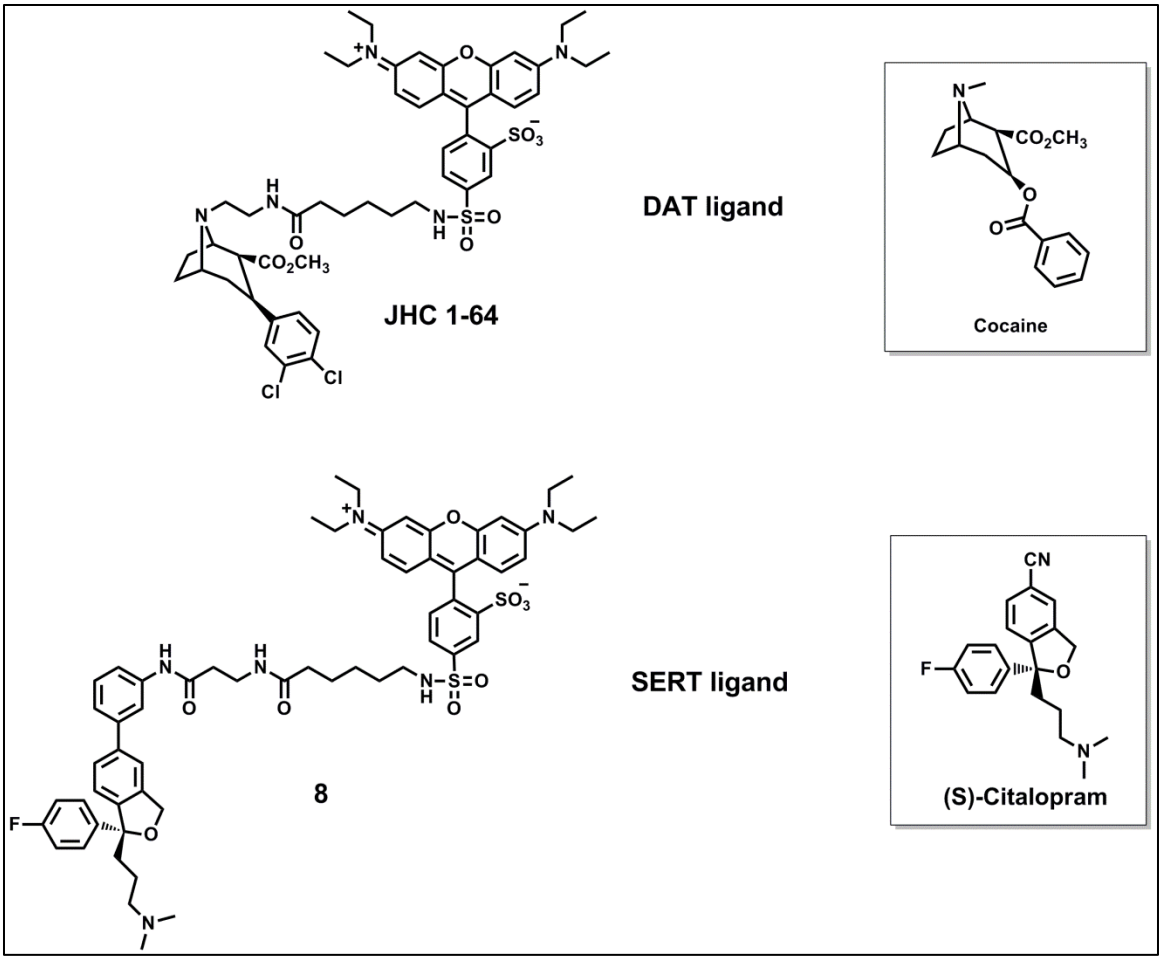

Figure 3.1. Fluorescently tethered probes developed in the Newman lab for the DAT[11] and SERT[13]

Although both ligands have proven to be useful fluorescent tools for labeling DAT and SERT, their effectiveness is somewhat limited as they must occupy the binding site for visualization of the receptors. As discussed previously in chapter 1, occupation of a binding site by an agonist or antagonist can cause conformational changes or differential trafficking patterns. In the case for the DAT, it has been determined that not all dopamine uptake blockers are cocaine-like and could possibly prove as effective medications without addictive liability. Understanding the mechanisms of the differences between cocaine and non-cocaine like ligands at the DAT may enable the development of

medications that are effective for the treatment of cocaine and methamphetamine addiction, as well as other neuropsychiatric disorders[15]. Since the fluorescent compound JHC 1-64 blocks the binding site, it would prevent other drugs such as cocaine or methamphetamine from binding. Hence, although constitutive activity of the DAT could be visualized, the effects of these drugs on the trafficking of DAT cannot.

3.1.1 Probe design

In collaboration with the Newman and Gether labs, we designed new fluorescent probes for the DAT and SERT utilizing our nanoprobe technology. In this work, we have redesigned nanoprobe 1 to label DAT and SERT by replacing the use dependant spermine ligand with a tropane analogue of cocaine and the antidepressant drug citalopram, respectively (Figure 3.2). Based on the previous binding data and imaging studies conducted by the Newman lab, we believe these new ligands will give specificity for these receptors and therefore allow for visualization on live cells. We have also replaced the Cy3 chromophore from nanoprobe 1 with a sulfonylrhodamine dye to display the modular nature of our nanoprobe technology. The synthesis of these probes should allow for silent labeling of endogenous DAT and SERT and expand the toolbox available for chemical biologists.

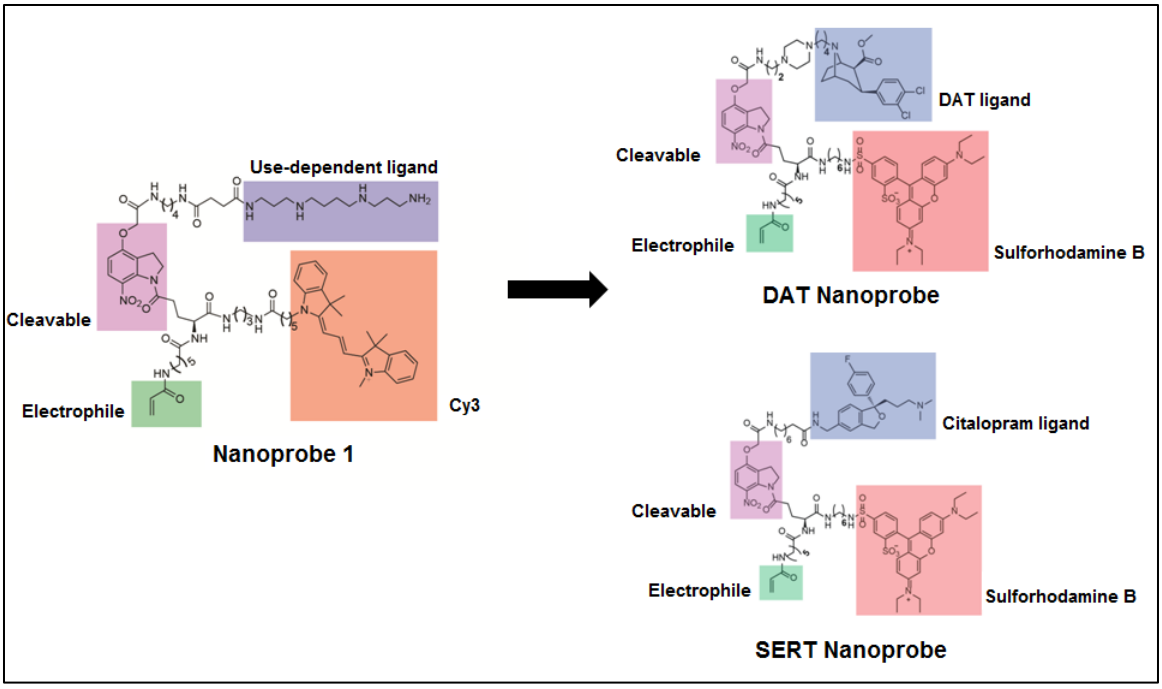

Figure 3.2. Conversion of nanoprobe 1 to DAT and SERT nanoprobes.

3.2 Experimental Methods

3.2.1 Probe synthesis

Borrowing from synthetic precedent[16], the probe was synthetically elaborated commencing with the nitroindoline core to provide two orthogonal protecting groups for further chemical modification. The tert-butyl ester of the nitroindoline core **1** was selectively deprotected under acidic conditions to yield carboxylic acid **2**. Carboxylic acid **2** was functionalized with rhodamine-cadaverine under standard peptide coupling conditions to form the fluorescent intermediate **3**. Rhodamine intermediate **3** then underwent basic hydrolysis to deprotect the methyl ester moiety to produce carboxylic acid **4**. Carboxylic acid **4** was treated with either dopamine ligand (MFZ-15-94) or serotonin ligand (VK03-45) under peptide coupling conditions to complete the synthesis

of the dopamine (SM-V-61) and serotonin (SM-V-37) nanoprobes in 30% yield for each probe (Scheme 3.1).

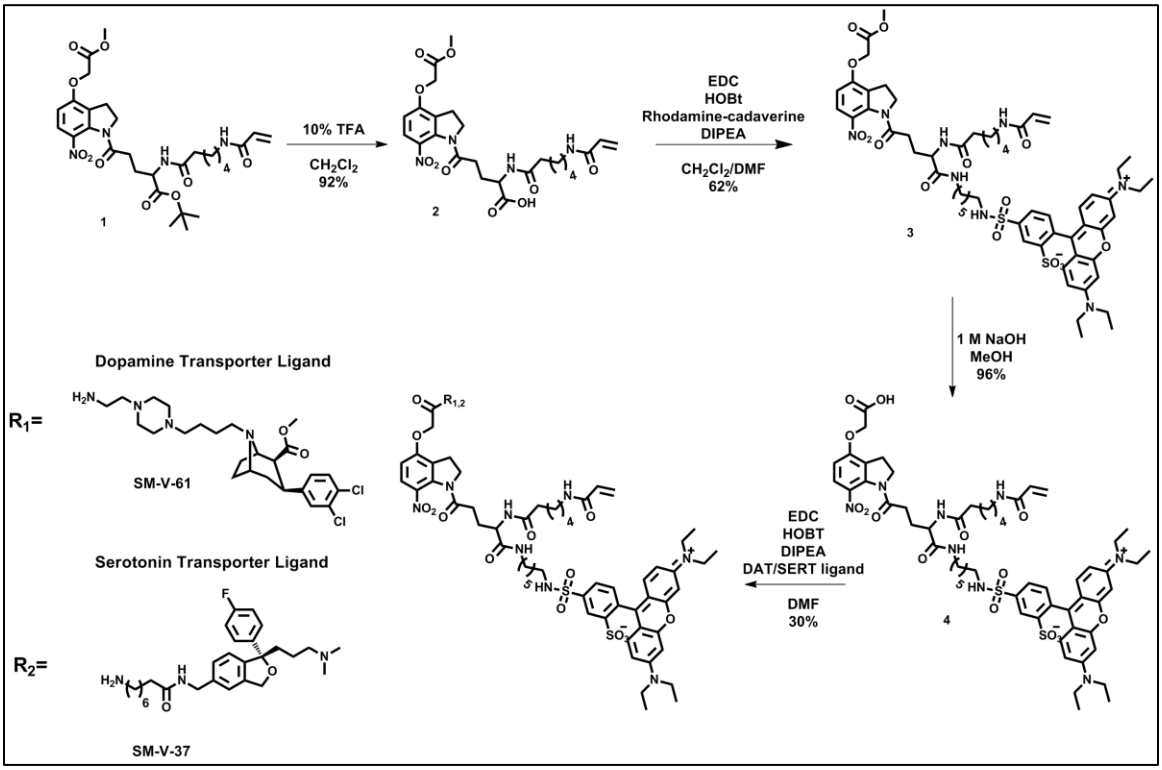

Scheme 3.1. Synthesis of DAT and SERT Nanoprobes from indoline 1.

3.3 Results and Discussion

The synthesis of both the DAT and SERT nanoprobes was based on previously prepared nanoprobe 1. The tert-butyl ester of indoline **1** could selectively be deprotected under mild acidic conditions with trifluoroacetic acid (TFA). The peptide coupling of the rhodamine fluorophore to carboxylic acid **2** proved to be challenging. Under standard peptide coupling conditions with EDC and HOBt, the reaction was found to take upwards of 3 days to produce a majority of the fluorescent intermediate **3**. This could be due to unfavorable steric interactions between carboxylic acid **2** and the rhodamine ligand, despite the fact that a 6 carbon linker was utilized. In the future, it might be interesting to observe the effect of linker length on the reactivity between carboxylic acid **2** and a

rhodamine ligand. To circumvent this issue, higher equivalents of EDC and HOBt were utilized to promote the production of intermediate **3**. This not only improved the yield of the reaction, but also lowered the reaction time to 18 hours. Completion of both nanoprobes was done through the peptide coupling of carboxylic acid **4** with dopamine or serotonin ligands supplied by the Newman lab. Carboxylic acid **4** proved to be more reactive than carboxylic acid **2**, likely due to less steric crowding at that position.

Upon completion of the DAT (SM-V-61) and SERT (SM-V-37) nanoprobes, they were sent to the Gether lab in Copenhagen for experiments to collect binding data and visualization of both receptors. We were interested in determining the binding affinity to ensure that the steric bulk from the nanoprobe structure did not completely disrupt the binding of either the dopamine or serotonin ligand utilized. As shown in table 3.1 and 3.2, both SM-V-61 and SM-V-37 displayed lower binding affinities towards their respective targets when compared to the previously synthesized fluorescent ligands from the Newman lab. However, to our delight, both nanoprobes were found to retain affinity for the DAT and SERT (244 nM and 202 nM, respectively), which should allow for visualization of these receptors on live cells.

Table 3.1. Binding affinity for SM-V-61 for the DAT. Uptake values were determined from uptake inhibition experiments in transfected COS-7 cells utilizing [^{3}H]dopamine. Binding affinity was determined from competition binding experiments on intact COS-7 cells using [^{3}H] CFT (2β-carbomethoxy-3β-94-fluorophenyl)tropane) as the radioligand.

	Uptake (K_i nM) **DAT**	**Binding (K_i nM)** **DAT**
SM-V-61	529	244
JHC 1-64	72	44

Table 3.2. Binding affinity for SM-V-37 for the SERT. Uptake values were determined from uptake inhibition experiments in transfected COS-7 cells utilizing [^{3}H]5-HT. Binding affinity was determined from competition binding experiments on intact COS-7 cells using [^{3}H] S-citalopram as the radioligand.

	Uptake (K_i nM) **DAT**	**Binding (K_i nM)** **DAT**
SM-V-37	603	202
Compound 8	225	N/A

To demonstrate specific labeling of DAT with SM-V-61, we utilized a HEK293 cell line stably expressing hDAT with EGFP fused to the N-terminus. Cells were incubated with 20 nM of SM-V-61 for 20 minutes at 37˚C with or without the specific DAT inhibitor nomifensine. As shown in Figure 3.3, live cell imaging using confocal microscopy revealed a uniform distribution of SM-V-61 (red) at the cell surface only where EGFP-DAT (green) was seen. The labeling of DAT by SM-V-61 is completely blocked in the presence of nomifensine as there is no fluorescence observed at the cell surface in the red channel. In addition, the transmission image shows that there are some cells that have not been transfected with the EGFP-DAT and SM-V-61 does not seem to label these cells. This evidence suggests that SM-V-61 is specific towards the EGFP-DAT and is not just labeling the cell surface. Another representation of EGFP-DAT labeling by SM-V-61 is shown in Figure 3.4. These images show complete labeling of the cell surface as displayed by the yellow color in the overlay box.

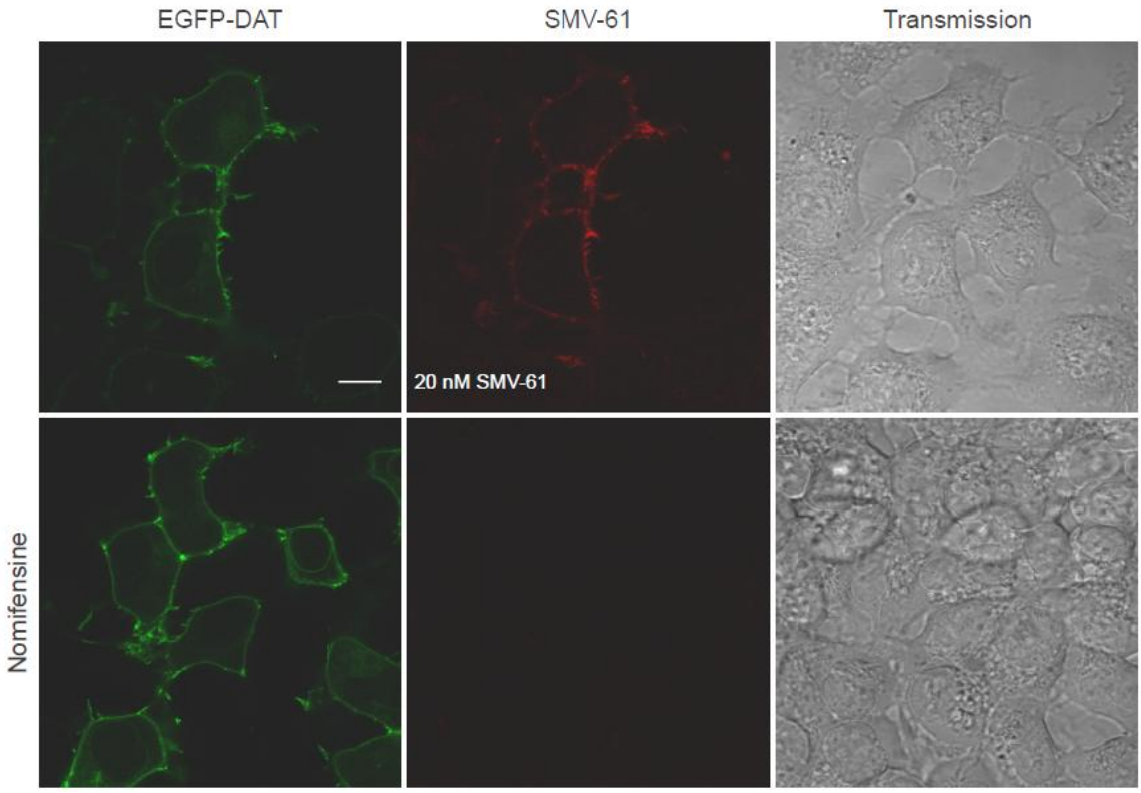

Figure 3.3. Visualizing SM-V-61 binding to hDAT in transfected HEK293 cells.

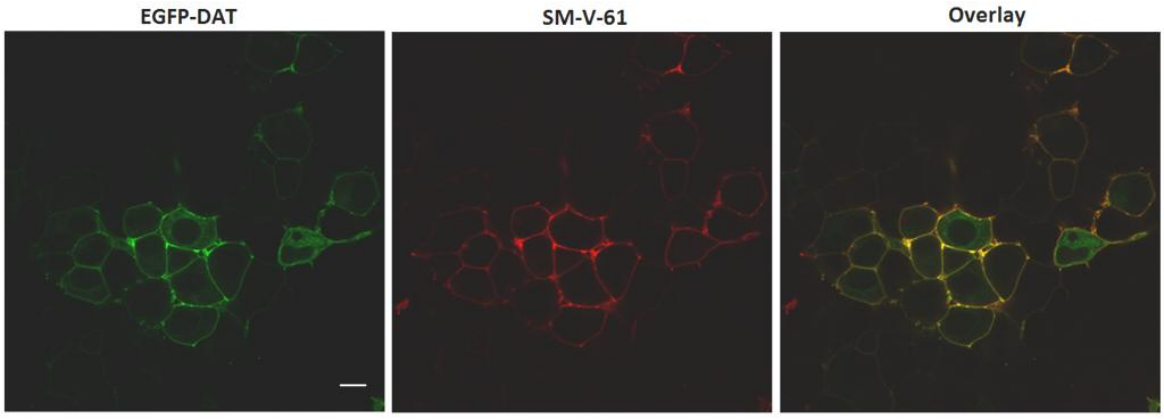

Figure 3.4. Overlay image of EFGP-DAT labeling by SM-V-61 in HEK293 cells.

To demonstrate specific labeling of SERT with SM-V-37, similar conditions were followed as previously discussed. A HEK293 cell line stably expressing EGFP-SERT was incubated with 20 nM of SM-V-37 for 20 minutes in the presence or absence of a SERT inhibitor, paroxetine. As seen previously, we observed red fluorescence from SM-

V-37 only in the areas of green fluorescence from EGFP-SERT. Receptor labeling is also completely blocked in the presence of paroxetine, showing no fluorescence in the red channel (Figure 3.5). These labeling results are also confirmed by the overlay image as seen in Figure 3.6, where the yellow color can be seen evenly distribution around the cell surface.

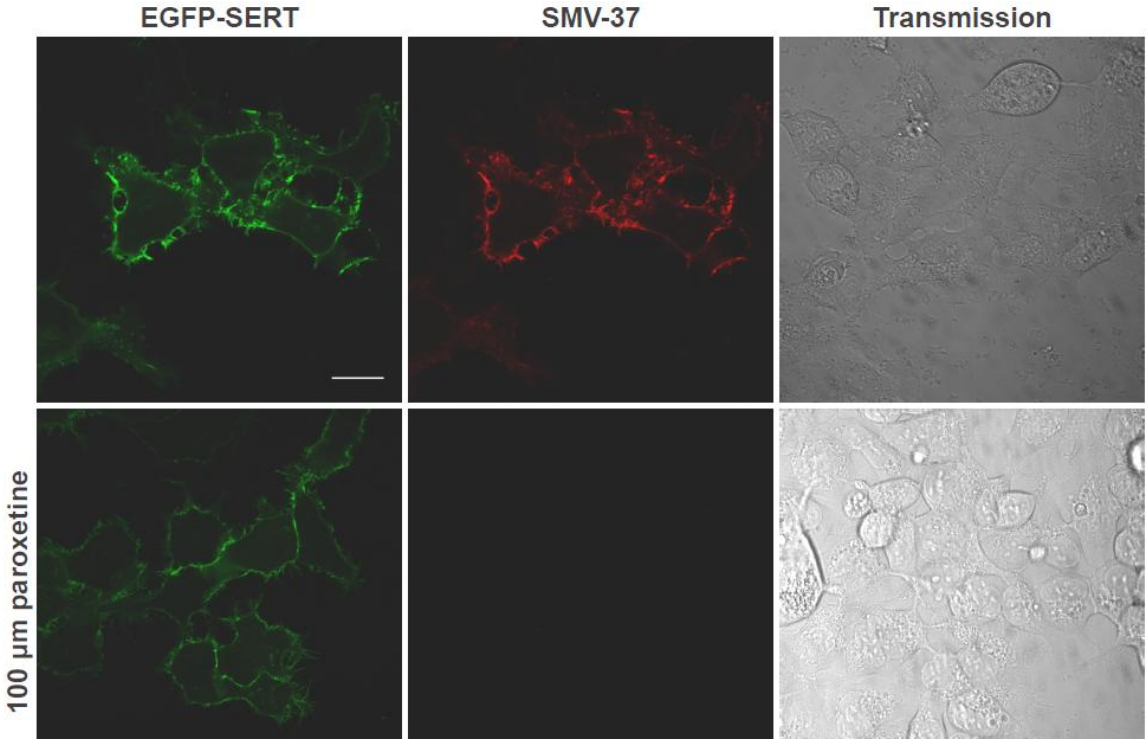

Figure 3.5. Visualizing SM-V-37 binding to hDAT in HEK293 cells.

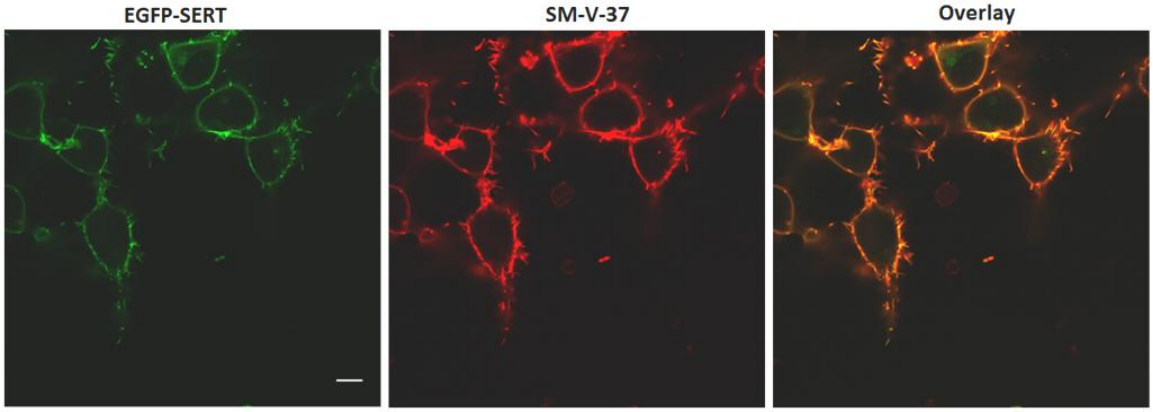

Figure 3.6. Overlay image of EFGP-SERT labeling by SM-V-37 in HEK293 cells.

The results of the fluorescent imaging of both nanoprobes suggest that they are specific towards their targeted receptor in transfected HEK cells. The labeling is due to the specificity of the DAT and SERT ligands employed based on the block of the red fluorescence in the presence of an inhibitor as well as a lack of labeling observed in non-transfected cells. Currently, work is being done in the Gether lab to optimize conditions for ligand displacement following uncaging of the nitroindoline core utilizing UV light. If fluorescence is still observed after uncaging, this would suggest the nanoprobe is covalently bond to the receptor of interest and the binding site should be unhindered. Future work will be to utilize either nanoprobe to label endogenous DAT or SERT in live neurons, enabling visualization of these receptors in their natural state.

3.4 Conclusion

The DAT and SERT nanoprobes synthesized in this work display the modular nature of our nanoprobe technology. The addition of either a DAT or SERT ligand to the nanoprobe scaffold maintained affinity towards either receptor (244 nm, 202 nm, respectively) and also allowed for visualization of these receptors in transfected HEK cells. Further studies conducted with cultured neurons will validate these probes as new tools available for neurobiologists to study both endogenous DAT and SERT.

3.5 Materials and Methods

3.5.1 General information

All reagents, biological and chemical, were purchased through Fisher Scientific (Fair Lawn, NJ, USA). All reactions involving air- and moisture-sensitive reagents were performed under an argon atmosphere using syringe-septum cap techniques. DMF and

CH_2Cl_2 were dried by storing over molecular sieves (4 Å). Analytical thin-layer chromatography (TLC) was carried out using Merck Silica gel 60 F254 aluminum sheets. Compounds were detected as single spots on TLC plates and visualized using UV light (254 or 366 nm) and $KMnO_4$ or ninhydrin. Merck silica gel (35–70 mesh) was used for flash chromatography. ^{1}H NMR spectra were recorded on a 400 MHz Bruker NMR spectrometer using the residual proton resonance of the solvent as the standard. Chemical shifts are reported in parts per million (ppm). When peak multiplicities are given, the following abbreviations are used: s, singlet; bs, broad singlet; d, doublet; t, triplet; q, quartet; m, multiplet. Mass spectra were measured on a Waters ZQ device for LRMS and at the UMass Mass Spectrometry facility for HRMS.

3.5.2 Synthesis of DAT and SERT Nanoprobes

Synthesis of 2-(6-acrylamidohexanamido)-5-(4-(2-methoxy-2-oxoethoxy)-7-nitroindolin-1-yl)-5-oxopentanoic acid (2)

Indoline **1** (0.200 g, 0.331 mmol) was dissolved in a 10% TFA/CH_2Cl_2 solution (2 mL) and stirred for 12 hours at room temperature. The solvent was removed via rotary evaporation to yield 0.202 grams (92% yield) of a yellow oil, was used in the next step without further purification.

^{1}H NMR same as previously reported[16]

Synthesis of 5-(N-(6-(2-(6-acrylamidohexanamido)-5-(4-(2-methoxy-2-oxoethoxy)-7-nitroindolin-1-yl)-5-oxopentanamido)hexyl)sulfamoyl)-2-(6-(diethylamino)-3-(diethyliminio)-3H-xanthen-9-yl)benzenesulfonate (3)

Carboxylic acid **2** (41 mg, 0.075 mmol), EDC (26 mg, 0.14 mmol), and HOBt (21 mg, 0.14 mmol) were dissolved in dry DMF (1 mL) under argon and stirred for 10

minutes. Rhodamine cadaverine (45 mg, 0.069 mmol) and DIPEA (24 μL, 0.14 mmol) were dissolved in dry DMF (1 mL) and added slowly to the reaction mixture over 2 minutes. After stirring the reaction for 16 hours the solvent was removed via rotary evaporation and column chromatography was performed utilizing 80:10:10 CH_2Cl_2:CH_3CN:MeOH as eluent to give 50 mg (62% yield) of a purple oil.

LCMS (ESI-TOF) Calc for $C_{58}H_{74}N_8O_{15}S_2$ [M+1]; 1187.38, Found: 1187.80

Synthesis of 5-(N-(6-(2-(6-acrylamidohexanamido)-5-(4-(carboxymethoxy)-7-nitroindolin-1-yl)-5-oxopentanamido)hexyl)sulfamoyl)-2-(6-(diethylamino)-3-(diethyliminio)-3H-xanthen-9-yl)benzenesulfonate (4)

Methyl ester **3** (40 mg, 0.034 mmol) was dissolved in MeOH (1 mL) and treated with 1 M NaOH (67 μL). The reaction mixture was stirred at room temperature for 4 hours then neutralized with 1 M citric acid (67 μL) and concentrated via rotary evaporation. The residue was diluted with water (2 mL), acidified to pH 2 with 1 M citric acid, and extracted with CH_2Cl_2 (3 x 4 mL). The organic layer was dried with $MgSO_4$, filtered, and the solvent removed via rotary evaporation to obtain 38 mg (96% yield) of a purple oil. The product was used without further purification.

LCMS (ESI-TOF) Calc for $C_{57}H_{72}N_8O_{15}S_2$ [M+1]; 1173.36, Found: 1173.20

Synthesis of Dopamine Nanoprobe (SM-V-61)

Carboxylic acid **4** (21 mg, 0.018 mmol), EDC (6.0 mg, 0.032 mmol), and HOBt (5.0 mg, 0.032 mmol) were dissolved in dry DMF (1 mL) under argon and stirred for 10 minutes. Dopamine ligand (MFZ15-94) (8.0 mg, 0.016 mmol) and DIPEA (11 μL, 0.063 mmol) were dissolved in dry DMF (1 mL) and added slowly to the reaction mixture. After stirring the reaction for 16 hours the solvent was removed via rotary evaporation

and the product was purified by preparative-HPLC to obtain 7.9 mg (30% yield) of a dark pink solid. (XBridge Prep C18 5µm (10 x 100 mm) column: H_2O and CH_3CN/0.1% formic acid as the mobile phase. Retention time=23.89 minutes)

^{1}H NMR (500 MHz, CD_3OD) δ ppm 8.54 (d, *J* = 1.68 Hz, 1 H) 8.45 (s, 8 H) 7.99 (dd, *J* = 7.93, 1.83 Hz, 1 H) 7.63 (d, *J* = 9.00 Hz, 1 H) 7.41 (d, *J* = 7.93 Hz, 1 H) 7.31 - 7.35 (m, 2 H) 7.09 (dd, *J* = 8.32, 1.91 Hz, 1 H) 6.98 - 7.03 (m, 2 H) 6.89 (d, *J* = 9.46 Hz, 2 H) 6.83 (d, *J* = 2.14 Hz, 2 H) 6.64 (d, *J* = 9.16 Hz, 1 H) 6.07 - 6.10 (m, 2 H) 5.51 (dd, *J* = 8.54, 3.51 Hz, 1 H) 4.59 (s, 2 H) 4.14 - 4.25 (m, 3 H) 3.56 (q, *J* = 7.12 Hz, 8 H) 3.31 (s, 3 H) 3.08 - 3.14 (m, 6 H) 2.91 (t, *J* = 6.87 Hz, 2 H) 2.60 (br. s., 1 H) 2.38 - 2.54 (m, 4 H) 2.25 - 2.32 (m, 2 H) 2.16 (t, *J* = 7.40 Hz, 3 H) 2.08 (d, *J* = 5.95 Hz, 1 H) 1.90 - 2.03 (m, 1 H) 1.79 - 1.88 (m, 2 H) 1.73 (d, *J* = 11.75 Hz, 1 H) 1.48 - 1.56 (m, 2 H) 1.31 - 1.45 (m, 11 H) 1.16 - 1.29 (m, 23 H)

LCMS (ESI-TOF) Calc for $C_{82}H_{109}Cl_2N_{12}O_{16}S_2$ $[M+1]^+$; 1653.85, Found: 1653.90

HRMS (ESI-TOF) Calc for $C_{82}H_{109}Cl_2N_{12}O_{16}S_2$ $[M+2]^+$; 827.349, Found: 827.348

Synthesis of Serotonin Nanoprobe (SM-V-37)

Carboxylic acid **4** (23 mg, 0.020 mmol), EDC (7.0 mg, 0.036 mmol), and HOBt (6.0 mg, 0.036 mmol) were dissolved in dry DMF (1 mL) under argon and stirred for 10 minutes. Serotonin ligand (VK03-45) (9.0 mg, 0.018 mmol) and DIPEA (12 µL, 0.069 mmol) were dissolved in dry DMF (1 mL) and added slowly to the reaction mixture. After stirring the reaction for 16 hours the solvent was removed via rotary evaporation and the product was purified by preparative-HPLC to obtain 8.3 mg (30% yield) of a dark pink solid. (XBridge Prep C18 5µm (10 x 100 mm) column: H_2O and CH_3CN/0.1% formic acid as the mobile phase. Retention time=25.73 minutes)

LCMS (ESI-TOF) Calc for $C_{85}H_{111}FN_{11}O_{16}S_2$ $[M+1]^+$; 1625.98, Found: 1625.8

HRMS (ESI-TOF) Calc for $C_{82}H_{109}Cl_2N_{12}O_{16}S_2$ $[M+1]^+$; 1625.7661, Found: 1625.7643

3.6. References

(1) Chen, R.; Furman, C. A.; Gnegy, M. E. *Future Neurol.* **2009**, *5*, 123.

(2) Kovtun, O.; Tomlinson, I. D.; Sakrikar, D. S.; Chang, J. C.; Blakely, R. D.; Rosenthal, S. J. *ACS Chem. Neurosci.* **2011**, *2*, 370.

(3) Sulzer, D. *Trends in Neurosciences*, 2007, *30*, 244–250.

(4) Mehler-Wex, C.; Riederer, P.; Gerlach, M. *Neurotox. Res.* **2006**, *10*, 167.

(5) Greenwood, T. A.; Alexander, M.; Keck, P. E.; McElroy, S.; Sadovnick, A. D.; Remick, R. A.; Kelsoe, J. R. *Am. J. Med. Genet.* **2001**, *105*, 145.

(6) Swanson, J. M.; Flodman, P.; Kennedy, J.; Spence, M. A.; Moyzis, R.; Schuck, S.; Murias, M.; Moriarity, J.; Barr, C.; Smith, M.; Posner, M. In *Neuroscience and Biobehavioral Reviews*; 2000; Vol. 24, pp. 21–25.

(7) Ingram, S. L.; Prasad, B. M.; Amara, S. G. *Nat. Neurosci.* **2002**, *5*, 971.

(8) Anderluh, A.; Klotzsch, E.; Reismann, A. W. a F.; Brameshuber, M.; Kudlacek, O.; Newman, A. H.; Sitte, H. H.; Schütz, G. J. *J. Biol. Chem.* **2014**, *289*, 4387.

(9) Kristensen, A. S.; Andersen, J.; Jørgensen, T. N.; Sørensen, L.; Eriksen, J.; Loland, C. J.; Strømgaard, K.; Gether, U. *Pharmacol. Rev.* **2011**, *63*, 585.

(10) Banala, A. K.; Zhang, P.; Plenge, P.; Cyriac, G.; Kopajtic, T.; Katz, J. L.; Loland, C. J.; Newman, A. H. *J. Med. Chem.* **2013**, *56*, 9709.

(11) Eriksen, J.; Rasmussen, S. G. F.; Rasmussen, T. N.; Vaegter, C. B.; Cha, J. H.; Zou, M.-F.; Newman, A. H.; Gether, U. *J. Neurosci.* **2009**, *29*, 6794.

(12) Cha, J. H.; Zou, M.-F.; Adkins, E. M.; Rasmussen, S. G. F.; Loland, C. J.; Schoenenberger, B.; Gether, U.; Newman, A. H. *J. Med. Chem.* **2005**, *48*, 7513.

(13) Zhang, P.; Jørgensen, T. N.; Loland, C. J.; Newman, A. H. *Bioorg. Med. Chem. Lett.* **2013**, *23*, 323.

(14) Rasmussen, S. G. F.; Carroll, F. I.; Maresch, M. J.; Jensen, A. D.; Tate, C. G.; Gether, U. *J. Biol. Chem.* **2001**, *276*, 4717.

(15) Newman, A. H.; Katz, J. L. *Design* **2009**, 95.

(16) Vytla, D.; Combs-Bachmann, R. E.; Hussey, A. M.; Hafez, I.; Chambers, J. J. *Org. Biomol. Chem.* **2011**, *9*, 7151.

CHAPTER 4

DEVELOPING A MODULAR KIT FOR TRACLESS LABELING OF ENDOGENOUS RECEPTORS

4.1 Introduction

The synthesis of the DAT and SERT nanoprobes discussed in Chapter 3 showed how the modular design of our nanoprobe technology could be utilized to target different receptors of interest. With an eye towards making this technique more general for other scientists who are interested in labeling endogenous receptors, we have designed and synthesized a new nanoprobe bearing an alkyne handle in place of a specific ligand. The alkyne moiety allows for ligand diversity at that point by utilizing a highly specific 1,3-dipolar cycloaddition reaction (click) with a ligand containing an azido linker. In addition, a free carboxylic acid in the molecule facilitates fluorophore diversity through reactions with commercially available amine terminated dyes (Figure 4.1). This modular and functional intermediate molecule allows for a vast library of compounds with different fluorescent profiles to be synthesized in a relatively short period of time. As a proof of concept, we functionalized a pharmacophore with an azido linker and then reacted it with the alkyne nanoprobe scaffold. Upon successful completion of the click reaction, the probe was then be used to fluorescently label a receptor of interest. One particular target of interest in our lab and in the field of neurobiology are the postsynaptic glutamatergic NMDA receptors.

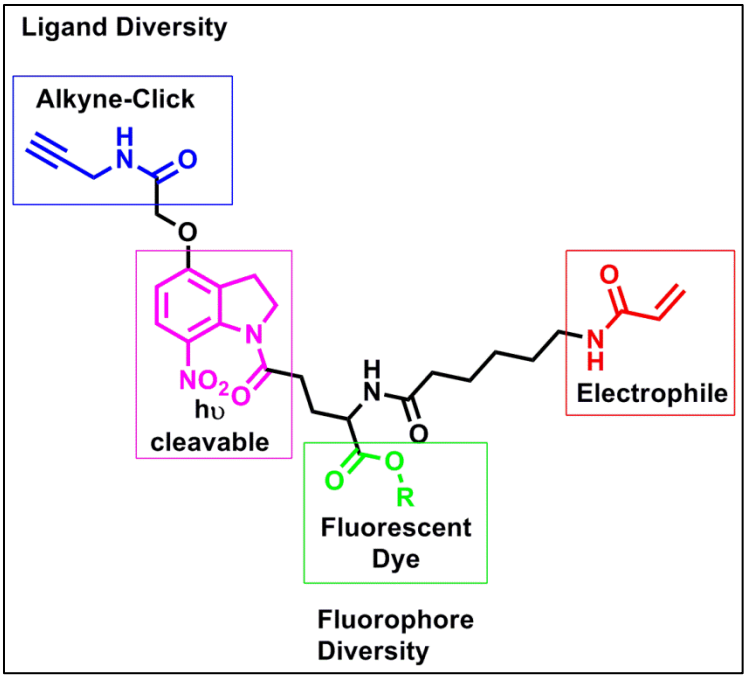

Figure 4.1. Structure of the alkyne based nanoprobe. This new probe will allow for ligand diversity through click reactions with a pharmacophore containing an azido-moiety.

The NMDA receptor is a subtype of glutamate receptor that is believed to be involved in processes of synaptic plasticity and memory formation[1]. In the hippocampus, NMDA receptors are tetrameric complexes composed of the NR1 subunit and a mixture of the two NR2 subunits, NR2A and NR2B, which are needed to form a functional ionotopic receptor[2]. Out of the three types of glutamate receptors, NMDA receptors are generally the most permeable to calcium ions. Thus, overactivation of these receptors result in excitotoxic neuronal cell death due to excess calcium influx[3]. It is known that several neurodegenerative diseases such as Alzheimer's disease, Parkinson's disease, ALS, as well as acute disorders including stroke and epilepsy, share a final common pathway to neuronal injury due to overstimulation of glutamate receptors[4]. Therefore, NMDA receptor pharmacophores have become a topic of interest for potential therapeutic use towards these disease states.

4.1.1 Probe design

The strategy that we employed for the synthesis of the alkyne based nanoprobe was slightly altered from the previously discussed nanoprobe scaffolds. Previously, the indoline scaffold was functionalized with a fluorophore first, then followed up two steps later with the peptide coupling of a specific pharmacophore. Here, we decided to attach our alkyne handle first, which would allow for modification with a fluorophore as the last step. This would allow for the alkyne nanoprobe to be reacted with a variety of fluorophores and produce an alkyne based probe with a multitude of colors and fluorescent profiles.

In collaboration with Dr. Doug Johnson at Pfizer Neuroscience (Cambridge, MA), we have devised a method to target NMDA receptors by utilizing a ketamine based ligand to react with our nanoprobe. Ketamine is a well-established anesthetic drug that has been in use for 50 years[5]. Ketamine acts as a non-competitive antagonist on NMDA receptors, where it binds at the phencyclidine (PCP) binding site[6]. The PCP binding site is localized within the receptor channel and partially overlaps with the magnesium binding site. Ketamine not only blocks the open channel and reduces the mean open time; it also decreases the frequency of channel opening by allosteric mechanisms[7]. Ketamine is often used as a racemic mixture, however, the S(+)-isomer has a 3-4 times higher affinity than the R-enantiomer[8]. To date, there have been limited structure-activity relationships for analogues of ketamine. Work by Jose et al. was aimed at the development of ketamine ester prodrugs for use as short-acting anestetics[9]. Several analogues of ketamine were synthesized by varying the length of the alkyl chain off the amine moiety and the type of ester employed (Figure 4.2a). Although the binding affinity

of each compound was not determined, their anesthetic effects were compared to ketamine in a rat infusion study. The short-chain aliphatic ester analogues broadly retained desirable anesthetic and analgesic activities, likely due to binding at the same site as the parent compound[9]. In all cases, the compounds conserved the secondary amine contained in ketamine, which is needed for a crucial interaction with asparagines in the NMDA receptor binding site[10,11,12]. Using this information we envisioned synthesizing a ketamine analogue containing an azido moiety through an extended alkyl chain (Figure 4.2b). This would conserve the basic secondary amine for binding and also extend the pharmacophore away from the alkyne nanoprobe to reduce unfavorable steric interactions between the receptor and probe.

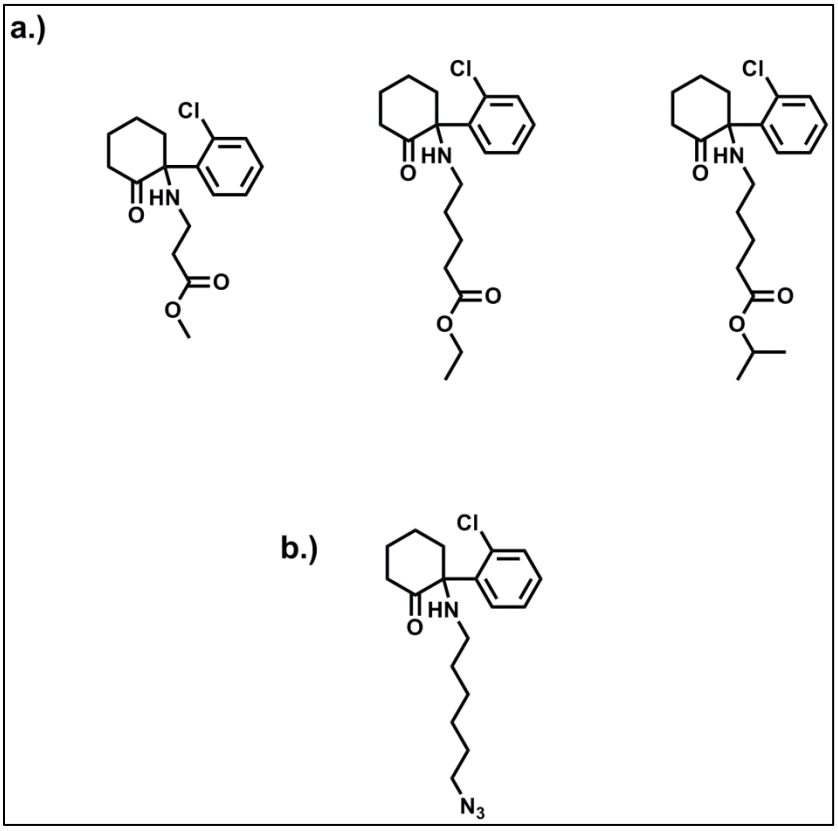

Figure 4.2. Structure of ketamine analogues. a.) Ester prodrugs of ketamine[9]. b.) Proposed azido analogue of ketamine

4.2 Methods

As discussed in the previous chapter, the nitroindoline core was synthesized following literature precedent[13]. The nitroindoline core **1** underwent base hydrolysis to deprotect the methyl ester providing carboxylic acid **2**. Carboxylic acid **2** was coupled to propargyl amine using standard peptide coupling conditions to provide the alkyne-containing nanoprobe scaffold **3**. Alkyne nanoprobe **3** was subsequently treated with trifluoroacetic acid to afford carboxylic acid **4**, which is the alkyne nanoprobe scaffold that will allow for a library of these probes to be synthesized (Scheme 4.1).

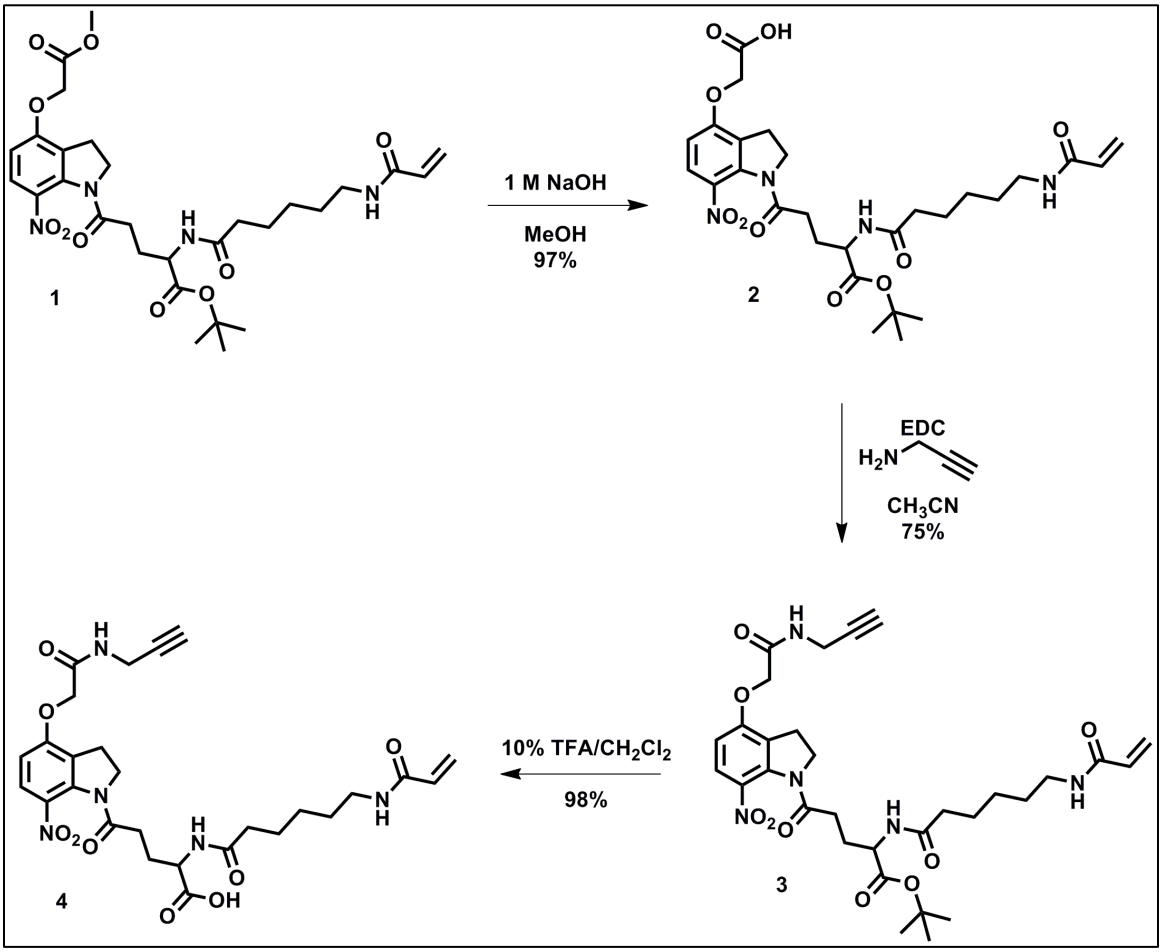

Scheme 4.1. Synthesis of alkyne nanoprobe 4 from indoline core 1.

To complete the synthesis of the ketamine based nanoprobe, carboxylic acid **4** was coupled to rhodamine-functionalized cadaverine to produce fluorescent probe **5**. The

ketamine analogue was functionalized by alkylation with 1-azido-6-bromohexane to afford compound **6**, which is then reacted with fluorescent probe **5** under standard "click" conditions to produce the final ketamine based nanoprobe **SM-V-127** (Scheme 4.2).

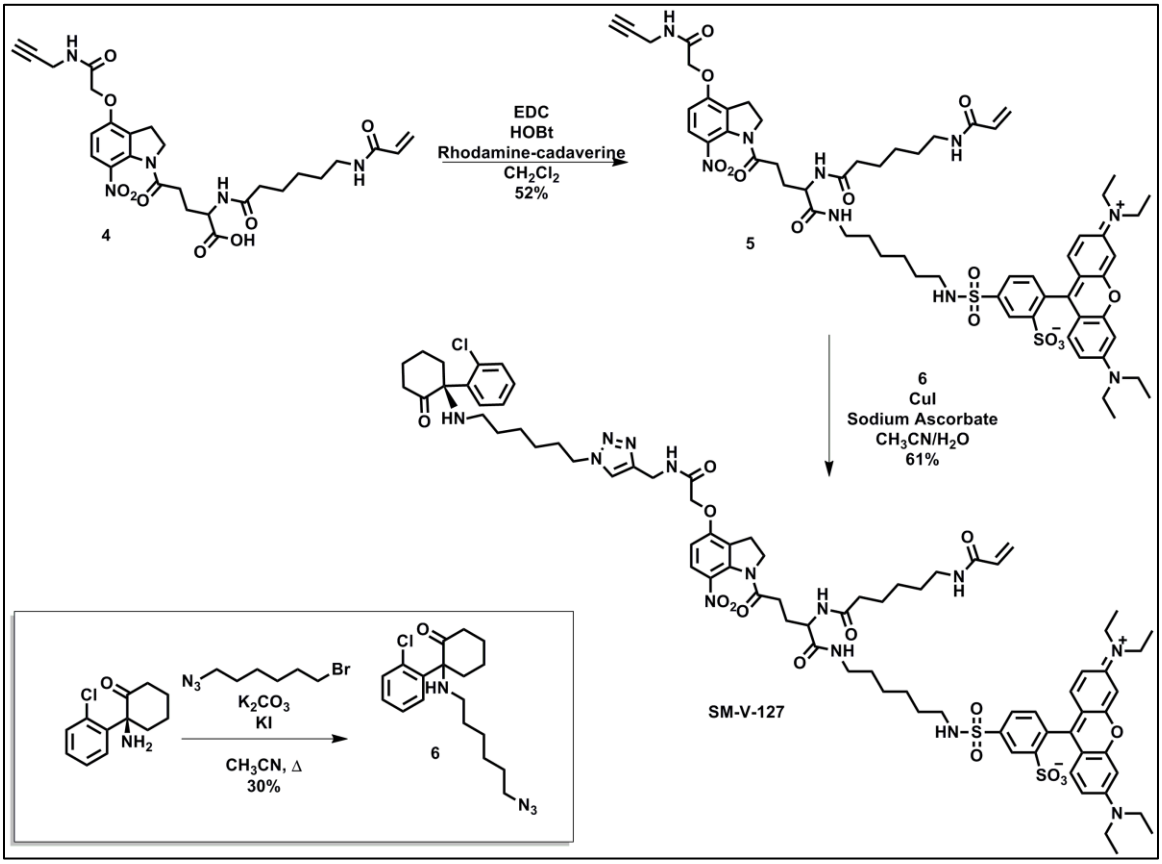

Scheme 4.2. Synthesis of ketamine based nanoprobe to target post synaptic NMDA receptors

4.3 Results and Discussion

The synthesis of the alkyne nanoprobe was slightly altered when compared to the previously discussed DAT and SERT nanoprobes in Chapter 3. Here, we peptide coupled the alkyne ligand first to allow for deprotection of the tert-butyl ester, which would leave a free carboxylic acid that could then be reacted with any amine terminated dye. Following base hydrolysis of the methyl ester in indoline **1**, alkyne nanoprobe **2** was synthesized through peptide coupling with propargyl amine. We chose this simple amine

compound because a longer linker on the pharmacophore could be utilized to extend the ligand out from the alkyne nanoprobe scaffold.

Following the synthesis of alkyne nanoprobe **4**, we chose to functionalize the probe with the sulfonyl rhodamine fluorophore utilized in the previous chapter because of its high quantum yield and the reaction conditions for this transformation has been optimized. Fluorescent compound **5** would allow for a multitude of nanoprobes targeting different receptors to be synthesized rapidly through copper mediated click reactions with pharmacophores containing an azido handle. As discussed previously, we chose to target glutamatergic NMDA receptors by utilizing a ketamine based pharmacophore with an azido linker, which was synthesized by alkylating (S)-2-amino-2-(2-chlorophenyl) cyclohexanone with 1-azido-6-bromohexane. Although a primary amine undergoing an alkylation under reflux conditions would normally be expected to proceed smoothly, the yield for the reaction was found to be quite poor. This may be due to the amine being bonded to a quaternary carbon, leading to unfavorable steric interactions. The addition of KI to encourage SN2 displacement of the alkyl halide only slightly improved the yield of the reaction. Fluorescent compound **5** was reacted with azido ketamine analogue **6** under standard click reaction conditions using copper iodide and sodium ascorbate to produce the ketamine based nanoprobe **SM-V-127** in 61% yield. The click reaction showed an improved yield and fewer side products observed over the previously synthesized DAT and SERT nanoprobes discussed in Chapter 3. This successful reaction displays how a ligand directed small molecule probe can be synthesized rapidly from the alkyne nanoprobe scaffold.

Labeling studies utilizing the ketamine nanoprobe were conducted on Chinese hamster ovary (CHO) cells stably transfected with an inducible vector containing the NR1A/NR2B NMDA receptor subunits. As discussed previously, ketamine is an open channel blocker of NMDA receptors and will require the addition of glutamate and glycine in order to open the binding site. The NMDA transfected cells were incubated with 20 μM of ketamine nanoprobe **SM-V-127** with or without the parent compound ketamine and images were acquired immediately to visualize any background fluorescence or labeling. Without any agonist added, no labeling should be seen due to the binding site being closed to the ligand. In both cases, minimal background fluorescence was observed for **SM-V-127** in the presence or absence of ketamine, as expected (Figure 4.3). As demonstrated in Figure 4.4, following the addition of glutamate and glycine, distinct fluorescent labeling is observed for **SM-V-127** and is completely blocked in the presence of ketamine itself. Cell labeling can be observed with probe concentrations as low as 100 nM and as short as 2.5 minutes following the addition of the agonists. The imaging results suggest that labeling is due to the specificity of the pharmacophore attached to the nanoprobe scaffold as fluorescent is blocked by the parent compound. Further imaging studies are being conducted to determine how specific the ketamine probe is for the NMDA receptors. This will be done by the addition of antibodies for the NR1A/NR2B subunits following labeling with the ketamine nanoprobe. If visualization of the antibodies and nanoprobe colocalize, it would indicate that the nanoprobe is likely labeling NMDA receptors. In-gel fluorescence experiments are also being run in parallel with the CHO cell labeling studies. These experiments will also help determine how specific the ketamine nanoprobe is for the NMDA receptor as

well as give insight into other proteins that the probe might label. Together, these results demonstrate that an alkyne based nanoprobe can be utilized to create multifunctional probes for receptor targeting.

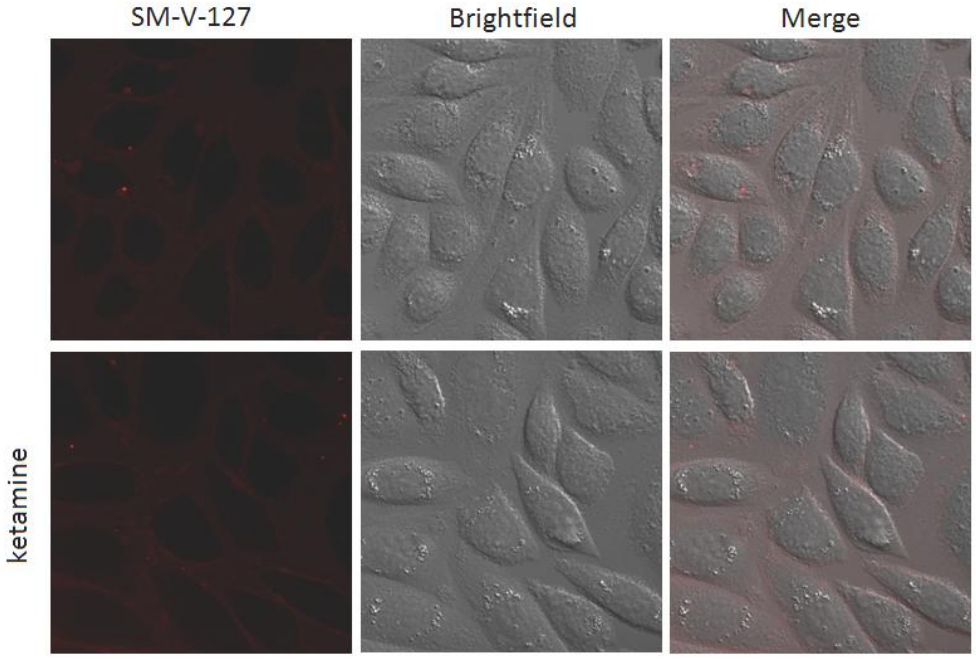

Figure 4.3. Fluorescent imaging of ketamine nanoprobe SM-V-127 pre-agonist addition.

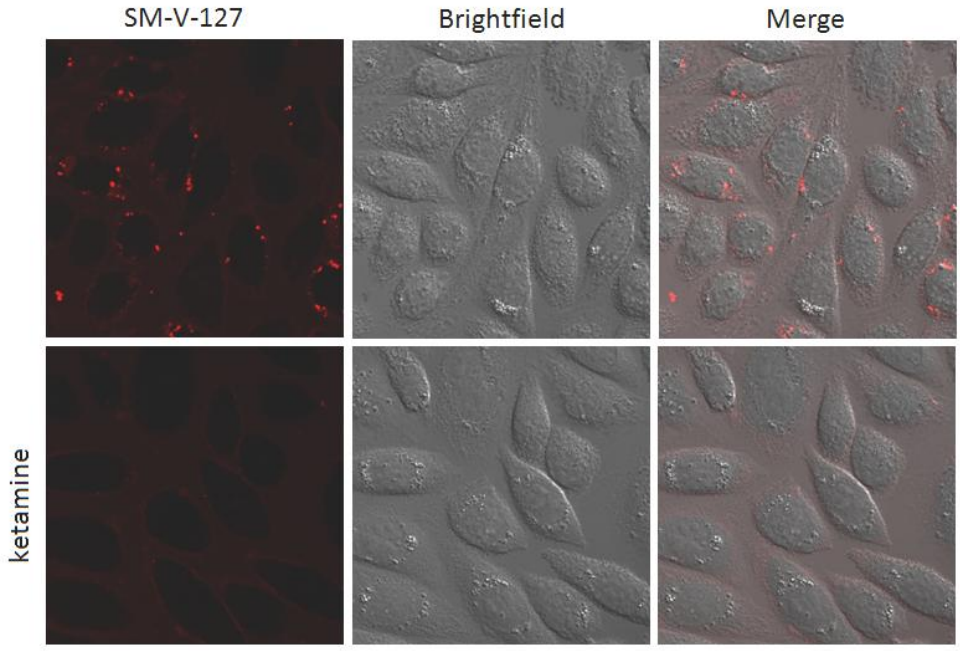

Figure 4.4. Fluorescent imaging of ketamine nanoprobe SM-V-127 post-agonist addition.

4.4 Conclusion

The alkyne based nanoprobe described in this work shows that the scaffold can be utilized to rapidly synthesize multifunctional probes to target receptors of interest. The addition of a ketamine ligand through a click reaction with the alkyne nanoprobe allowed for visualization of NMDA receptors in transfected CHO cells. The alkyne nanoprobe can provide a general labeling tool available for scientists to study various membrane bound endogenous receptors.

4.5 Materials and Methods

4.5.1 General information

All reagents, biological and chemical, were purchased through Fisher Scientific (Fair Lawn, NJ, USA). All reactions involving air- and moisture-sensitive reagents were performed under an argon atmosphere using syringe-septum cap techniques. DMF and CH_2Cl_2 were dried by storing over molecular sieves (4Å). Analytical thin-layer chromatography (TLC) was carried out using Merck Silica gel 60 F254 aluminum sheets. Compounds were detected as single spots on TLC plates and visualized using UV light (254 or 366 nm) or ninhydrin. Merck silica gel (35–70 mesh) was used for flash chromatography. ^{1}H NMR spectra were recorded on a 500 MHz Bruker NMR spectrometer using the residual proton resonance of the solvent as the standard. Chemical shifts are reported in parts per million (ppm). When peak multiplicities are given, the following abbreviations are used: s, singlet; bs, broad singlet; d, doublet; t, triplet; q, quartet; m, multiplet. ^{13}C NMR spectra were proton decoupled and recorded on a 500 MHz spectrometer using carbon signal of the deuterated solvent as the internal

standard. Mass spectra were measured either on a Waters ZQ device for LRMS and at the UMass Mass Spectrometry facility for HRMS.

4.5.2 Synthesis of alkyne nanoprobe

Synthesis of 2-((1-(4-(6-acrylamidohexanamido)-5-(tert-butoxy)-5-oxopentanoyl)-7-nitroindolin-4-yl)oxy)acetic acid (2)

Indoline **1** (0.400 g, 0.662 mmol) was dissolved in MeOH (22 mL) and treated with 1 M NaOH (993 μL). The reaction mixture was stirred at room temperature for 16 hours then neutralized with 1 M citric acid (993 μL) and concentrated via rotary evaporation. The residue was diluted with H_2O (10 mL), acidified to pH 2 with 1 M citric acid, and extracted with CH_2Cl_2 (3 x 20 mL). The organic layer was dried with $MgSO_4$, filtered, and the solvent removed via rotary evaporation to yield 380 mg (97% yield) of product. The product was used without further purification.

^{1}H NMR (400 MHz, CD_3OD) δ ppm 7.73 (d, *J* = 9.09 Hz, 1 H) 6.78 (d, *J* = 9.09 Hz, 1 H) 6.21 - 6.24 (m, 2 H) 5.64 (dd, *J* = 8.34, 3.79 Hz, 1 H) 5.51 (s, 1 H) 4.30 - 4.34 (m, 2 H) 3.24 - 3.29 (m, 2 H) 3.20 (t, *J* = 7.96 Hz, 2 H) 2.83 (s, 2 H) 2.24 - 2.33 (m, 2 H) 1.53 - 1.71 (m, 5 H) 1.47 - 1.50 (s, 9 H) 1.38 - 1.45 (m, 3 H)

Synthesis of tert-butyl 2-(6-acrylamidohexanamido)-5-(7-nitro-4-(2-oxo-2-(prop-2-yn-1-ylamino)ethoxy)indolin-1-yl)-5-oxopentanoate (3)

Carboxylic acid **2** (0.600 g, 1.02 mmol) and EDC (0.290 g, 1.53 mmol) were dissolved in dry CH_2Cl_2 (3 mL) under argon and stirred for 10 min. Propargylamine (196 μL, 3.06 mmol) dissolved in dry CH_2Cl_2 (2 mL) was added slowly to the reaction mixture and allowed to stir for 16 hours. The solvent was removed via rotary evaporation and the residue was dissolved with EtOAc (20 mL) and washed with 1 M citric acid, aq. sat.

$NaHCO_3$, brine, dried with $MgSO_4$, and the solvent removed to yield 480 mg (75% yield) of a red oil.

^{1}H NMR (500 MHz, $CDCl_3$) δ ppm 7.66 (d, *J* = 9.00 Hz, 1 H), 6.98 (t, *J* = 5.42 Hz, 1 H), 6.55 (d, *J* = 9.00 Hz, 1 H), 6.47 (d, *J* = 7.63 Hz, 1 H), 5.99 - 6.11 (m, 2 H), 5.52 (dd, *J* = 10.22, 1.53 Hz, 1 H), 4.57 (d, *J* =1.68 Hz, 2 H), 4.41 (ddd, *J* = 9.12, 7.67, 3.97 Hz, 1 H), 4.16 (t, *J* = 8.16 Hz, 2 H), 4.08 (dd, *J* = 5.26, 2.06 Hz, 2 H), 3.13 (d, *J* = 2.59 Hz, 1 H), 3.12 (t, *J* = 6.56 Hz, 2 H), 2.44 - 2.59 (m, 2 H), 2.11 - 2.25 (m, 4 H), 1.99 - 2.07 (m, 1 H), 1.98 (s, 1 H), 1.64 (s, 2 H), 1.51 - 1.58 (m, 2 H), 1.40 (s, 9 H), 1.26 (d, *J* = 7.32 Hz, 2 H), 1.19 (t, *J* = 7.17 Hz, 1 H).

^{13}C NMR (500 MHz, $CDCl_3$) δ ppm 173.46, 171.15, 170.76, 166.87, 165.71, 156.33, 136.71, 136.05, 131.01, 126.06, 125.47, 123.33, 107.60, 82.33, 79.00, 71.78, 67.72, 60.41, 52.61, 49.90, 39.03, 35.89, 32.05, 28.86, 26.79, 26.27, 26.04, 24.69, 21.06, 14.20.

LCMS (ESI-TOF) Calc for $C_{31}H_{41}N_5O_9$[M+1] ; 628.69, Found: 628.50

Synthesis of 2-(6-acrylamidohexanamido)-5-(7-nitro-4-(2-oxo-2-(prop-2-yn-1-ylamino)ethoxy)indolin-1-yl)-5-oxopentanoic acid (4)

Alkyne **3** (0.110 mg, 0.175 mmol) was dissolved in a 10% TFA/CH_2Cl_2 solution (2 mL) and stirred for 12 hours at room temperature. The solvent was removed via rotary evaporation to yield 120 mg (98% yield) of a red oil. The product was used without further purification.

^{1}H NMR (500 MHz, CD_3OD) δ ppm 7.74 (d, *J* = 9.00 Hz, 1 H), 6.79 (d, *J* = 9.16 Hz, 1 H), 6.20 - 6.24 (m, 2 H), 5.64 (dd, *J* = 9.08, 2.98 Hz, 1 H), 4.73 (s, 2 H), 4.46 (dd, *J* = 9.00, 5.04 Hz, 1 H), 4.32 (t, *J* = 8.01 Hz, 2 H), 4.06 (d, *J* = 2.59 Hz, 2 H), 3.22 - 3.28 (m,

4 H), 2.64 - 2.75 (m, 2 H), 2.62 (t, *J* = 2.52 Hz, 1 H), 2.27 - 2.31 (m, 3 H), 2.00 - 2.09 (m, 3 H), 1.63 - 1.70 (m, 2 H), 1.52 - 1.61 (m, 2 H), 1.36 - 1.44 (m, 2 H).

^{13}C NMR (500 MHz, CD_3OD) δ ppm 174.96, 173.53, 171.36, 168.43, 166.72, 157.00, 136.33, 135.79, 130.70, 125.11, 124.67, 124.16, 107.65, 78.92, 70.88, 67.06, 51.78, 49.98, 38.88, 35.23, 31.50, 28.58, 27.89, 26.09, 25.07.

LCMS (ESI-TOF) Calc for $C_{27}H_{33}N_5O_9$[M+1] ; 572.23, Found: 572.20

Synthesis of rhodamine-alkyne nanoprobe 5

Carboxylic acid **4** (24 mg, 0.042 mmol), EDC (12 mg, 0.063 mmol), and HOBt (10 mg, 0.063 mmol) were dissolved in dry DMF (1 mL) under argon and stirred for 10 min. Rhodamine cadaverine (27 mg, 0.042 mmol) and DIPEA (15 μL, 0.084 mmol) were dissolved in dry DMF (1 mL) and added slowly to the reaction mixture. After stirring the reaction for 16 hours, the solvent was removed via rotary evaporation and column chromatography was performed utilizing 80:10:10 CH_2Cl_2:CH_3CN:MeOH as eluent to yield 26 mg (52% yield) of a deep purple oil.

^{1}H NMR (500 MHz, CD_3OD) δ ppm 8.66 (s, 1 H) 8.08 - 8.14 (m, 1 H) 7.86 (d, *J* = 7.17 Hz, 1 H) 7.68 (d, *J* = 8.85 Hz, 1 H) 7.44 - 7.54 (m, 2 H) 7.12 (d, *J* = 9.46 Hz, 2 H) 6.99 (d, *J* = 9.46 Hz, 2 H) 6.92 (s, 2 H) 6.75 (d, *J* = 9.00 Hz, 1 H) 6.15 - 6.24 (m, 2 H) 4.68 (s, 2 H) 4.33 (d, *J* = 7.32 Hz, 1 H) 4.26 (t, *J* = 7.86 Hz, 2 H) 4.03 (s, 2 H) 3.67 (q, *J* = 6.56 Hz, 10 H) 3.14 - 3.25 (m, 8 H) 3.02 (t, *J* = 6.33 Hz, 2 H) 2.61 (d, *J* = 2.29 Hz, 3 H) 2.27 (t, *J* = 7.32 Hz, 3 H) 2.04 - 2.14 (m, 1 H) 1.95 (dd, *J* = 14.42, 7.10 Hz, 1 H) 1.59 - 1.67 (m, 3 H) 1.45 - 1.57 (m, 8 H) 1.25 - 1.39 (m, 20 H)

^{13}C NMR (500 MHz, CD_3OD) δ ppm 174.74, 171.32, 168.28, 167.90, 166.62, 157.90, 156.98, 156.42, 155.70, 145.86, 142.74, 136.32, 135.71, 133.86, 132.28, 131.10, 130.78,

127.92, 126.43, 126.32, 125.08, 124.71, 124.11, 113.87, 113.67, 107.68, 95.64, 79.03, 78.13, 77.88, 77.62, 70.95, 67.06, 53.02, 50.01, 45.49, 42.68, 38.88, 35.37, 31.56, 29.13, 28.77, 28.54, 27.96, 27.93, 27.06, 26.17, 25.92, 25.83, 25.04, 11.58

LCMS (ESI-TOF) Calc for $C_{60}H_{75}N_9O_{14}S_2$ [M+1] ; 1210.42, Found: 1210.40

4.5.3 Synthesis of ketamine nanoprobe (6)

Rhodamine-alkyne nanoprobe **5** (17 mg, 0.0140 mmol) was combined with CuI (1.2 mg, 0.0040 mmol) and sodium ascorbate (1.2 mg, 0.0040 mmol) and dissolved in CH_3CN/H_2O (1 mL/0.1 mL). Ketamine azide ligand **7** (3.0 mg, 0.0094 mmol) dissolved in CH_3CN (1 mL) was then added and the reaction mixture was allowed to stir for 16 hours. The solvent was removed via rotary evaporation and the product was purified by preparative-HPLC to obtain 8.8 mg (61% yield) of product as a pink solid. (XBridge Prep C18 5µm (10 x 100 mm) column: H_2O and CH_3CN/0.1% formic acid as the mobile phase.)

LCMS (ESI-TOF) Calc for $C_{78}H_{100}ClN_{13}O_{15}S_2$ [M+1] ; 1559.29, Found: 1558.90

HRMS (ESI-TOF) Calc for $C_{78}H_{100}ClN_{13}O_{15}S_2$ $[M+2]^+$; 780.8376, Found: 780.8393

4.5.4 Synthesis of ketamine azide ligand (7)

To a suspension of K_2CO_3 (110 mg, 0.670) in CH_3CN (3 mL) was added 2-amino-2-(2-chlorophenyl)cyclohexanone (50.0 mg, 0.223 mmol) and a catalytic amount of KI. 1-azido-6-bromohexane (55.0 mg, 0.268 mmol) dissolved in CH_3CN (2 mL) was then added dropwise and the solution was heated to reflux and stirred for 16 hours. After cooling to room temperature the solvent was removed via rotary evaporation. H_2O (10 mL) was added to the residue and was extracted with EtOAc (3 x 10 mL). The combined

organic layers were combined, washed with brine (10 mL), dried with $MgSO_4$, and evaporated via rotary evaporation. The crude material was purified by column chromatography use 1:1 EtOAc:hexanes as eluent to yield 23 mg (30% yield) as a clear oil.

LCMS (ESI-TOF) Calc for $C_{18}H_{25}ClN_4O$[M+1] ; 349.17, Found: 349.20

4.6 References

(1) Gitto, R.; De Luca, L.; Ferro, S.; Scala, A.; Ronsisvalle, S.; Parenti, C.; Prezzavento, O.; Buemi, M. R.; Chimirri, A. *Bioorg. Med. Chem.* **2014**, *22*, 393.

(2) Barria, A.; Malinow, R. *Neuron* **2002**, *35*, 345.

(3) Chen, H.-S. V.; Lipton, S. a. *J. Neurochem.* **2006**, *97*, 1611.

(4) Lipton, S. A. *Nat. Rev. Drug Discov.* **2006**, *5*, 160.

(5) Domino, E.F., Chodoff, P., Corssen, G. *Clin. Pharmacol. Ther.* **1965**, *6*, 279.

(6) Sinner, B.; Graf, B. M. In *Modern Anesthetics SE - 15*; Schüttler, J.; Schwilden, H., Eds.; *Handbook of Experimental Pharmacology*; Springer Berlin Heidelberg, 2008; Vol. 182, pp. 313–333.

(7) Sleigh, J.; Harvey, M.; Voss, L.; Denny, B. *Trends Anaesth. Crit. Care* **2014**, *4*, 76.

(8) Zeilhofer, H. U.; Swandulla, D.; Geisslinger, G.; Brune, K. *Eur. J. Pharmacol.* **1992**, *213*, 155.

(9) Jose, J.; Gamage, S. a; Harvey, M. G.; Voss, L. J.; Sleigh, J. W.; Denny, W. a. *Bioorg. Med. Chem.* **2013**, *21*, 5098.

(10) Johnson, J. W.; Glasgow, N. G.; Povysheva, N. V. *Curr. Opin. Pharmacol.* **2015**, *20*, 54.

(11) Kashiwagi, K.; Masuko, T.; Nguyen, C. D.; Kuno, T.; Tanaka, I.; Igarashi, K.; Williams, K. *Mol. Pharmacol.* **2002**, *61* , 533.

(12) Chen, H.-S. V.; Lipton, S. A. *J. Pharmacol. Exp. Ther.* **2005**, *314* , 961.

(13) Vytla, D.; Combs-Bachmann, R. E.; Hussey, A. M.; Hafez, I.; Chambers, J. J. *Org. Biomol. Chem.* **2011**, *9*, 7151.

CHAPTER 5

CAGED AZIRIDINIUM-PHOTOCONTROL OVER ALKYLATION OF NUCLEOPHILES

Adapted with permission from McCarron, S.T.; Feliciano, M.; Johnson, J.N.; Chambers, J.J. Photoinitiated release of an aziridinium ion precursor for the temporally controlled alkylation of nucleophiles. Bioorganic and Medicinal Chemistry Letters. 2013, 8, 2395-2398.

5.1 Introduction

The development of novel and efficient methods aimed at the facile alkylation of biological substrates has been a topic of much effort in the field of chemical biology[1,2,3,4]. The application of small molecule probes to a biological target allows for subcellular imaging and the study of dynamic protein motions in and on cells. The power of these molecules can be synergistic with new sub-diffraction resolution microscopy methods, which typically rely on the delivery and attachment of fluorophores to proteins of interest[5,6,7]. As mentioned in previous chapters, these fluorophores are usually delivered by one of two methods: genetic tagging of the protein of interest using a naturally fluorescent reporter protein such as GFP or by non-covalent labeling using the tried-and-true antibody method. However, these methods either require genetic engineering of the target protein or non-covalent interactions of fairly large antibodies for highlighting the location of the target biomolecules.

One method for the delivery of a small molecule probes to a protein target is through the application of photochemically activated moieties that utilize small molecules to target proteins and then covalently modify the protein of interest for downstream analysis[8,9,10]. In particular, there are three classes of commonly used photoreactive moieties that allow for photo-crosslinking to proteins, which include aryl azides, diazirines, and substituted benzophenones. Each of these functional groups is chemically-inert under dark conditions but can revert to a reactive species by the application of high energy, ultraviolet light. Upon photo-activation, azides and diazirine groups produce a nitrene-like or a carbene intermediate, respectively, while benzophenones depend on radical aryl ketylintermediates for reactivity[11,12]. However, the reactivity of these compounds is difficult to tune and often react with the solubilizing media or buffer, thereby reducing their labeling efficiency.

Recently, there has been the development of multifunctional probes that allow for traceless labeling of endogenous proteins[13,14,15]. As discussed in Chapters 3 and 4, these probes consist of a ligand for binding to the target protein, a fluorophore for visualization, and some electrophilic moiety that forms a new covalent bond with the target upon binding to the protein. Generally, the native nucleophile is the sulfhydryl of cysteine that is intrinsic to the target protein and the small molecule-based electrophile contains a maleimide for selective bioconjugation to this residue. While these probes offer many advantages in terms of their size and their ability to be ‘traceless’, they all are limited by the electrophile delivered to the biological system and electrophiles are known to react with off-target nucleophiles[16]. Here, we report the development of a small, photoactivated, electrophilic moiety that is compatible with aqueous buffer.

This chapter will focus on a method to photoinitiate the release of 2-chloro-N,N-dimethylethylamine; a molecule that is similar in reactivity to the nitrogen mustard alkylating agent bis(2-chloroethyl) ethylamine (HN1). This particular compound is known to form the promiscuous N,N-dialkylaziridinium electrophile under biologically-relevant conditions[17,18,19]. In addition, the N,N-dialkylaziridinium ion formed from HN1 has been implicated in the alkylation of biological nucleophiles, most commonly the guanine of DNA after exposure to this nitrogen mustard. We reasoned that the formation of N,N-dimethylaziridinium from 2-chloro-N,N-dimethylethylamine can be initiated with light if we were to chemically mask the important lone pair of electrons on the tertiary amine of the latter in the form of a photoreleasable quaternary amine from molecule **2** (Scheme 5.1). The photocage we chose to employ is the 4-methyl-7-methoxycoumarin chromophore for a number of reasons: (1) this chromophore will undergo heterolytic bond cleavage resulting in the release of a tertiary amine in neutral form with the lone pair of electrons made available for subsequent ring closure. (2) the coumarin can be activated by either ultraviolet light or two-photon infrared light which could allow for more precise spatial control of labeling and, (3) the quantum yield of release from this chromophore is highly efficient[20]. The N,N-dimethylaziridinium that is formed is expected to be relatively long lived in biological conditions. Reports on similar aziridinium species suggest that the half-life of the aziridinium in phosphate buffered saline solution (PBS) at 37˚C is about 70 minutes[21].

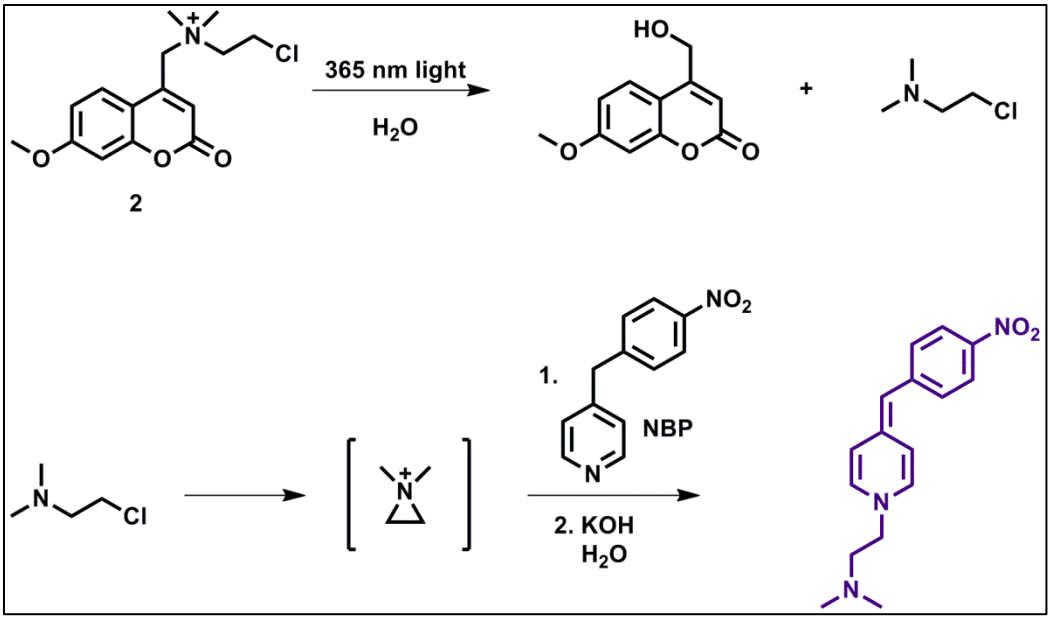

Scheme 5.1. Photo-induced aziridinium formation and subsequent alkylation of the pyridine-based nucleophile, NBP.

5.2 Experimental methods

The caged molecule **2** was synthesized by alkylating N,N-dimethylaminoethanol with 4-chloromethyl-7-methoxycoumarin[22] to form **1** in 72% yield followed by substitution of the hydroxyl with chloride using thionyl chloride to afford **2** in 81% yield (Scheme 5.2). To explore the photoinitiated release of the 2-chloro-N,N-dimethylethylamine and the subsequent formation of an aziridinium ion, we employed a colorimetric assay to determine nucleophile alkylation. 4-Nitrobenzylpyridine (NBP) has been utilized as a detector of alkylation in the literature because N-alkylation and facile work-up produces a deep purple color that is easy to quantify using a UV/Vis spectrophotometer[23,24]. The pyridinium nitrogen is quarternized by the electrophile and under basic work up a benzylic proton is removed, which conjugates the aryl rings to produce a deep purple color that can be rapidly measured (Scheme 5.1). We used this method of analysis to follow the evolution of N,N-dimethylaziridinium formation of the

non-caged 2-chloro-N,N-dimethylethylamine, the caged molecule **2** kept in the dark, and of the caged molecule after exposure to a short pulse of 365 nm light from an LED light source. In addition, 2-chloro-N,N-dimethylethylamine and caged **2** were incubated with four amino acids (cysteine, lysine, serine, and arginine) that are biologically relevant nucleophiles at physiological pH and temperature. We chose these amino acids to give insight to protein labeling studies that can be done in the future. The 2-chloro-N,N-dimethylethylamine and caged **2** were allowed to react with each amino acid and the reaction was analyzed by LC/MS to determine the extent of labeling.

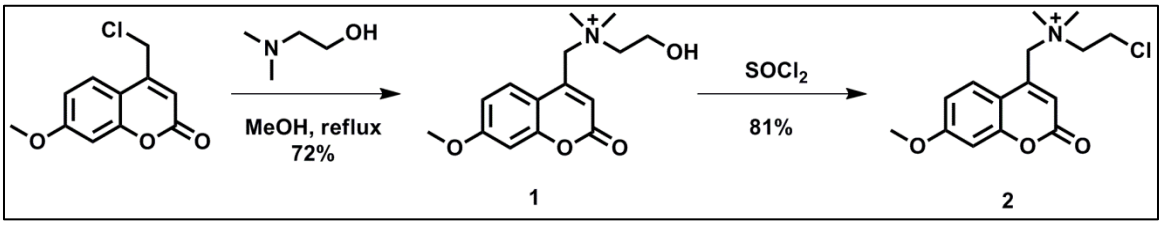

Scheme 5.2. Synthesis of caged N,N-dimethylaziridinium precursor 2.

5.3 Results and Discussion

5.3.1 NBP alkylation assay

Our investigation began with the measurement of aziridinium formation from 2-chloro-N,N-dimethylethylamine (hydrochloride) in aqueous buffer in the presence of NBP at 37˚C and pH 7.4. We decided to perform these reactions at physiological pH and temperature due to our future plans to employ this photochemistry on live mammalian cells. We followed the time course of NBP alkylation by removing aliquots of the reaction mixture and incubating them with stop solution followed by ethyl acetate extraction of the colored product (Figure 5.1). The OD535 of the ethyl acetate layer was then quantified and all data points were measured in triplicate from three different

reaction runs. In parallel, we prepared an identical solution of compound **2** and allowed it to react with the NBP in the dark. We expected some background reactivity due to SN2 displacement of the alkyl chloride on the caged molecule by the nucleophilic pyridine. However, the caged molecule did not react at a detectable level, suggesting that the quarternization of the tertiary amine is sufficient to eliminate much of the electrophilic character of this alkyl chloride (Figure 5.2). Upon photoinitiated release of 2-chloro-N,N-dimethylethylamine from the coumarin cage, NBP alkylation was observed and was quite similar in reaction rate to the non-caged 2-chloro-N,N dimethylethylamine. The photoinitiated release of 2-chloro-N,N-dimethylethylamine allows the aziridinium formation to begin at a prescribed time and results in identical alkylation of the NBP reporter molecule.

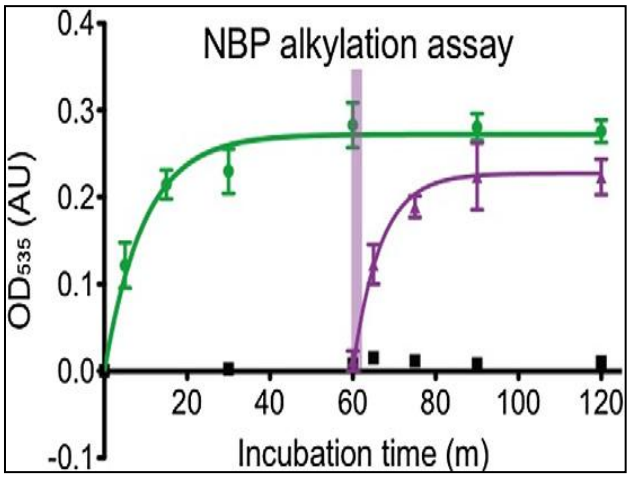

Figure 5.1. Rate of NBP alkylation. Data points represent average of three independent experiments (n=3 for each experiment) of reaction between alkylating molecule and NBP following work-up and analysis. Lines are calculated as exponential associations. Green circles are for 2-chloro-N,N-dimethylethylamine, black boxes are for caged molecule 2 maintained in the dark, and purple triangles are for caged molecule 2 (at the same concentration and quantity as that used for the green circles) after exposure to 1 min of 365 nm light as represented by purple bar at 60 min mark.

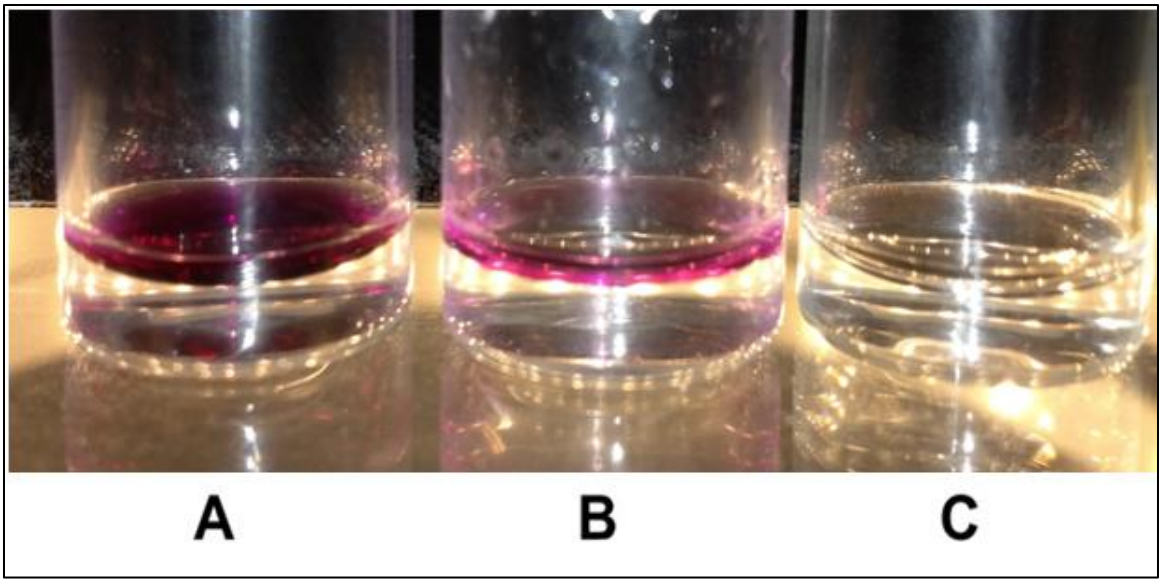

Figure 5.2. Photographs of alkylation reactions post-workup. (a) 2-chloro N,N-dimethylethylamine incubated with NBP at 30 min, (b) caged molecule 2 irradiated at 365 nm for 1 min and incubated with NBP for 30 min, and (c) caged molecule 2 kept in the dark with NBP at 30 min. The top, color-containing layer is the ethyl acetate extract that is normally analyzed via UV/vis.

5.3.2 Mass spectroscopy analysis

Next, we investigated the selectivity of the photo-initiated release of 2-chloro-N,N-dimethylethylamine towards four amino acids that represent biologically-relevant potential nucleophiles. The N-terminus of the amino acids were Fmoc-protected to discourage the alkylation of the free amine versus the side chain functional groups. As a positive control, 2-chloro-N,N-dimethylethylamine hydrochloride was incubated with Fmoc-serine, lysine, arginine, or cysteine for 2 hours at 37˚C and pH 7.4 in 2.5 mL of PBS/DMSO (4:1) solution. After incubation, 50 μL of the reaction mixture was diluted to 1 mL in methanol and analyzed by LC/MS. Under these conditions only cysteine was found to be alkylated by 2-chloro-N,N-dimethylethylamine (MW = 415.2). Likewise, caged **2** was incubated with of each Fmoc-protected amino acid under the same

conditions in the dark and after irradiation with UV light. After 2 hours of incubation, the mass corresponding to the alkylated amino acids were not found for caged **2** with no UV irradiation. In addition, the mass corresponding to unreacted caged **2** was present, indicating that the cage was not reactive to the buffer at a detectible level. However, following exposure to 1 min of 365 nm light, the mass corresponding to the alkylated amino acids was only found in the case of cysteine (MW = 415.2). This finding parallels the results from the positive control experiment with 2-chloro-N,N-dimethylethylamine.

5.4 Conclusion

In summary, we have developed a convenient method for the photoinitiated release of the electrophile N,N-dimethylaziridinium from 2-chloro-N,N-dimethylethylamine in situ. While our data does not conclusively confirm the production of the aziridinium moiety, we have shown that our caged molecule is unreactive before the release with light. Going forward, we plan to synthesize a similar molecule that contains a ligand and a propargyl handle to allow for the electrophilic attachment to a protein of interest. This alkyne will allow for a subsequent [3+2] cyclization (click reaction) with an azido-based fluorophore or biotin. The present molecular system that is the subject of this chapter is chemically-inert when kept in the dark and is stable in PBS solution for >30 days at room temperature. The reactive species is only generated after light is applied to unmask the tertiary amine. The application of this technology to protein labeling studies could offer new tools to spatially limit protein modification for the purpose of protein tracking on cells. The technology will also add another versatile tool to the arsenal of spatially and temporarily controlled protein labeling bioorganic chemistry.

5.5 Material and Methods

5.5.1 General information

All reagents were purchased through Fisher Scientific (Fair Lawn, NJ, USA). Merck silica gel (35–70 mesh) was used for flash chromatography. NMR spectra were recorded on a 400 MHz Bruker NMR spectrometer using the residual proton resonance of the solvent as the standard for proton spectra and the carbon signal of the deuterated solved as the internal standard for carbon spectra. Chemical shifts are reported in parts per million (ppm). When peak multiplicities are given, the following abbreviations are used: s, singlet; br s, broad singlet; d, doublet; t, triplet; q, quartet; m, multiplet. Mass spectra were measured on a Waters ZQ device for LRMS while HRMS data was collected at the University of Massachusetts Mass Facility which is supported, in part, by the National Science Foundation. The colorimetric absorption measurements were made on an Evolution 100 UV/Vis spectrometer.

5.5.2 Synthesis of caged electrophile

Synthesis of 2-Hydroxy-N-((7-methoxy-2-oxo-2Hchromen-4-yl)methyl)-N,N-dimethylethanaminium (1)

To a stirred solution of 4-chloromethyl-7-methoxycoumarin (500 mg, 2.23 mmol), prepared according to a previous report[22] in methanol (15 mL) was added N,N-dimethylethanolamine (896 μL, 8.92 mmol). The reaction mixture was heated to reflux and allowed to stir for 24 hours. The reaction mixture was cooled to room temperature and the solvent was removed via rotary evaporation. The crude product was dissolved in a minimal amount of hot methanol (4 mL) and hexanes were added slowly until 503 mg

(72% yield) of a white solid precipitated. The solid was collected by filtration and was rinsed with hexanes and used without further purification.

^{1}H NMR (400 MHz, D_2O) δ ppm = 7.78 (ds, *J* = 9.09, 2.53 Hz, 1H) 6.99 (dd *J* = 9.09, 2.53 Hz, 1H) 6.95 (d, *J* = 2.53 Hz, 1H) 6.58 (s, 1H) 4.73–4.76 (m, 2H) 4.03–4.09 (m, 2H) 3.83 (s, 3H) 3.59–3.64 (m, 2H) 3.13 (s, 6H).

^{13}C NMR (400 MHz, D_2O) δ = 163.32, 162.62, 155.31, 142.70, 126.19, 119.26, 113.48, 112.22, 101.64, 67.30, 62.53, 56.03, 55.49, 51.46.

HRMS (FAB+) Calcd for $C_{15}H_{20}NO_4$ [M+]: 278.1387. Found: 278.1389.

Synthesis of 2-chloro-N-((7-methoxy-2-oxo-2H-chromen-4-yl)methyl)-N,N-dimethylethanaminium (2)

To the previously-produced alcohol **1** (100 mg, 0.319 mmol) was added thionyl chloride (2.0 mL, 28 mmol) and the solution stirred at room temperature for 16 hours. The volatiles were removed via rotary evaporation followed by high vacuum to leave a white solid that was recrystallized from isopropanol to yield 86 mg (81% yield) of a white solid.

^{1}H NMR (400 MHz, D_2O) δ ppm = 7.79 (d, *J* = 8.59 Hz, 1H) 6.97–7.05 (m, 2H) 6.58 (s, 1H) 4.76 (s, 2H) 4.00–4.07 (m, 2 H) 3.86–3.92 (m, 2H) 3.84 (s, 3H) 3.17 (s, 6H).

^{13}C NMR (400 MHz, D_2O) δ = 163.39, 162.47, 155.31, 142.26, 126.10, 119.36, 113.52, 112.10, 101.68, 66.18, 62.58, 56.05, 51.23, 35.38.

HRMS (FAB+) Calcd for $C_{15}H_{19}ClNO_3$ [M+]: 296.1048. Found: 296.1059.

5.5.3 Photolysis and NBP alkylation assay conditions

All solutions were kept in the dark (aluminum foil wrapped) except during UV irradiation conditions. Solutions of 2-chloro-N,N-dimethylethylamine or caged molecule

2 were prepared by dissolving the hydrochloride salt of 2-chloro-N,N-dimethylethylamine or the chloride salt of **2** in PBS buffer to a final concentration of 25 mM. Nitrobenzylpyridine solution was prepared in dry acetone to a final concentration of 25 mM. Alkylation assays were performed by mixing 1.0 mL of PBS, 500 μL of test solution containing either **2** or 2-chloro-N,N-dimethylethylamine, and 500 μL of NBP solution and allowing them to incubate at 37˚C. Aliquots of the reaction mixture (100 μL) were removed at various times and were immediately quenched by the addition of 400 μL ethyl acetate, 500 μL of water, and 63 μL of 1.0 M aqueous KOH. Mixtures were vortexed for 1 minute and centrifuged to efficiently separate the layers. The organic layer was removed via pipette and was either directly analyzed by UV absorption or, if highly colored, diluted 10x or 100x in order to produce OD535 measurements between 0.0 and 1.0 AU. Each sample was measured after zeroing the UV/Vis detector to pure ethyl acetate and each data point was measured in triplicate. Each data point used in the time course plot is defined by three separate reactions, aliquot removal, and workup. Photolysis of the protecting group was accomplished by irradiating the sample from the top of an open 1 dram vial with the light from a LedEngin High Power LED 365 nm source (Mouser Electronics, Mansfield, TX, USA) situated 5 mm from the top of the vial driven by 600 mA of current.

5.5.4 Mass spectrometry analysis of amino acid labeling assay

Stock solutions of the corresponding Fmoc-protected amino acids (Lys, Ser, Cys, Arg) were dissolved in DMSO to a final concentration of 14 mM. Control experiments were conducted by dissolving the hydrochloride salt of 2-chloro-N,N-dimethylethylamine (0.007 mmol) in 200 μL of PBS followed by the addition of 50 μL of the amino acid

DMSO solution for a final concentration of 28 and 2.8 mM, respectively. Each reaction was conducted at pH 7.4 and 37˚C for 2 hours at which time a 50 μL aliquot was removed, diluted to 1 mL in methanol, and analyzed by mass spectrometry. In similar fashion, caged **2** was dissolved in 200 μL of PBS followed by the addition of 50 μL of each amino acid DMSO solution and allowed to react for 2 hours at 37˚C and pH 7.4 in the dark. The reaction mixture was then analyzed as previously described. Lastly, for the photolysis experiment, caged **2** was dissolved in 200 μL of PBS followed by the addition of 50 μL of each amino acid DMSO solution and warmed to 37˚C. The sample was irradiated for 1 min from a LedEngin High Power LED 365 nm source and then allowed to react for 2 hours at 37˚C and pH 7.4. The reaction mixture was analyzed as previously described.

5.6 References

(1) Lapinsky, D. J. *Bioorg. Med. Chem.* **2012**, *20*, 6237.

(2) Wombacher, R.; Cornish, V. W. *J. Biophotonics* **2011**, *4*, 391.

(3) Puliti, D.; Warther, D.; Orange, C.; Specht, A.; Goeldner, M. *Bioorg. Med. Chem.* **2011**, *19*, 1023.

(4) Loving, G. S.; Sainlos, M.; Imperiali, B. *Trends Biotechnol.* **2015**, *28*, 73.

(5) Betzig, E.; Patterson, G. H.; Sougrat, R.; Lindwasser, O. W.; Olenych, S.; Bonifacino, J. S.; Davidson, M. W.; Lippincott-Schwartz, J.; Hess, H. F. *Sci.* **2006**, *313* , 1642.

(6) Lacoste, T. D.; Michalet, X.; Pinaud, F.; Chemla, D. S.; Alivisatos, A. P.; Weiss, S. *Proc. Natl. Acad. Sci.* **2000**, *97* , 9461.

(7) Shroff, H.; White, H.; Betzig, E. In *Current Protocols in Cell Biology*; John Wiley & Sons, Inc., 2001.

(8) Knowles, J. R. *Acc. Chem. Res.* **1972**, *5*, 155.

(9) Chambers, J. J.; Gouda, H.; Young, D. M.; Kuntz, I. D.; England, P. M. *J. Am. Chem. Soc.* **2004**, *126*, 13886.

(10) Kamiya, H.. *Journal of Neuroscience*, 2012, *32*, 6517–6524.

(11) Dormán, G.; Prestwich, G. D. *Biochemistry* **1994**, *33*, 5661.

(12) Brunner, J. *Annu. Rev. Biochem.* **1993**, *62*, 483.

(13) Vytla, D.; Combs-Bachmann, R. E.; Hussey, A. M.; Hafez, I.; Chambers, J. J. *Org. Biomol. Chem.* **2011**, *9*, 7151.

(14) Tsukiji, S.; Miyagawa, M.; Takaoka, Y.; Tamura, T.; Hamachi, I. *Nat Chem Biol* **2009**, *5*, 341.

(15) Tamura, T.; Tsukiji, S.; Hamachi, I. *J. Am. Chem. Soc.* **2012**, *134*, 2216.

(16) Lord, S. J.; Lee, H. D.; Moerner, W. E. *Anal. Chem.* **2010**, *82*, 2192.

(17) Lawley, P. B. and P. D. *Biochem. J.* **1961**, *80*, 496.

(18) Rink, S. M.; Hopkins, P. B. *Biochemistry* **1995**, *34*, 1439.

(19) Kohn, K. W.; Hartley, J. A.; Mattes, W. B. *Nucleic Acids Res.* **1987**, *15* , 10531.

(20) Dore, T. M.; Wilson, H. C. *Neuromethods* **2011**, *55*, 57.

(21) Ransom, R. W.; Kammerer, R. C.; Cho, A. K. *Mol. Pharmacol.* **1982**, *21* , 380.

(22) Nam, N.-H.; Kim, Y.; You, Y.-J.; Hong, D.-H.; Kim, H.-M.; Ahn, B.-Z. *Bioorg. Med. Chem. Lett.* **2002**, *12*, 2345.

(23) Gómez-Bombarelli, R.; González-Pérez, M.; Calle, E.; Casado, J. *Chem. Res. Toxicol.* **2012**, *25*, 1176.

(24) Thaens, D.; Heinzelmann, D.; Böhme, A.; Paschke, A.; Schüürmann, G. *Chem. Res. Toxicol.* **2012**, *25*, 2092.

CHAPTER 6

FUTURE DIRECTIONS

6.1 Nanoprobe development

The alkyne nanoprobe discussed in Chapter 4 provides a method for facile synthesis of a multifunctional probe that could be targeted to a variety of receptors. To explore the modular nature of this probe further, several portions of the probe can be altered to develop a kit for fluorescent labeling of endogenous proteins. In this chapter there will be a discussion of the synthesis of a new ligand for targeting NMDA receptors, new fluorophore combinations with the probe, and an exploration of linker length for the acrylamide electrophile.

6.1.1 Ifenprodil-based NMDA receptor targeting

We have previously developed an azido-analogue of ketamine for functionalization of the alkyne nanoprobe, which would give specificity for postsynaptic NMDA receptors. Another pharmacophore that targets a subclass of NMDA receptors is the drug ifenprodil. Ifenprodil is a lead compound for a major class of antagonists of the NMDA receptor with marked selectivity for the NR2B unit. To date, there have been several studies to characterize its subtype-specific binding to NMDA receptors both in vitro and in vivo[1,2,3,4]. The NR2B containing NMDA receptors are particularly interesting to study because they are preferentially enriched in extrasynaptic sites and may participate in processes linked to glutamatergic overstimulation, which can cause excitotoxicity[5]. Therefore, NR2B-selective antagonists are quite attractive for the development of therapeutic agents for neuroprotection[6].

Ifenprodil contains two asymmetric centers that give rise to two diastereoisomeric forms, threo (R*R*) and the erythro (R*S*) forms seen in Figure 6.1. The threo racemate was found to be five times more potent neuroprotective agent than the erythro diastereomer in an in vitro glutamate neurotoxicity test[2]. Investigation of the interaction of ifenprodil on NMDA receptors places the binding site at the N-terminal domain of the NR2B unit. The potency of this compound is due to the key structural elements that incorporate a phenolic aromatic ring connected to a second phenyl ring through a linker containing a tertiary amine[7,8,9]. The piperazine ring provides a scaffold to hold the two aryl rings in an optimum orientation in the binding site, which contain a lipophilic pocket to accommodates the phenyl ring and a hydrophobic pocket that accepts the phenol group[10].

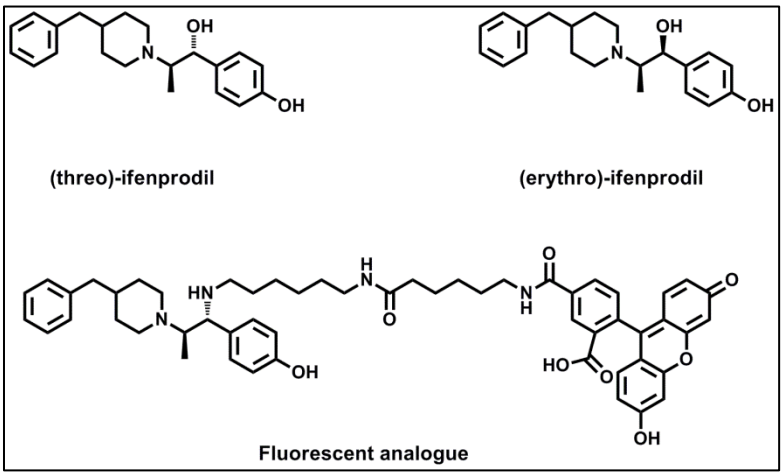

Figure 6.1. Structures of ifenprodil and fluorescent analogue by Marchand et al[10]

Work done by Marachand et al. utilized ifenprodil as a ligand for the development of small molecule fluorescent probes to characterize the microenvironment of the binding site at the NMDA receptor (Figure 6.1)[10]. The authors determined that chemical modification of the benzylic hydroxyl moiety for the attachment of linkers is preferable to the modification on the phenol moiety due to a hydrogen bond of the benzylic

hydroxyl with a glutamine residue from NR2B. In addition, a linker bearing a secondary amine or amide functional group was necessary to maintain affinity for the NMDA receptor[11]. Using this information, we have designed two azido-containing analogues of ifenprodil to react with the alkyne nanoprobe to create a multifunctional probe that will target NMDA receptors containing the NR2B subunit.

The first azido-analogue compound **4** can be synthesized in two steps starting from compound **1**, which was provided by Dr. Doug Johnson at Pfizer Neuroscience (Cambridge, MA). Compound **1** was converted to the azido compound **3** according to a stereospecific mesylation/amination sequence through the use of 6-azidohexan-1-amine (**2**), which was synthesized from the corresponding 1,6-diazidohexane. This transformation occurs with a retention of configuration as a result of a mechanism with anchimeric assistance due to the in situ formation of an aziridinium intermediate[10]. Acidic deprotection of the benzyl protected phenol is expected to yield the azido-analogue **4** (Scheme 6.1).

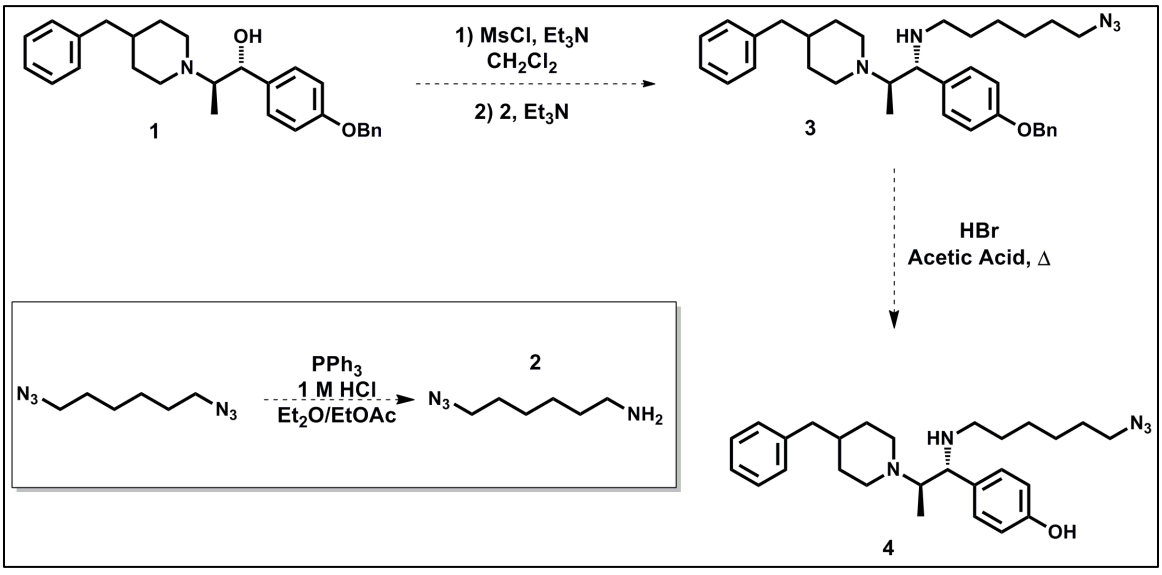

Scheme 6.1. Synthesis of ifenprodil azido-analogue 4.

The second azido-analogue compound **7** can be synthesized in three steps starting from compound **1**. Under similar reaction conditions used previously, compound **1** will be reacted with mono-Boc protected hexyldiamine to produce intermediate **5**. Acid deprotection of compound **5** is expected to yield amine compound **6**, which can react with 6-azidohexanoic acid under standard peptide coupling conditions to obtain the azido-analogue **7** (Scheme 6.2).

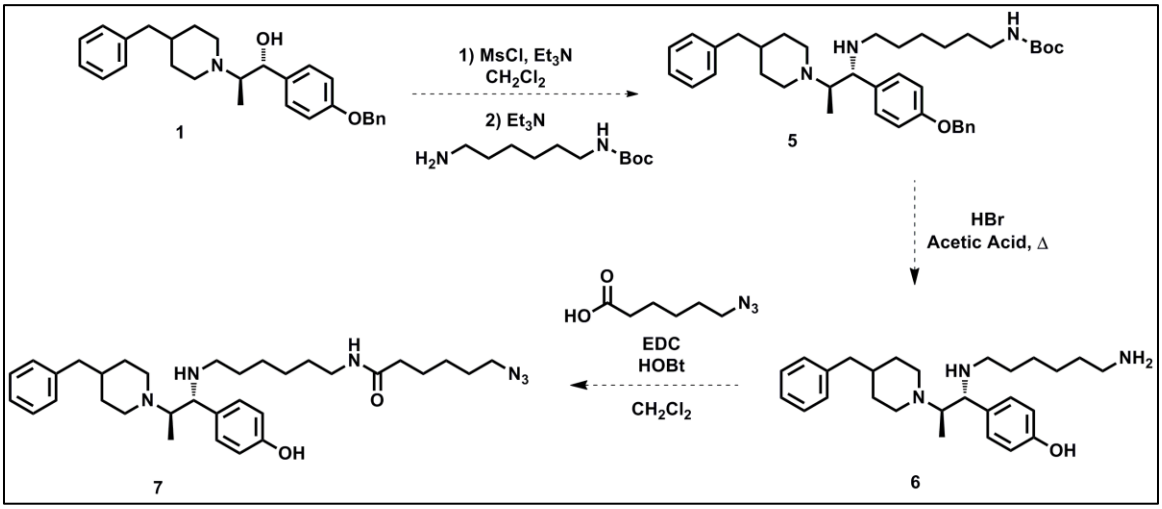

Scheme 6.2. Synthesis of ifenprodil azido-analogue 7.

Using the rhodamine linked alkyne nanoprobe synthesized previously, we could develop two NMDA receptor probes specific for the NR2B subunit by utilizing click chemistry with azido-analogues **4** and **7** (Scheme 6.3). Although the pharmacophore is the same in both cases, the linker length is varied by 6 carbons. This would allow us to determine the effects of linker length on binding affinity and provide insight into which probe would be more useful for visualization of the NMDA receptors.

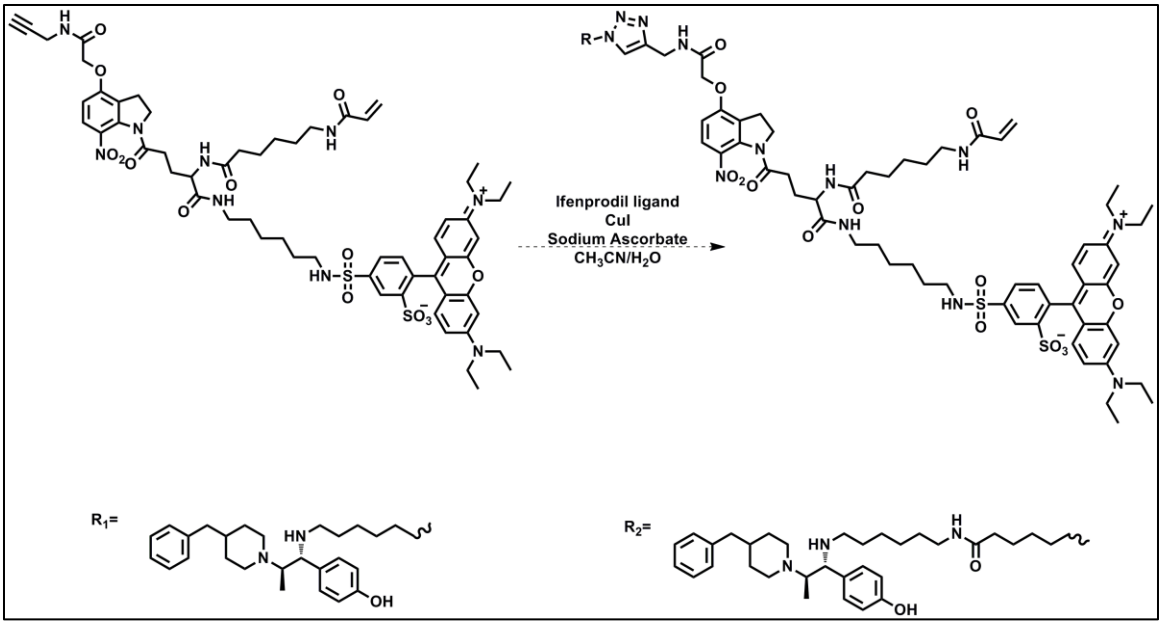

Scheme 6.3. Synthesis of ifenprodil based nanoprobes for the NMDA receptor

6.1.2 Fluorophore modification

Another site on the alkyne nanoprobe scaffold for potential modification is the addition of different fluorophores to allow for visualization of receptors with different colors or photochemical properties. Changing the fluorophore will allow for pulse-chase experiments, single molecule imaging, and if the fluorophore is pH or otherwise environmentally sensitive, can provide information about the surrounding environment. There are a multitude of commercially available fluorophores that are amine-terminated, or are easily modified with an amine linker. Of these available fluorophores, several have been used to visualize receptors of interest both in vitro and in vivo[12,13,14]. We can synthesize several fluorescent nanoprobes starting from the alkyne nanoprobe scaffold through peptide coupling with a fluorophore with an amine linker (Figure 6.2). This will allow for a fluorescent library of these compounds that can easily be modified with a pharmacophore utilizing click chemistry, as seen in Chapter 4.

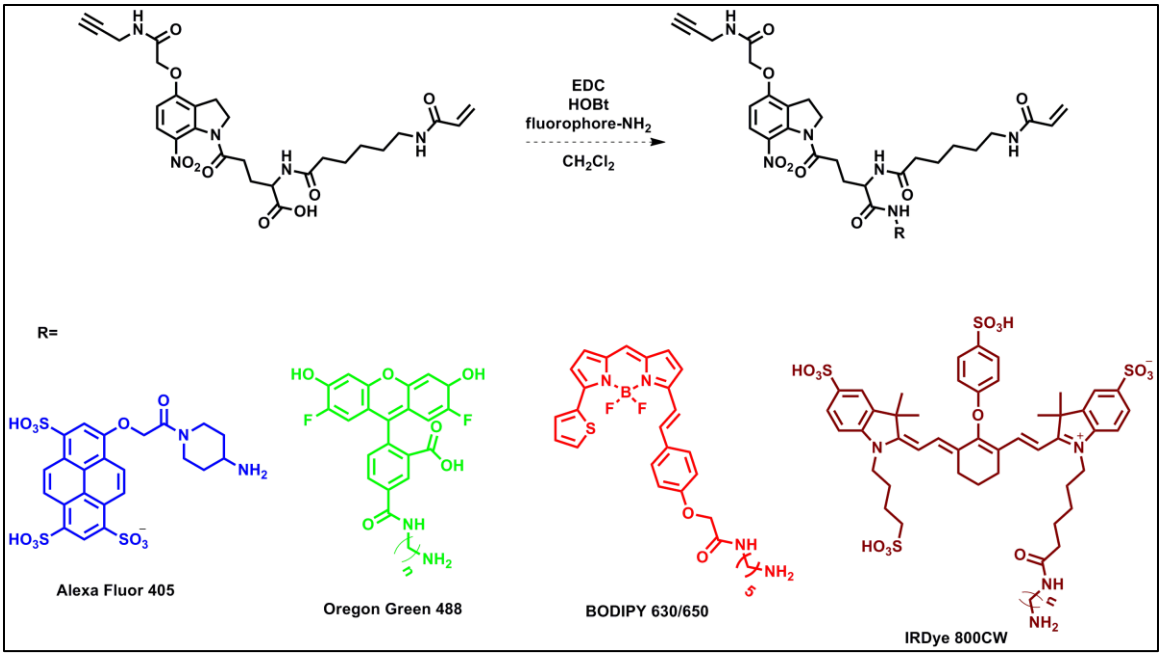

Figure 6.2. Fluorescent analogues for conjugation to the alkyne nanoprobe

6.1.3 Electrophile linker length

An area of chemical space on the nanoprobe scaffold that has not been evaluated is the length of the linker containing the acrylamide electrophile. Previously, we have discussed the effect on changing the pharmacophore for targeting different receptors of interest or changing the fluorophore used to visualize the receptor. The linker length between the pharmacophore and the alkyne scaffold is important because it will affect the binding affinity of the probe for the receptor being studied. However, the linker length for the electrophile also needs to be considered in case there are no endogenous nucleophiles in the chemical space of the linker with six carbons. The alkyne nanoprobe scaffold can be redesigned to contain an electrophile with a short 3 carbon linker derived from 3-aminopropanoic acid or a much longer 12 carbon linker derived from 12-aminododecanoic acid (Figure 6.3). Varying the linker length of the electrophile, coupled with different fluorophores discussed in previous section will allow for a kit of these

alkyne nanoprobes that can be applied to various receptors of interest. If there was a situation where the pharmacophore used did not lead to labeling of the receptor, now there will be more options to optimize conditions for binding and crosslinking of the probe.

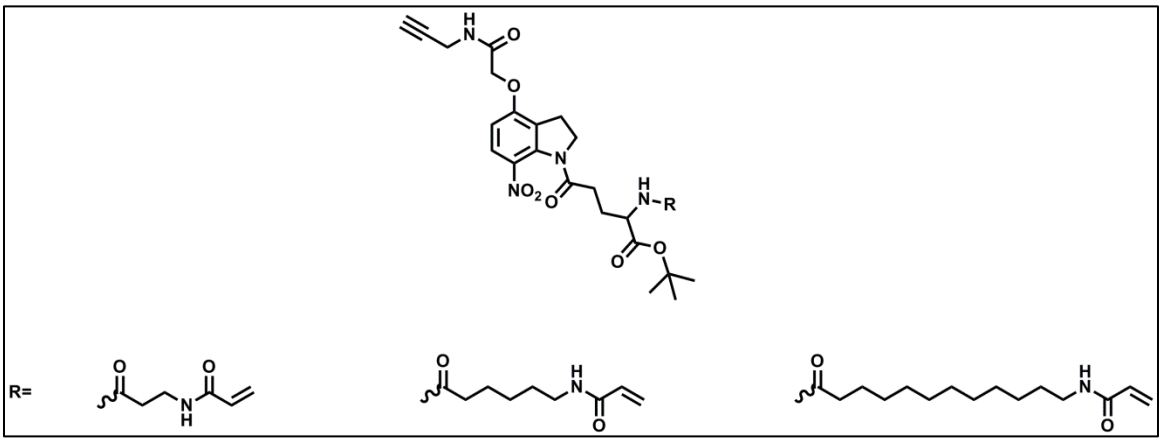

Figure 6.3. Linker length modification of alkyne nanoprobe

6.2 Caged alkyne electrophile development

The caged aziridinium compound discussed in Chapter 5 allowed for control of the alkylation of nucleophiles using UV light. Although the aziridinium compound that was generated could be visualized using a colormetric assay, it would be difficult to monitor electrophilic addition to a protein of interest. Going forward, we will synthesize a similar caged compound as discussed before; however, this new molecule will contain an alkyne handle for click reactions with a fluorophore or biotin-azide. This new molecule can be used for protein labeling and could possibly be used as a new core for future iterations of the nanoprobe technology. In essence, this new labeling technology would be a hybrid between caged compounds and photoaffinity labeling.

The synthesis of the caged alkyne electrophile **11** can be completed in 3 steps from 2-(methylamino)ethanol. 2-(methylamino)ethanol will be alkylated with propargyl bromide to yield compound **8**. Compound **8** will be used in a reaction with thionyl chloride to form the control alkyne-chloro compound **9**, as well as to alkylate 4-chloromethyl-7-methoxycoumarin under reflux conditions to yield caged compound **10**. The synthesis of caged compound **11** is then completed following the reaction of caged compound **10** with thionyl chloride to form the alkyl chloride compound **11** (Scheme 6.4).

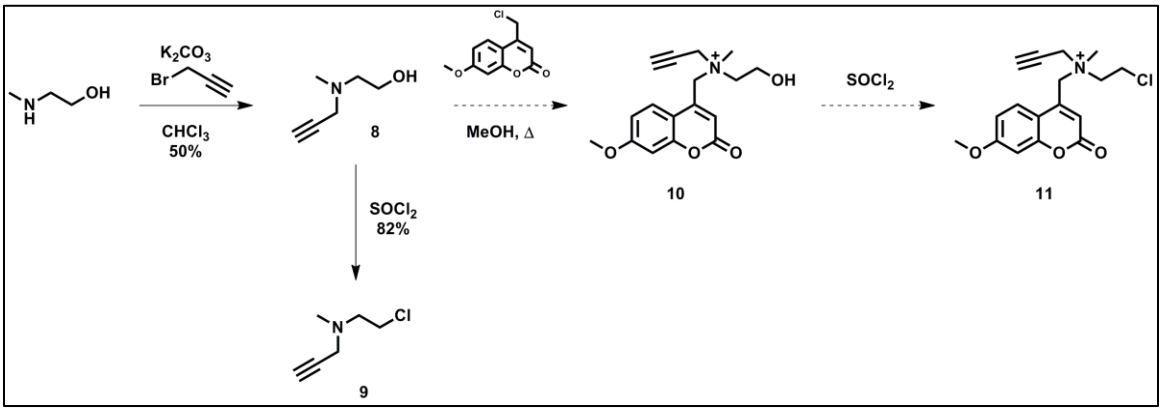

Scheme 6.4. Synthesis of a caged alkyne nitrogen mustard

To determine whether the addition of the propargyl handle will have an effect on aziridinium formation, compound **9** was tested in a NBP alkylation assay to determine if it will act similarly to the 2-chloro-N,N-dimethylethylamine control compound from the previous study. As shown in Figure 6.4, the alkyne electrophile was able to alkylate NBP, which show similar results as the 2-chloro-N,N-dimethylethylamine compound used before[15]. In addition, compound **8** was unable to alkylate NBP because it contains an alcohol moiety instead of an alkyl chloride like the other two compound tested. This suggests that compound **9** is still able to form an aziridinium intermediate and may possibly be rendered inert following addition to the coumarin photocage. Further studies

with both compound **9** and caged compound **11** should determine if this technology can be utilized to spatially limit protein modification for the purpose of protein tracking on cells.

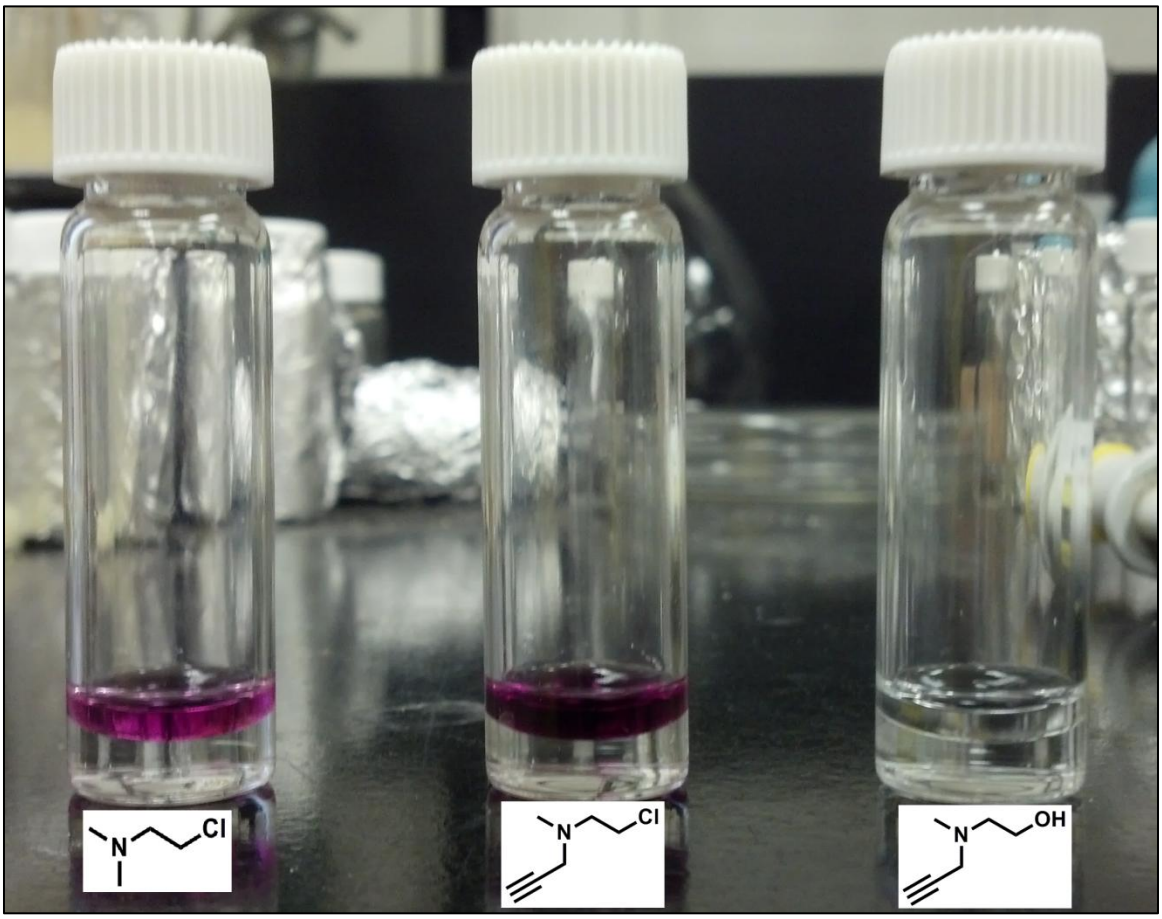

Figure 6.4. NBP alkylation assay for alkyne mustard. Left) 2-chloro-N,N-dimethylethylamine Center) Compound **9**. Right) Compound **8**.

6.3 References

(1) Reynolds, I. J.; Miller, R. J. *Mol. Pharmacol.* **1989**, *36* , 758.

(2) Chenard, B. L.; Shalaby, I. A.; Koe, B. K.; Ronau, R. T.; Butler, T. W.; Prochniak, M. A.; Schmidt, A. W.; Fox, C. B. *J. Med. Chem.* **1991**, *34*, 3085.

(3) Rosahl, T. W.; Wingrove, P. B.; Hunt, V.; Fradley, R. L.; Lawrence, J. M. K.; Heavens, R. P.; Treacey, P.; Usala, M.; Macaulay, A.; Bonnert, T. P.; Whiting, P. J.; Wafford, K. A. *Mol. Cell. Neurosci.* **2006**, *33*, 47.

(4) Grimwood, S.; Richards, P.; Murray, F.; Harrison, N.; Wingrove, P. B.; Hutson, P. H. *J. Neurochem.* **2000**, *75*, 2455.

(5) Hardingham, G. E.; Fukunaga, Y.; Bading, H. *Nat Neurosci* **2002**, *5*, 405.

(6) Mony, L.; Kew, J. N. C.; Gunthorpe, M. J.; Paoletti, P. *Br. J. Pharmacol.* **2009**, *157*, 1301.

(7) Tamiz, A. P.; Whittemore, E. R.; Zhou, Z.-L.; Huang, J.-C.; Drewe, J. A.; Chen, J.-C.; Cai, S.-X.; Weber, E.; Woodward, R. M.; Keana, J. F. W. *J. Med. Chem.* **1998**, *41*, 3499.

(8) Mony, L.; Krzaczkowski, L.; Leonetti, M.; Le Goff, A.; Alarcon, K.; Neyton, J.; Bertrand, H.-O.; Acher, F.; Paoletti, P. *Mol. Pharmacol.* **2009**, *75* , 60.

(9) Ng, F.-M.; Geballe, M. T.; Snyder, J. P.; Traynelis, S. F.; Low, C.-M. *Mol. Brain* **2008**, *1*, 16.

(10) Marchand, P.; Becerril-Ortega, J.; Mony, L.; Bouteiller, C.; Paoletti, P.; Nicole, O.; Barré, L.; Buisson, A.; Perrio, C. *Bioconjug. Chem.* **2012**, *23*, 21.

(11) Dhilly, M.; Becerril-Ortega, J.; Colloc'h, N.; MacKenzie, E. T.; Barré, L.; Buisson, A.; Nicole, O.; Perrio, C. *ChemBioChem* **2013**, *14*, 759.

(12) Eriksen, J.; Rasmussen, S. G. F.; Rasmussen, T. N.; Vaegter, C. B.; Cha, J. H.; Zou, M.-F.; Newman, A. H.; Gether, U. *J. Neurosci.* **2009**, *29*, 6794.

(13) Kozma, E.; Suresh Jayasekara, P.; Squarcialupi, L.; Paoletta, S.; Moro, S.; Federico, S.; Spalluto, G.; Jacobson, K. A. *Bioorg. Med. Chem. Lett.* **2013**, *23*, 26.

(14) Bai, M.; Sexton, M.; Stella, N.; Bornhop, D. J. *Bioconjug. Chem.* **2008**, *19*, 988.

(15) McCarron, S. T.; Feliciano, M.; Johnson, J. N.; Chambers, J. J. *Bioorg. Med. Chem. Lett.* **2013**, *23*, 2395.

CHAPTER 7

SUPPLEMENTARY INFORMATION

Table 7.1 List of abbreviations

1-ethyl-3-(3-dimethylamino propyl)carbodiimide	EDC	*N*,*N*-Diisopropylethylamine	DIPEA
1,3-di(2-toyl)guanidine	DTG	*N*,*N*-Dimethylformamide	DMF
4-nitrobenzylpyridine	NBP	N-methyl-D-aspartate	NMDA
Acetonitrile	CH_3CN	Nitrobenzodiazole	NBD
Amyloid lateral sclerosis	ALS	Photoaffinity labeling	PAL
α-amino-3-hydroxy-5-methyl 4-isoxazolepropioic acid	AMPA	Potassium carbonate	K_2CO_3
Chinese hamster ovaries	CHO	Potassium iodide	KI
Central nervous system	CNS	Potassium tert-butoxide	KOTBu
Dichloromethane	CH_2Cl_2	Serotonin transporter	SERT
Dimethyl sulfoxide	DMSO	Sodium azide	NaN_3
Dopamine transporter	DAT	Sodium bicarbonate	$NaHCO_3$
Endoplasmic reticulum	ER	Sodium hydroxide	NaOH
Ethanol	EtOH	Sodium nitrite	$NaNO_2$
Ethyl acetate	EtoAc	Thin layer chromatography	TLC
Hydrochloric acid	HCl	Thionyl chloride	$SOCl_2$
Hydroxybenzotriazole	HOBt	Tin (II) chloride	$SnCl_2$
Magnesium sulfate	$MgSO_4$	Triethylamine	Et_3N
Methanesulfonyl chloride	MsCl	Trifluoroacetic acid	TFA
Mitochondrion-associated ER membrane	MAM	Water	H_2O

7.1 Mass spectroscopy data

LC-MS data for DAT nanoprobe (SM-V-61)

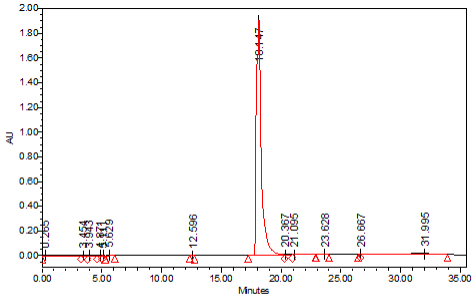

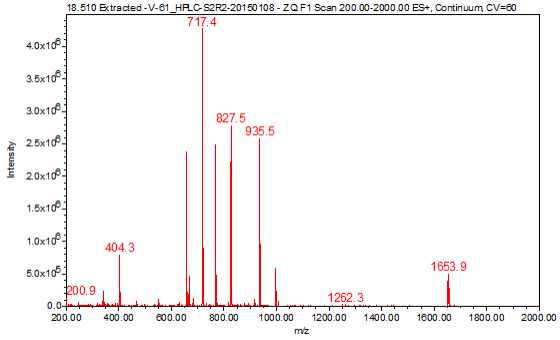

LC-MS data for SERT nanoprobe (SM-V-37)

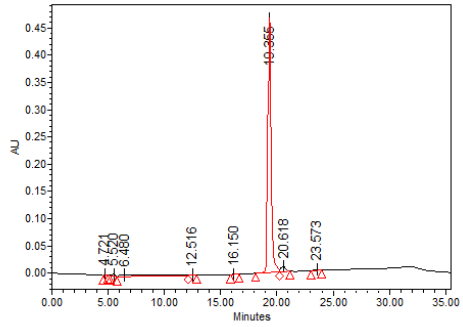

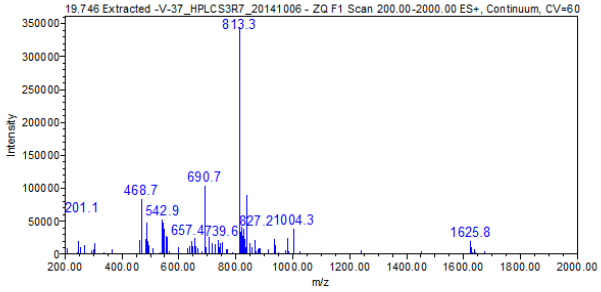

LC-MS data for ketamine nanoprobe (SM-V-127)

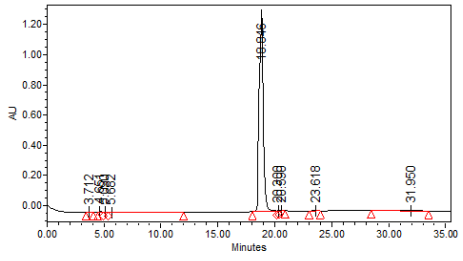

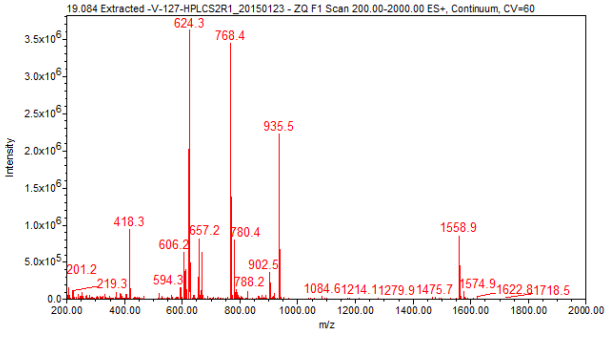

High resolution mass spectroscopy of DAT nanoprobe (SM-V-61)

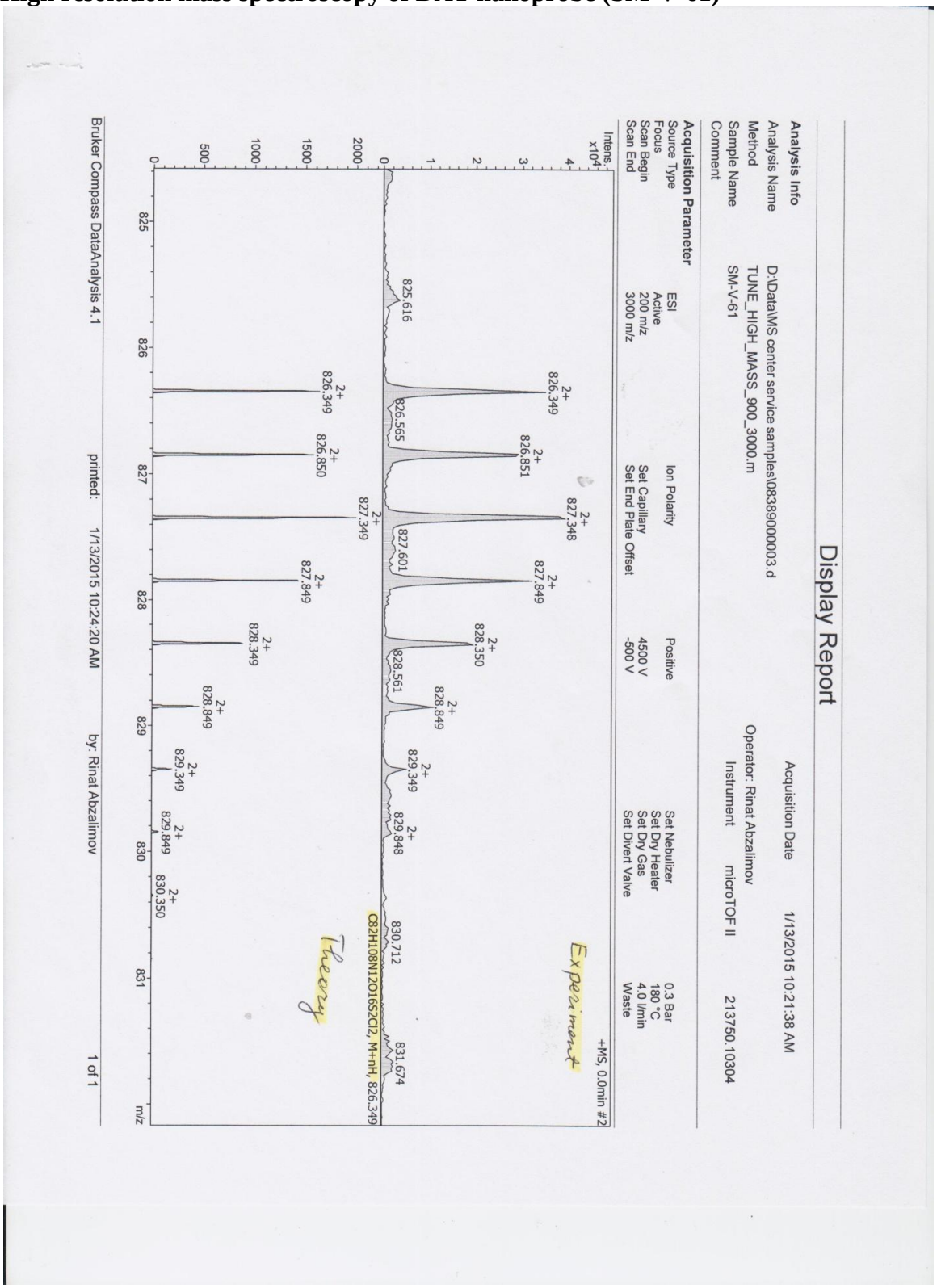

High resolution mass spectroscopy of SERT nanoprobe (SM-V-37)

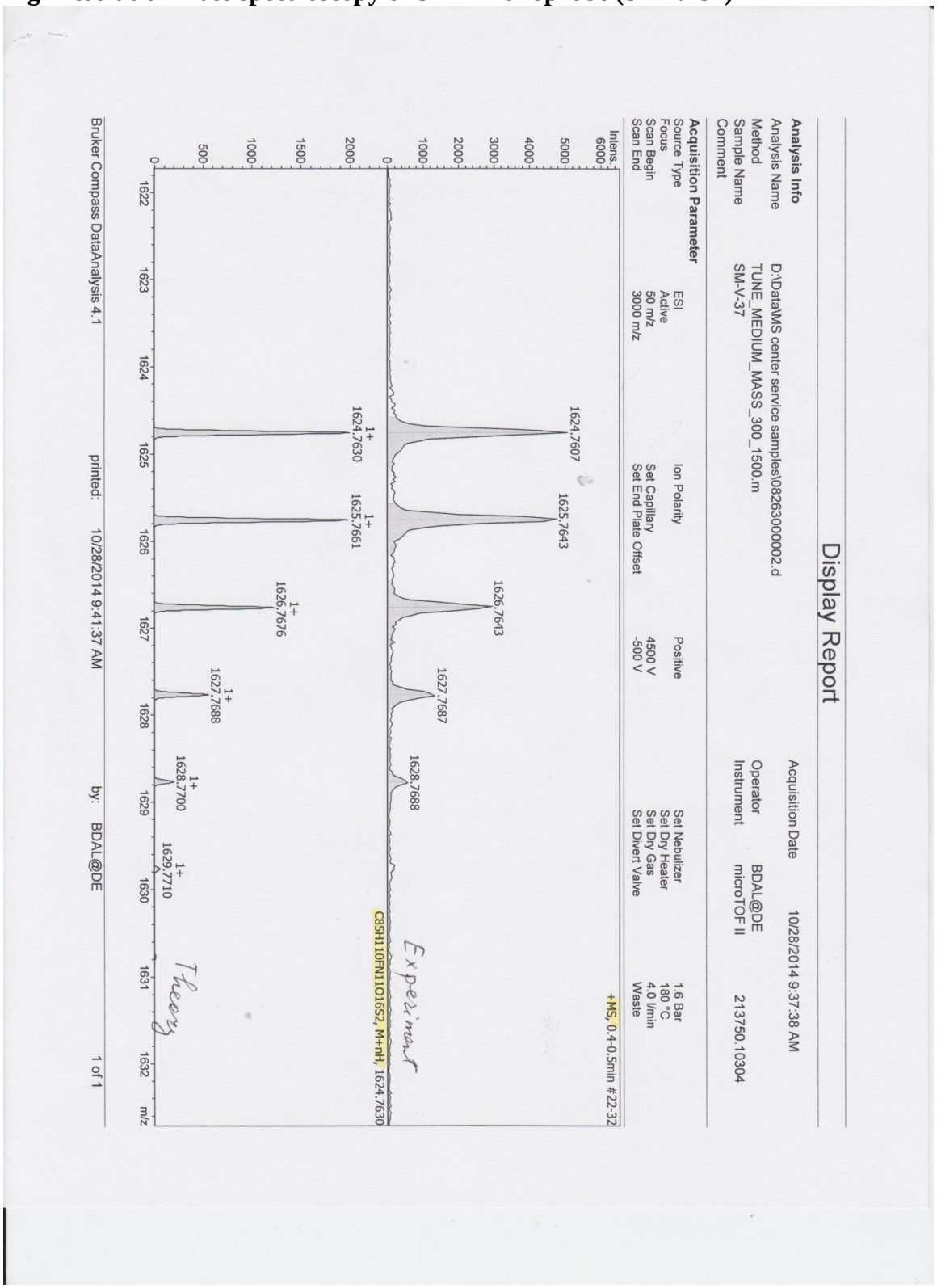

High resolution mass spectroscopy of ketamine nanoprobe (SM-V-127)

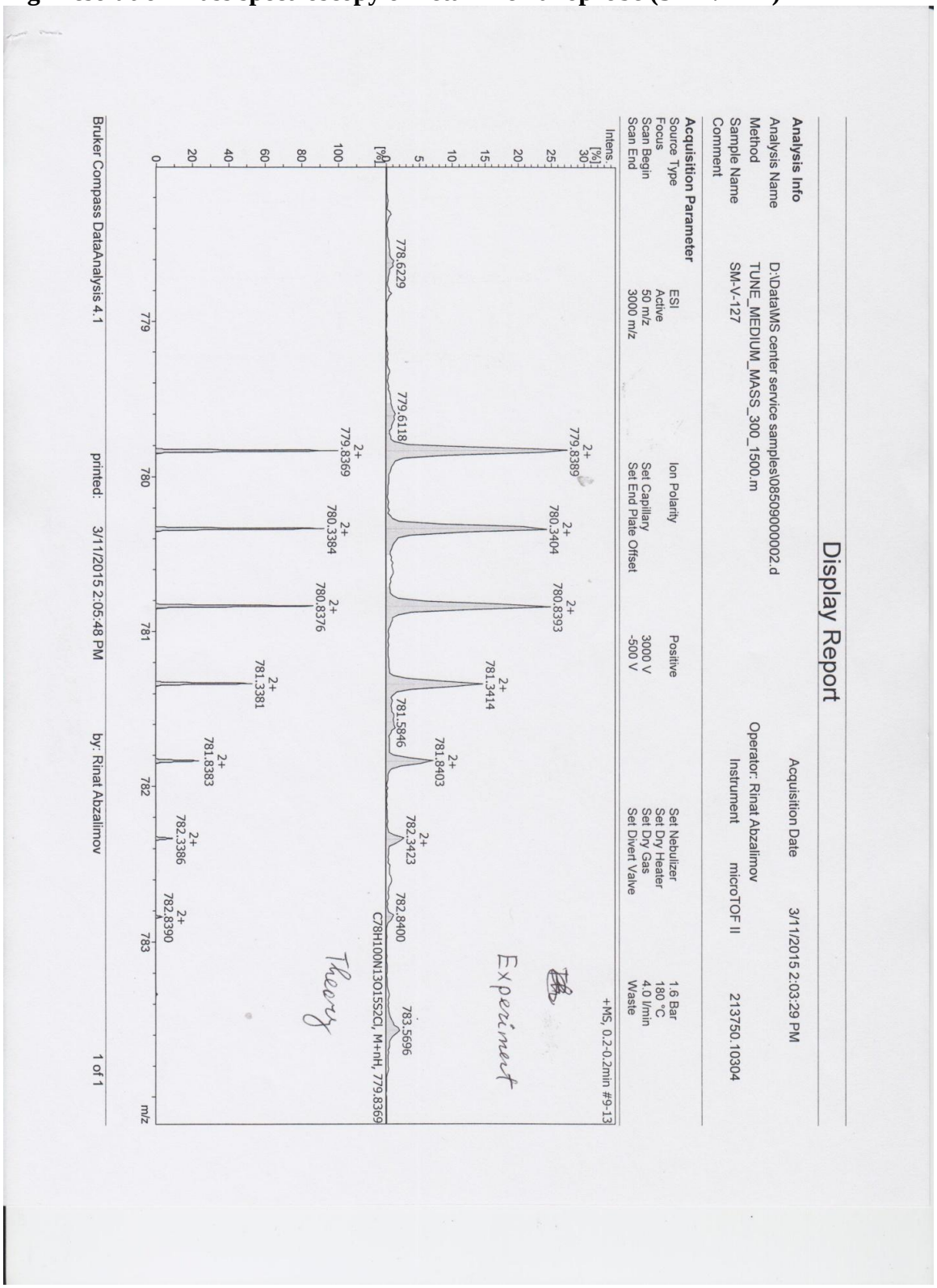

BIBLIOGRAPHY

A. Fleming, S., (1995). Chemical reagents in photoaffinity labeling. *Tetrahedron* 51, 12479–12520.

Ablordeppey, S.Y., Fischer, J.B., Law, H., Glennon, R.A., (2002). Probing the proposed phenyl-A region of the sigma-1 receptor. *Bioorg. Med. Chem.* 10, 2759–2765.

Al-Saif, A., Al-Mohanna, F., Bohlega, S., (2011). A mutation in sigma-1 receptor causes juvenile amyotrophic lateral sclerosis. *Ann. Neurol*. 70, 913–919.

Anderluh, A., Klotzsch, E., Reismann, A.W. a F., Brameshuber, M., Kudlacek, O., Newman, A.H., Sitte, H.H., Schütz, G.J., (2014). Single molecule analysis reveals coexistence of stable serotonin transporter monomers and oligomers in the live cell plasma membrane. *J. Biol. Chem*. 289, 4387–94.

Bai, M., Sexton, M., Stella, N., Bornhop, D.J., (2008). MBC94, a Conjugable Ligand for Cannabinoid CB2 Receptor Imaging. *Bioconjug. Chem*. 19, 988–992.

Baker, J.G., Middleton, R., Adams, L., May, L.T., Briddon, S.J., Kellam, B., Hill, S.J., (2010). Influence of fluorophore and linker composition on the pharmacology of fluorescent adenosine A1 receptor ligands. *Br. J. Pharmacol*. 159, 772–786.

Banala, A.K., Zhang, P., Plenge, P., Cyriac, G., Kopajtic, T., Katz, J.L., Loland, C.J., Newman, A.H., (2013). Design and Synthesis of 1-(3-(Dimethylamino)propyl)-1-(4-fluorophenyl)-1,3-dihydroisobenzofuran-5-carbonitrile (Citalopram) Analogues as Novel Probes for the Serotonin Transporter S1 and S2 Binding Sites. *J. Med. Chem*. 56, 9709–9724.

Barria, A., Malinow, R., (2002). Subunit-specific NMDA receptor trafficking to synapses. *Neuron*. 35, 345–53.

Berardi, F., Abate, C., Ferorelli, S., Colabufo, N.A., Perrone, R., (2009). 1-Cyclohexylpiperazine and 3,3-dimethylpiperidine derivatives as sigma-1 (sigma1) and sigma-2 (sigma2) receptor ligands: a review. *Cent. Nerv. Syst. Agents Med. Chem.* 9, 3, 205-219

Berque-Bestel, I., Soulier, J.-L., Giner, M., Rivail, L., Langlois, M., Sicsic, S., (2003). Synthesis and Characterization of the First Fluorescent Antagonists for Human 5-HT4 Receptors. *J. Med. Chem*. 46, 2606–2620.

Betzig, E., Patterson, G.H., Sougrat, R., Lindwasser, O.W., Olenych, S., Bonifacino, J.S., Davidson, M.W., Lippincott-Schwartz, J., Hess, H.F., (2006). Imaging Intracellular Fluorescent Proteins at Nanometer Resolution. *Sci*. 313 , 1642–1645.

Brunner, J., (1993). New Photolabeling and Crosslinking Methods. *Annu. Rev. Biochem*. 62, 483–514.

Carroll, R.C., Beattie, E.C., von Zastrow, M., Malenka, R.C., (2001). Role of ampa receptor endocytosis in synaptic plasticity. *Nat Rev Neurosci*. 2, 315–324.

Cha, J.H., Zou, M.-F., Adkins, E.M., Rasmussen, S.G.F., Loland, C.J., Schoenenberger, B., Gether, U., Newman, A.H., (2005). Rhodamine-labeled 2beta-carbomethoxy-3beta-(3,4-dichlorophenyl)tropane analogues as high-affinity fluorescent probes for the dopamine transporter. *J. Med. Chem*. 48, 7513–7516.

Chambers, J.J., Gouda, H., Young, D.M., Kuntz, I.D., England, P.M., (2004). Photochemically Knocking Out Glutamate Receptors in Vivo. *J. Am. Chem. Soc*. 126, 13886–13887.

Chen, H.-S.V., Lipton, S. a, (2006). The chemical biology of clinically tolerated NMDA receptor antagonists. *J. Neurochem*. 97, 1611–26.

Chen, H.-S.V., Lipton, S.A., (2005). Pharmacological Implications of Two Distinct Mechanisms of Interaction of Memantine with N-Methyl-d-aspartate-Gated Channels. *J. Pharmacol. Exp. Ther*. 314 , 961–971.

Chen, R., Furman, C.A., Gnegy, M.E., (2009). Dopamine transporter trafficking: rapid response on demand. *Future Neurol*. 5, 123–134.

Chenard, B.L., Shalaby, I.A., Koe, B.K., Ronau, R.T., Butler, T.W., Prochniak, M.A., Schmidt, A.W., Fox, C.B., (1991). Separation of .alpha.1-adrenergic and N-methyl-D-aspartate antagonist activity in a series of ifenprodil compounds. *J. Med. Chem*. 34, 3085–3090.

Combs-Bachmann, R.E., Johnson, J.N., Vytla, D., Hussey, A.M., Kilfoil, M.L., Chambers, J.J., (2015). Ligand-directed delivery of fluorophores to track native calcium-permeable AMPA receptors in neuronal cultures. *J. Neurochem*. 133, 320–329.

Dhami, G.K., Ferguson, S.S.G., (2006). Regulation of metabotropic glutamate receptor signaling, desensitization and endocytosis. *Pharmacol. Ther*. 111, 260–271.

Dhilly, M., Becerril-Ortega, J., Colloc'h, N., MacKenzie, E.T., Barré, L., Buisson, A., Nicole, O., Perrio, C., (2013). Synthesis and in Vitro Characterisation of Ifenprodil-Based Fluorescein Conjugates as GluN1/GluN2B N-Methyl-D-aspartate Receptor Antagonists. *ChemBioChem*. 14, 759–769.

Domino, E.F., Chodoff, P., Corssen, G., (1965). Pharmacologic Effects of CI-561, a New Dissociative Anestetic, *In Man. Clin. Pharmacol*. Ther. 6, 279–291.

Dore, T.M., Wilson, H.C., (2011). Chromophores for the delivery of bioactive molecules with two-photon excitation. *Neuromethods*. 55, 57–92.

Dormán, G., Prestwich, G.D., (1994). Benzophenone photophores in biochemistry. *Biochemistry*. 33, 5661–5673.

Dormán, G., Prestwich, G.D., (2000). Using photolabile ligands in drug discovery and development. *Trends Biotechnol*. 18, 64–77.

Eriksen, J., Rasmussen, S.G.F., Rasmussen, T.N., Vaegter, C.B., Cha, J.H., Zou, M.-F., Newman, A.H., Gether, U., (2009). Visualization of dopamine transporter trafficking in live neurons by use of fluorescent cocaine analogs. *J. Neurosci*. 29, 6794–808.

Fernandez-Suarez, M., Baruah, H., Martinez-Hernandez, L., Xie, K.T., Baskin, J.M., Bertozzi, C.R., Ting, A.Y., (2007). Redirecting lipoic acid ligase for cell surface protein labeling with small-molecule probes. *Nat Biotech*. 25, 1483–1487.

Giepmans, B.N.G., Adams, S.R., Ellisman, M.H., Tsien, R.Y., (2006). The fluorescent toolbox for assessing protein location and function. *Science*. 312, 217–24.

Gironacci, M.M., Adamo, H.P., Corradi, G., Santos, R.A., Ortiz, P., Carretero, O.A., (2011). Angiotensin (1-7) Induces Mas Receptor Internalization. *Hypertens*. 58 , 176–181.

Gitto, R., De Luca, L., Ferro, S., Scala, A., Ronsisvalle, S., Parenti, C., Prezzavento, O., Buemi, M.R., Chimirri, A., (2014). From NMDA receptor antagonists to discovery of selective σ receptor ligands. *Bioorg. Med. Chem*. 22, 393–7.

Glennon, R. a., Ablordeppey, S.Y., Ismaiel, A.M., El-Ashmawy, M.B., Fischer, J.B., Howie, K.B., (1994). Structural Features Important for .sigma 1 Receptor Binding. *J. Med. Chem*. 37, 1214–1219.

Glennon, R.A., (2005). Pharmacophore Identification for Sigma-1 (σ1) Receptor Binding: Application of the "Deconstruction - Reconstruction - Elaboration" Approach. *Mini Rev. Med. Chem.*

Gómez-Bombarelli, R., González-Pérez, M., Calle, E., Casado, J., (2012). Potential of the NBP Method for the Study of Alkylation Mechanisms: NBP as a DNA-Model. *Chem. Res. Toxicol*. 25, 1176–1191.

Greenwood, T.A., Alexander, M., Keck, P.E., McElroy, S., Sadovnick, A.D., Remick, R.A., Kelsoe, J.R., (2001). Evidence for linkage disequilibrium between the dopamine transporter and bipolar disorder. *Am. J. Med. Genet*. 105, 145–151.

Griffin, B. Albert, Adams, Stephen R., Tsien, R.Y., (1998). Specific Covalent Labeling of Recombinant Protein Molecules Inside Live Cells. *Science*. (80-.). 281, 269–272.

Grimwood, S., Richards, P., Murray, F., Harrison, N., Wingrove, P.B., Hutson, P.H., (2000). Characterisation of N-Methyl-D-Aspartate Receptor-Specific [3H]Ifenprodil Binding to Recombinant Human NR1a/NR2B Receptors Compared with Native Receptors in Rodent Brain Membranes. *J. Neurochem*. 75, 2455–2463.

Halo, T.L., Appelbaum, J., Hobert, E.M., Balkin, D.M., Schepartz, A., (2009). Selective recognition of protein tetraserine motifs with a cell-permeable, pro-fluorescent bis-boronic acid. *J. Am. Chem. Soc*. 131, 438–9.

Hardingham, G.E., Fukunaga, Y., Bading, H., (2002). Extrasynaptic NMDARs oppose synaptic NMDARs by triggering CREB shut-off and cell death pathways. *Nat Neurosci*. 5, 405–414.

Höltke, C., von Wallbrunn, A., Kopka, K., Schober, O., Heindel, W., Schäfers, M., Bremer, C., (2007). A Fluorescent Photoprobe for the Imaging of Endothelin Receptors. *Bioconjug. Chem*. 18, 685–694.

Ingram, S.L., Prasad, B.M., Amara, S.G., (2002). Dopamine transporter-mediated conductances increase excitability of midbrain dopamine neurons. *Nat. Neurosci*. 5, 971–978.

Jansen, K.L.R., Faull, R.L.M., Storey, P., Leslie, R.A., (1993). Loss of sigma binding sites in the CA1 area of the anterior hippocampus in Alzheimer's disease correlates with CA1 pyramidal cell loss. *Brain Res*. 623, 299–302.

Jasper, A., Schepmann, D., Lehmkuhl, K., Vela, J.M., Buschmann, H., Holenz, J., Wünsch, B., (2009). Synthesis of σ receptor ligands with unsymmetrical spiro connection of the piperidine moiety. *Eur. J. Med. Chem*. 44, 4306–4314.

John, C.S., Gulden, M.E., Li, J., Bowen, W.D., McAfee, J.G., Thakur, M.L., (2015). Synthesis, In Vitro Binding, and Tissue Distribution of Radioiodinated 2-[125I]N-(N-Benzylpiperidin-4-yl)-2-Iodo Benzamide, 2-[125I]BP: A Potential σ Receptor Marker for Human Prostate Tumors. *Nucl. Med. Biol*. 25, 189–194.

Johnson, J.W., Glasgow, N.G., Povysheva, N. V, (2015). Recent insights into the mode of action of memantine and ketamine. *Curr. Opin. Pharmacol*. 20, 54–63.

Jones, T.R., Smithers, M.J., Betteridge, R.F., Taylor, M.A., Jackman, A.L., Calvert, A.H., Davies, L.C., Harrap, K.R., (1986). Quinazoline antifolates inhibiting thymidylate synthase. Variation of the amino acid. *J. Med. Chem*. 29, 1114–1118.

Jose, J., Gamage, S. a, Harvey, M.G., Voss, L.J., Sleigh, J.W., Denny, W. a, (2013). Structure-activity relationships for ketamine esters as short-acting anaesthetics. *Bioorg. Med. Chem*. 21, 5098–106.

Joubert, J., Dyk, S. V, Malan, S.F., (2013). Small molecule fluorescent ligands as central nervous system imaging probes. *Mini Rev. Med. Chem*. 13, 682–96.

Kamiya, H., (2012). Photochemical Inactivation Analysis of Temporal Dynamics of Postsynaptic Native AMPA Receptors in Hippocampal Slices. *J. Neurosci*.

Kashiwagi, K., Masuko, T., Nguyen, C.D., Kuno, T., Tanaka, I., Igarashi, K., Williams, K., (2002). Channel Blockers Acting atN-Methyl-d-aspartate Receptors: Differential Effects of Mutations in the Vestibule and Ion Channel Pore. *Mol. Pharmacol*. 61 , 533–545.

Katoono, R., Kawai, H., Fujiwara, K., Suzuki, T., (2004). [10]Paracyclophanediamides and their octadehydro derivatives: novel exotopic receptors with hydrogen-bonding sites on the bridge. *Tetrahedron Lett*. 45, 8455–8459.

Kawamura, K., Elsinga, P.H., Kobayashi, T., Ishii, S., Wang, W.-F., Matsuno, K., Vaalburg, W., Ishiwata, K., (2015). Synthesis and evaluation of 11C- and 18F-labeled 1-[2-(4-alkoxy-3-methoxyphenyl)ethyl]-4-(3-phenylpropyl)piperazines as sigma receptor ligands for positron emission tomography studies. *Nucl. Med. Biol*. 30, 273–284.

Knowles, J.R., (1972). Photogenerated reagents for biological receptor-site labeling. A*cc. Chem. Res*. 5, 155–160.

Kohn, K.W., Hartley, J.A., Mattes, W.B., (1987). Mechanisms of DNA sequence selective alkylation of guanine-N7 positions by nitrogen mustards. *Nucleic Acids Res*. 15 , 10531–10549.

Korlipara, V., Ells, J., Wang, J., Tam, S., Elde, R., Portoghese, P., (1997). Fluorescent N-benzylnaltrindole analogues as potential delta opioid receptor selective probes. *Eur. J. Med. Chem*. 32, 171–174.

Kovtun, O., Tomlinson, I.D., Sakrikar, D.S., Chang, J.C., Blakely, R.D., Rosenthal, S.J., (2011). Visualization of the cocaine-sensitive dopamine transporter with ligand-conjugated quantum dots. *ACS Chem. Neurosci*. 2, 370–8.

Kozma, E., Suresh Jayasekara, P., Squarcialupi, L., Paoletta, S., Moro, S., Federico, S., Spalluto, G., Jacobson, K.A., (2013). Fluorescent ligands for adenosine receptors. *Bioorg. Med. Chem. Lett*. 23, 26–36.

Krieger, F., Mourot, A., Araoz, R., Kotzyba-Hibert, F., Molgó, J., Bamberg, E., Goeldner, M., (2008). Fluorescent agonists for the torpedo nicotinic acetylcholine receptor. *ChemBioChem*. 9, 1146–1153.

Kristensen, A.S., Andersen, J., Jørgensen, T.N., Sørensen, L., Eriksen, J., Loland, C.J., Strømgaard, K., Gether, U., (2011). SLC6 neurotransmitter transporters: structure, function, and regulation. *Pharmacol. Rev*. 63, 585–640.

Lacoste, T.D., Michalet, X., Pinaud, F., Chemla, D.S., Alivisatos, A.P., Weiss, S., (2000). Ultrahigh-resolution multicolor colocalization of single fluorescent probes. *Proc. Natl. Acad. Sci*. 97 , 9461–9466.

Laggner, C., Schieferer, C., Fiechtner, B., Poles, G., Hoffmann, R.D., Glossmann, H., Langer, T., Moebius, F.F., (2005). Discovery of High-Affinity Ligands of σ1 Receptor, ERG2, and Emopamil Binding Protein by Pharmacophore Modeling and Virtual Screening. *J. Med. Chem*. 48, 4754–4764.

Lapinsky, D.J., (2012). Tandem photoaffinity labeling–bioorthogonal conjugation in medicinal chemistry. *Bioorg. Med. Chem*. 20, 6237–6247.

Lawley, P.B. and P.D., (1961). The reaction of mono- and di-functional alkylating agents with nucleic acids. *Biochem. J*. 80, 496–503.

Leopoldo, M., Lacivita, E., Berardi, F., Perrone, R., (2009). Developments in fluorescent probes for receptor research. *Drug Discov. Today*. 14, 706–712.

Lin, M.Z., Wang, L., (2008). Selective Labeling of Proteins with Chemical Probes in Living Cells. *Physiology*. 23, 131–141.

Lipton, S.A., (2006). Paradigm shift in neuroprotection by NMDA receptor blockade: memantine and beyond. *Nat. Rev. Drug Discov*. 5, 160–170.

Lord, S.J., Lee, H.D., Moerner, W.E., (2010). Single-Molecule Spectroscopy and Imaging of Biomolecules in Living Cells. *Anal. Chem*. 82, 2192–2203.

Loving, G.S., Sainlos, M., Imperiali, B., (2015). Monitoring protein interactions and dynamics with solvatochromic fluorophores. *Trends Biotechnol*. 28, 73–83.

Lu, W., Shi, Y., Jackson, A.C., Bjorgan, K., During, M.J., Sprengel, R., Seeburg, P.H., Nicoll, R.A., (2014). Subunit Composition of Synaptic AMPA Receptors Revealed by a Single-Cell Genetic Approach. *Neuron*. 62, 254–268.

Mach, R.H., Huang, Y., Buchheimer, N., Kuhner, R., Wu, L., Morton, T.E., Wang, L.-M., Ehrenkaufer, R.L., Wallen, C.A., Wheeler, K.T., (2015). [18F]N-4′-Fluorobenzyl-4-(3-bromophenyl) acetamide for imaging the sigma receptor status of tumors: comparison with [18F]FDG and [125I]IUDR. *Nucl. Med. Biol*. 28, 451–458.

Mach, R.H., Smith, C.R., Al-Nabulsi, I., Whirrett, B.R., Childers, S.R., Wheeler, K.T., (1997). σ2 Receptors as Potential Biomarkers of Proliferation in Breast Cancer. *Cancer Res*. 57 , 156–161.

Madsen, B.W., Beglan, C.L., Spivak, C.E., (2000). Fluorescein-labeled naloxone binding to mu opioid receptors on live Chinese hamster ovary cells using confocal fluorescent microscopy. *J. Neurosci. Methods*. 97, 123–131.

Marchand, P., Becerril-Ortega, J., Mony, L., Bouteiller, C., Paoletti, P., Nicole, O., Barré, L., Buisson, A., Perrio, C., (2012). Confocal microscopy imaging of NR2B-containing NMDA receptors based on fluorescent ifenprodil-like conjugates. *Bioconjug. Chem*. 23, 21–26.

Martin, W.R., Eades, C.G., Thompson, J.A., Huppler, R.E., Gilbert, P.E., (1976). The effects of morphine- and nalorphine- like drugs in the nondependent and morphine-dependent chronic spinal dog. *J. Pharmacol. Exp. Ther*. 197 , 517–532.

Maurice, T., Urani, A., Phan, V.-L., Romieu, P., (2001). The interaction between neuroactive steroids and the σ1 receptor function: behavioral consequences and therapeutic opportunities. *Brain Res. Rev*. 37, 116–132.

McCarron, S.T., Feliciano, M., Johnson, J.N., Chambers, J.J., (2013). Photoinitiated release of an aziridinium ion precursor for the temporally controlled alkylation of nucleophiles. *Bioorg. Med. Chem. Lett*. 23, 2395–2398.

Mehler-Wex, C., Riederer, P., Gerlach, M., (2006). Dopaminergic dysbalance in distinct basal ganglia neurocircuits: Implications for the pathophysiology of parkinson's disease, schizophrenia and attention deficit hyperactivity disorder. *Neurotox. Res*. 10, 167–179.

Melamed, E., Lahav, M., Atlas, D., (1976). Beta-adrenergic receptors in rat myocardium: Direct detection by a new fluorescent beta-blocker. *Experientia*. 32, 1387–1389.

Michalet, X., Weiss, S., Jäger, M., (2006). Single-molecule fluorescence studies of protein folding and conformational dynamics. *Chem. Rev*. 106, 5, 1785-1813

Middleton, R.J., Briddon, S.J., Cordeaux, Y., Yates, A.S., Dale, C.L., George, M.W., Baker, J.G., Hill, S.J., Kellam, B., (2007). New fluorescent adenosine A1-receptor agonists that allow quantification of ligand-receptor interactions in microdomains of single living cells. *J. Med. Chem*. 50, 782–93.

Middleton, R.J., Kellam, B., (2005). Fluorophore-tagged GPCR ligands. *Curr. Opin. Chem. Biol*. 9, 517–525.

Mishina, M., Ishiwata, K., Ishii, K., Kitamura, S., Kimura, Y., Kawamura, K., Oda, K., Sasaki, T., Sakayori, O., Hamamoto, M., Kobayashi, S., Katayama, Y., (2005). Function of sigma1 receptors in Parkinson's disease. *Acta Neurol. Scand*. 112, 103–107.

Mishina, M., Ohyama, M., Ishii, K., Kitamura, S., Kimura, Y., Oda, K., Kawamura, K., Sasaki, T., Kobayashi, S., Katayama, Y., Ishiwata, K., (2008). Low density of sigma1 receptors in early Alzheimer's disease. *Ann. Nucl. Med*. 22, 151–156.

Mizukami, S., Hori, Y., Kikuchi, K., (2014). Small-molecule-based protein-labeling technology in live cell studies: probe-design concepts and applications. *Acc. Chem. Res*. 47, 247–56.

Monnet, F.P., Debonnel, G., de Montigny, C., (1992). In vivo electrophysiological evidence for a selective modulation of N-methyl-D-aspartate-induced neuronal activation in rat CA3 dorsal hippocampus by sigma ligands. *J. Pharmacol. Exp. Ther*. 261 , 123–130.

Mony, L., Kew, J.N.C., Gunthorpe, M.J., Paoletti, P., (2009a). Allosteric modulators of NR2B-containing NMDA receptors: molecular mechanisms and therapeutic potential. *Br. J. Pharmacol*. 157, 1301–1317.

Mony, L., Krzaczkowski, L., Leonetti, M., Le Goff, A., Alarcon, K., Neyton, J., Bertrand, H.-O., Acher, F., Paoletti, P., (2009b). Structural Basis of NR2B-Selective Antagonist Recognition by N-Methyl-d-aspartate Receptors. *Mol. Pharmacol*. 75 , 60–74.

Nam, N.-H., Kim, Y., You, Y.-J., Hong, D.-H., Kim, H.-M., Ahn, B.-Z., (2002). Preliminary Structure–Antiangiogenic Activity Relationships of 4-Senecioyloxymethyl-6,7-dimethoxycoumarin. *Bioorg. Med. Chem. Lett*. 12, 2345–2348.

Newman, A.H., Katz, J.L., (2009). Atypical Dopamine Uptake Inhibitors that Provide Clues About Cocaine' s Mechanism at the Dopamine Transporter. *Design*. 95–129.

Ng, F.-M., Geballe, M.T., Snyder, J.P., Traynelis, S.F., Low, C.-M., (2008). Structural insights into phenylethanolamines high-affinity binding site in NR2B from binding and molecular modeling studies. *Mol. Brain*. 1, 16.

Popp, M.W.-L., Ploegh, H.L., (2011). Making and Breaking Peptide Bonds: Protein Engineering Using Sortase. *Angew. Chemie Int. Ed*. 50, 5024–5032.

Puliti, D., Warther, D., Orange, C., Specht, A., Goeldner, M., (2011). Small photoactivatable molecules for controlled fluorescence activation in living cells. *Bioorg. Med. Chem*. 19, 1023–1029.

Ransom, R.W., Kammerer, R.C., Cho, A.K., (1982). Chemical transformations of xylamine (N-2'-chloroethyl-N-ethyl-2-methylbenzylamine) in solution. Pharmacological activity of the species derived from this irreversible norepinephrine uptake inhibitor. *Mol. Pharmacol*. 21 , 380–386.

Rasmussen, S.G.F., Carroll, F.I., Maresch, M.J., Jensen, A.D., Tate, C.G., Gether, U., (2001). Biophysical Characterization of the Cocaine Binding Pocket in the Serotonin Transporter Using a Fluorescent Cocaine Analogue as a Molecular Reporter. *J. Biol. Chem*. 276, 4717–4723.

Reynolds, I.J., Miller, R.J., (1989). Ifenprodil is a novel type of N-methyl-D-aspartate receptor antagonist: interaction with polyamines. *Mol. Pharmacol*. 36 , 758–765.

Rink, S.M., Hopkins, P.B., (1995). A mechlorethamine-induced DNA interstrand cross-link bends duplex DNA. *Biochemistry*. 34, 1439–1445.

Robinette, D., Neamati, N., Tomer, K.B., Borchers, C.H., (2006). Photoaffinity labeling combined with mass spectrometric approaches as a tool for structural proteomics. *Expert Rev. Proteomics*. 3, 399–408.

Rosahl, T.W., Wingrove, P.B., Hunt, V., Fradley, R.L., Lawrence, J.M.K., Heavens, R.P., Treacey, P., Usala, M., Macaulay, A., Bonnert, T.P., Whiting, P.J., Wafford, K.A., (2006). A genetically modified mouse model probing the selective action of ifenprodil at the N-methyl-d-aspartate type 2B receptor. *Mol. Cell. Neurosci*. 33, 47–56.

Shroff, H., White, H., Betzig, E., (2001). Photoactivated Localization Microscopy (PALM) of Adhesion Complexes, in: *Current Protocols in Cell Biology*. Chap 4.

Singh, A., Thornton, E.R., Westheimer, F.H., (1962). The Photolysis of Diazoacetylchymotrypsin. *J. Biol. Chem*. 237 , PC3006–PC3008.

Sinner, B., Graf, B.M., (2008). Ketamine, in: Schüttler, J., Schwilden, H. (Eds.), Modern Anesthetics SE - 15, *Handbook of Experimental Pharmacology*. Springer Berlin Heidelberg, pp. 313–333.

Sleigh, J., Harvey, M., Voss, L., Denny, B., (2014). Ketamine – More mechanisms of action than just NMDA blockade. *Trends Anaesth. Crit. Care*. 4, 76–81.

Sobolevsky, A.I., Rosconi, M.P., Gouaux, E., (2009). X-ray structure , symmetry and mechanism of an AMPA-subtype glutamate receptor. *Nature*. 462, 745–756.

Su, T.-P., Hayashi, T., Maurice, T., Buch, S., Ruoho, A.E., (2010). The sigma-1 receptor chaperone as an inter-organelle signaling modulator. *Trends Pharmacol. Sci*. 31, 12, 557-566

Sulzer, D., (2007). Multiple hit hypotheses for dopamine neuron loss in Parkinson's disease. *Trends Neurosci*. 30, 5, 244-250

Swanson, J.M., Flodman, P., Kennedy, J., Spence, M.A., Moyzis, R., Schuck, S., Murias, M., Moriarity, J., Barr, C., Smith, M., Posner, M., (2000). Dopamine genes and ADHD, in: *Neuroscience and Biobehavioral Reviews*. pp. 21–25.

Tahtaoui, C., Parrot, I., Klotz, P., Guillier, F., Galzi, J.-L., Hibert, M., Ilien, B., (2004). Fluorescent Pirenzepine Derivatives as Potential Bitopic Ligands of the Human M1 Muscarinic Receptor. *J. Med. Chem*. 47, 4300–4315.

Tamiz, A.P., Whittemore, E.R., Zhou, Z.-L., Huang, J.-C., Drewe, J.A., Chen, J.-C., Cai, S.-X., Weber, E., Woodward, R.M., Keana, J.F.W., (1998). Structure−Activity Relationships for a Series of Bis(phenylalkyl)amines: Potent Subtype-Selective Inhibitors of N-Methyl-d-aspartate Receptors. *J. Med. Chem*. 41, 3499–3506.

Tamura, T., Tsukiji, S., Hamachi, I., (2012). Native FKBP12 Engineering by Ligand-Directed Tosyl Chemistry: Labeling Properties and Application to Photo-Cross-Linking of Protein Complexes in Vitro and in Living Cells. *J. Am. Chem. Soc*. 134, 2216–2226.

Thaens, D., Heinzelmann, D., Böhme, A., Paschke, A., Schüürmann, G., (2012). Chemoassay Screening of DNA-Reactive Mutagenicity with 4-(4-Nitrobenzyl)pyridine – Application to Epoxides, Oxetanes, and Sulfur Heterocycles. *Chem. Res. Toxicol*. 25, 2092–2102.

Thiagarajan, T.C., Lindskog, M., Tsien, R.W., (2005). Adaptation to Synaptic Inactivity in Hippocampal Neurons. *Neuron*. 47, 725–737.

Toseland, C.P., (2013). Fluorescent labeling and modification of proteins. *J. Chem. Biol*. 6, 85–95.

Tsukiji, S., Miyagawa, M., Takaoka, Y., Tamura, T., Hamachi, I., (2009). Ligand-directed tosyl chemistry for protein labeling in vivo. *Nat Chem Biol*. 5, 341–343.

Turcatti, G., Zoffmann, S., Lowe, J.A., Drozda, S.E., Chassaing, G., Schwartz, T.W., Chollet, A., (1997). Characterization of non-peptide antagonist and peptide agonist binding sites of the NK1 receptor with fluorescent ligands. *J. Biol. Chem*. 272, 21167–21175.

Vázquez, M.E., Blanco, J.B., Salvadori, S., Trapella, C., Argazzi, R., Bryant, S.D., Jinsmaa, Y., Lazarus, L.H., Negri, L., Giannini, E., Lattanzi, R., Colucci, M., Balboni, G., (2006). 6-N,N-dimethylamino-2,3-naphthalimide: a new environment-sensitive fluorescent probe in delta- and mu-selective opioid peptides. *J. Med. Chem*. 49, 3653–3658.

Vilner, B.J., John, C.S., Bowen, W.D., (1995). Sigma-1 and Sigma-2 Receptors Are Expressed in a Wide Variety of Human and Rodent Tumor Cell Lines. *Cancer Res*. 55 , 408–413.

Vivero-Pol, L., George, N., Krumm, H., Johnsson, K., Johnsson, N., (2005). Multicolor Imaging of Cell Surface Proteins. *J. Am. Chem. Soc*. 127, 12770–12771.

Vodovozova, E.L., (2007). Photoaffinity labeling and its application in structural biology. Biochem. 72, 1, 1-20

Vytla, D., Combs-Bachmann, R.E., Hussey, A.M., Hafez, I., Chambers, J.J., (2011). Silent, fluorescent labeling of native neuronal receptors. *Org. Biomol. Chem*. 9, 7151–7161.

Walker, J.M., Bowen, W.D., Walker, F.O., Matsumoto, R.R., De Costa, B., Rice, K.C., (1990). Sigma receptors: biology and function. *Pharmacol. Rev*. 42 , 355–402.

Weber, P.J.A., Beck-Sickinger, A.G., (1997). Comparison of the photochemical behavior of four different photoactivatable probes. *J. Pept. Res*. 49, 375–383.

Wheeler, K.T., Wang, L.-M., Wallen, C.A., Childers, S.R., Cline, J.M., Keng, P.C., Mach, R.H., (2000). Sigma-2 receptors as a biomarker of proliferation in solid tumours. *Br J Cancer*. 82, 1223–1232.

Wombacher, R., Cornish, V.W., (2011). Chemical tags: Applications in live cell fluorescence imaging. *J. Biophotonics*. 4, 391–402.

Yates, A.S., Doughty, S.W., Kendall, D.A., Kellam, B., (2005). Chemical modification of the naphthoyl 3-position of JWH-015: In search of a fluorescent probe to the cannabinoid CB2 receptor. *Bioorg. Med. Chem. Lett*. 15, 3758–3762.

Zeilhofer, H.U., Swandulla, D., Geisslinger, G., Brune, K., (1992). Differential effects of ketamine enantiomers on NMDA receptor currents in cultured neurons. *Eur. J. Pharmacol*. 213, 155–158.

Zhang, P., Jørgensen, T.N., Loland, C.J., Newman, A.H., (2013). A rhodamine-labeled citalopram analogue as a high-affinity fluorescent probe for the serotonin transporter. *Bioorg. Med. Chem. Lett*. 23, 323–6.